The Thesis Committee for Joseph Robert Klein
Certifies that this is the approved version of the following thesis:

Behavior of Slender Beams without Stirrups: Effects of Load Distribution and Member Depth

APPROVED BY
SUPERVISING COMMITTEE:

Supervisor:

Oguzhan Bayrak

Trevor Hrynyk

Behavior of Slender Beams without Stirrups: Effects of Load Distribution and Member Depth

by

Joseph Robert Klein, B.S.C.E.

Thesis

Presented to the Faculty of the Graduate School of

The University of Texas at Austin

in Partial Fulfillment

of the Requirements

for the Degree of

Master of Science in Engineering

The University of Texas at Austin

December 2015

Dedication

To my family, whose love and support put me where I am today

Acknowledgements

This research was the result of much hard work and dedication, not just from me, but from many individuals. Documents such as this rarely reflect all of the people that contributed to them so I will attempt to remedy that here.

I want to thank MPR Associates, Inc. Though this research was not part of the main project, the funding they provided made this work possible. In addition, they taught me two important lessons. First, quality control, though sometimes vexing, ultimately leads to a better end product. Second, never work in the nuclear industry; there is quality control and then there is *nuclear* quality control.

I will always cherish the mentorship I received during this project. Dr. Bayrak not only gave me direction, but he loved discussing every aspect of the project with me. Though I did not always enjoy the questions he asked me afterwards, I always enjoyed telling him something and seeing the wheels turning in his head. Dean Deschenes and Mike Brown both provided me with much guidance and practical experience at different times during my work. Though each are very unique individuals, I felt that both were always there for whatever I needed. I consider both to be not only mentors, but friends. Thanks to Dr. Bayrak, Dr. Hrynyk, and Mike for their help in reading and editing this document.

A special thank you to all of the FSEL staff. David Braley not only told the best stories, but also continually taught me about the different types of intelligence. Dennis Fillip was constantly helping me, and I'm sure I learned more from him than he ever intended. I can't count the number of times that Blake Stasney walked by and made a comment that completely changed how I was going about a task. All three of them made

this research possible with their instruction in lab tools and equipment, and their operation of the cranes and forklifts. Thank you to Michelle Damvar and Deanna Mueller for their administrative work, and John Bacon for his terrible jokes.

The other FSEL students were always willing to lend a helping hand when I needed it. Thank you to all of the students I worked with day-in and day-out: Trey Dondrea, Daniel Elizondo, Cody Lambert, Alistair Longshaw, Alissa Neuhausen, Sara Watts, Heather Wilson, and Beth Zetzman. A special thank you must go out to Gloriana Arrieta Martinez and Katelyn Beiter, who were with me for the entirety of this project, and Nick Dassow, who showed me the ropes and whose work formed a basis for my own. There are too many students to list that helped me cast my specimens, but I greatly appreciate every one of them.

Finally, I want to thank my entire family. My parents taught me more lessons than I can count, but most importantly they instilled in me the values of love and family above all. My brothers always knew the right things to say to help me through any problem I had. My cousin cooked me dinner and gave me a place to get away from school. Last, but not least, I want to thank my girlfriend, Beth Anne. Her love and laughter did more for me than she will ever know. Already, the times we have shared are some of my most cherished.

Abstract

Behavior of Slender Beams without Stirrups: Effects of Load Distribution and Member Depth

Joseph Robert Klein, M.S.E.

The University of Texas at Austin, 2015

Supervisor: Oguzhan Bayrak

Though uniform loading is common in structures, the vast majority of all shear strength tests on slender reinforced concrete members without stirrups have been performed using concentrated loading. Furthermore, the uniform load tests that have been conducted typically involve members with smaller specimen depths (d) and larger reinforcement ratios (ρ) than are commonly used in practice. Previous studies usually agree that a noticeable increase in shear strength can be expected when a specimen is subjected to uniform loading as opposed to concentrated loading.

Six shear tests were performed on four slender beams without stirrups at The University of Texas at Austin. Two of the specimens had approximately double the effective depth (d) as the other two. For a given depth, two concentrated load tests were carried out on either end of one specimen, and one uniform load test was carried out on the second specimen. Thus, four reinforced concrete beams were used to perform a total of four concentrated load tests and two uniform load tests, with the objective of determining the influence of load distribution as member depth (d) increases. To ensure

that a direct comparison could be made between each load distribution, the ratio between maximum bending moment and maximum shear force was maintained for all tests. Additionally, to provide consistency with typical design practice, the reinforcement ratio (ρ) was selected to match that of a typical beam.

The experimental results presented an influence of load distribution opposite to that of previous studies, with a range of increase in shear strength at first diagonal cracking of concentrated load tests of -16 to 50 percent, with an average increase of 18 percent, over uniform load tests. Additionally, the tests with smaller effective depths (d) saw a percent increase in shear strength of 31 to 68 percent, with an average increase of 50 percent, over tests with larger effective depths (d).

Table of Contents

List of Tables

List of Figures

Chapter 1: Introduction

1.1 OVERVIEW

With the failure of a reinforced concrete beam without shear reinforcement at the Wilkins Air Force Base in 1955 (Elstner and Hognestad 1957), came a surge in shear strength tests to better comprehend the factors affecting shear strength. Presently, over 1,000 shear tests on slender members without stirrups have been performed on a variety of different members, as presented in the ACI-DAfStb shear database (Reineck et al. 2013).

The vast majority of these tests, however, have been performed on members with effective depths (d) less than 12 in. (305 mm) and reinforcement ratios (ρ) greater than 2 percent. Furthermore, only approximately 7 percent of the shear tests were performed using a uniform load configuration. In a desire to test specimens more representative of field conditions, the specimens presented in this thesis have effective depths (d) of 21.3 in. (541 mm) and 45.3 in. (1,151 mm), reinforcement ratios of 1 percent, and were subjected to either uniform or concentrated loading.

Existing technical literature would suggest that uniformly loaded specimens should exhibit an increase in shear strength over specimens tested under concentrated loading. With the small effective depths (d) and high reinforcement ratios (ρ) seen in most of the literature, it was unclear at the onset of testing whether the difference between uniform and concentrated loading holds true as member depth (d) increases and reinforcement ratio (ρ) decreases. Rather than observing the increased shear strength of uniform load tests seen in the literature, the six results presented here had the opposite trend. However, the difference between load distributions decreased as effective member depth (d) increased, which is in agreement with the difference reported in the literature.

Test results obtained within this study were compared to shear provisions in ACI 318-14 and AASHTO LRFD 2014. Not only was the desire to assess the safety provided by code provisions, but also to determine if assumptions such as the location of the critical section and failure at first diagonal cracking instead of ultimate load were sound. In general, both codes, ACI 318 and AASHTO LRFD, overestimated the shear strength of slender reinforced concrete members without stirrups. ACI 318-14 code provisions more accurately captured the shear strength of specimens with an effective depth of 21.3 in. (541 mm), and AASHTO LRFD 2014 more accurately captured the shear strength of specimens with an effective depth of 45.3 in. (1,151 mm). There was little difference in the accuracy of code-calculated strengths in regards to load distribution. Furthermore, the assumptions of the location of the critical section were found to be reasonable for both codes. Test results in literature and those presented herein agreed that load carrying capacity after first diagonal cracking is unreliable and unpredictable.

In general, size effect was found to be more critical for shear strength than was load distribution. In members such as thick slabs and footings, it is often thought that the presence of uniform loads offsets the decrease in shear strength due to large effective depths (d) (Uzel et al. 2011). The tests presented here and in some of the literature would suggest otherwise. Additionally, based on conclusions by Sherwood et al. (2006), one-way shear strength is largely independent of member width. For those reasons, provisions such as minimum shear reinforcement ($A_{v,min}$) should not vary between different member types, especially when dealing with large effective depths (d).

1.2 RESEARCH SIGNIFICANCE

The results from this study allow for a direct comparison between the deepest identical members tested under both concentrated and uniform load configurations.

Furthermore, these results have expanded upon the existing literature by providing specimens with effective depths (d) and reinforcement ratios (ρ) likely seen in practice and tested under more realistic loading schemes. The six tests performed were examined in the context of the assumptions and provisions of ACI 318-14 and AASHTO LRFD 2014. Though some assumptions were sound, each code document overestimated the shear strength of the slender reinforced concrete members without shear reinforcement tested in this study.

Chapter 2: Experimental Investigation

2.1 Beam Designation and Specimen Geometry

Four reinforced concrete specimens were constructed as shown in Figure 2-1 to obtain six structural tests. Two specimens (LD6 and LD7) were each tested under a concentrated load. One test was performed on each end of these two members for a total of four concentrated load tests. Stirrups were placed outside of the test region in specimens LD6 and LD7 to minimize damage so that a second concentrated load test could occur. Two other specimens (LD5 and LD8) were tested under a uniform load applied along the entire length.

Each specimen was constructed slightly differently, as shown in Figure 2-1. LD5 and LD6 were 24 in. (0.61 m) tall, while LD7 and LD8 were 48 in. (1.22 m) tall. The test regions for each beam are also depicted in gray in Figure 2-1. The naming convention is summarized as follows:

- LD5: Uniform load test on a specimen of height (h) 24 in. (0.61 m). Total load span was equal to 256 in. (6.50 m).
- LD6-N, LD6-S: Concentrated load tests on a specimen of height (h) 24 in. (0.61 m). Shear span (a) was equal to 64 in. (1.63 m).
- LD7-N, LD7-S: Concentrated load tests on a specimen of height (h) 48 in. (1.22 m). Shear span (a) was equal to 136 in. (3.45 m).
- LD8: Uniform load test on a specimen of height (h) 48 in. (1.22 m). Total load span was equal to 544 in. (13.82 m).

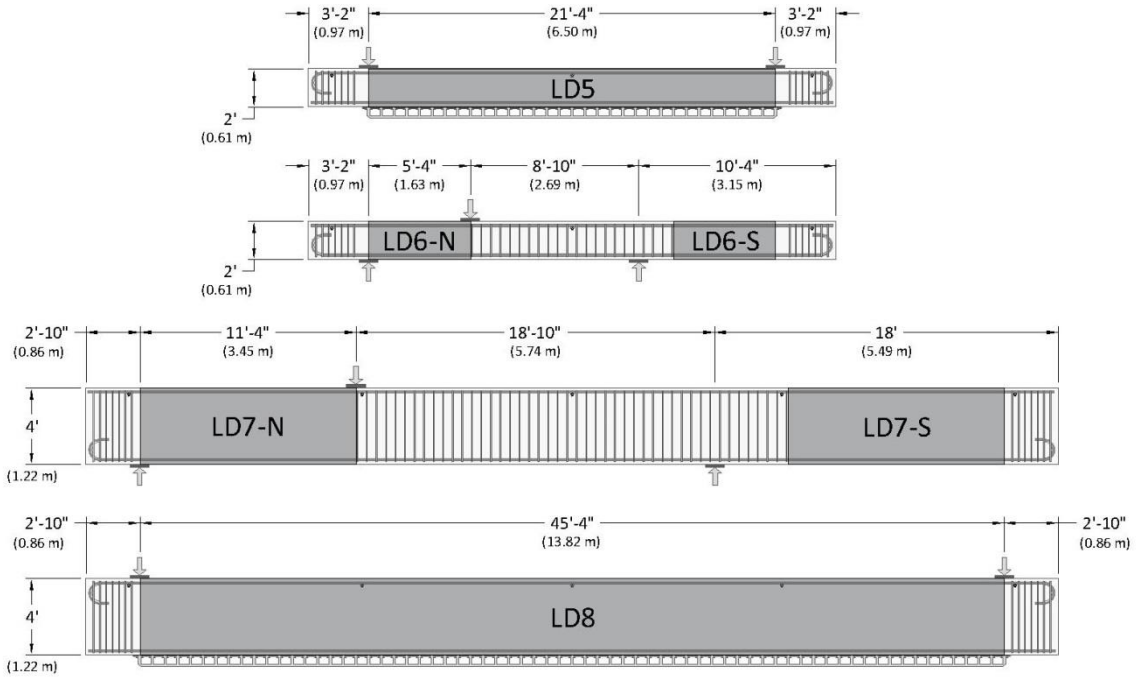

Figure 2-1: Specimen Geometry and Test Regions

The width (b_w) of each specimen was 21 in. (0.53 m), while the length was 332 in. (8.43 m) for LD5 and LD6 and 612 in. (15.54 m) for LD7 and LD8. In all specimens, flexural reinforcement consisted of No. 11 reinforcing bars, with equal amounts of reinforcement on tension and compression faces. In LD5 and LD6, 3-No. 11 reinforcing bars led to a longitudinal reinforcement ratio (ρ) of 1.05 percent, and in LD7 and LD8, 6-No. 11 reinforcing bars led to a reinforcement ratio of 0.98 percent. Concrete clear cover was 2 in. (0.05 m) on both the tension and compression sides for all specimens. The effective depth (d) was 21.3 in. (0.54 m) for LD5 and LD6, and the effective depth (d) was 45.3 in. (1.15 m) for LD7 and LD8. The end region of each beam contained 7-No. 5 stirrups spaced at 4 in. (0.10 m) on-center and 180 degree hooks to satisfy code-specified development length and to avoid anchorage failure during testing. Additionally, the middle regions of both LD6 and LD7 contained No. 5 stirrups spaced at 6 in. (0.10 m)

on-center to minimize damage outside of the test span. The specimen cross-sections are summarized in Figure 2-2.

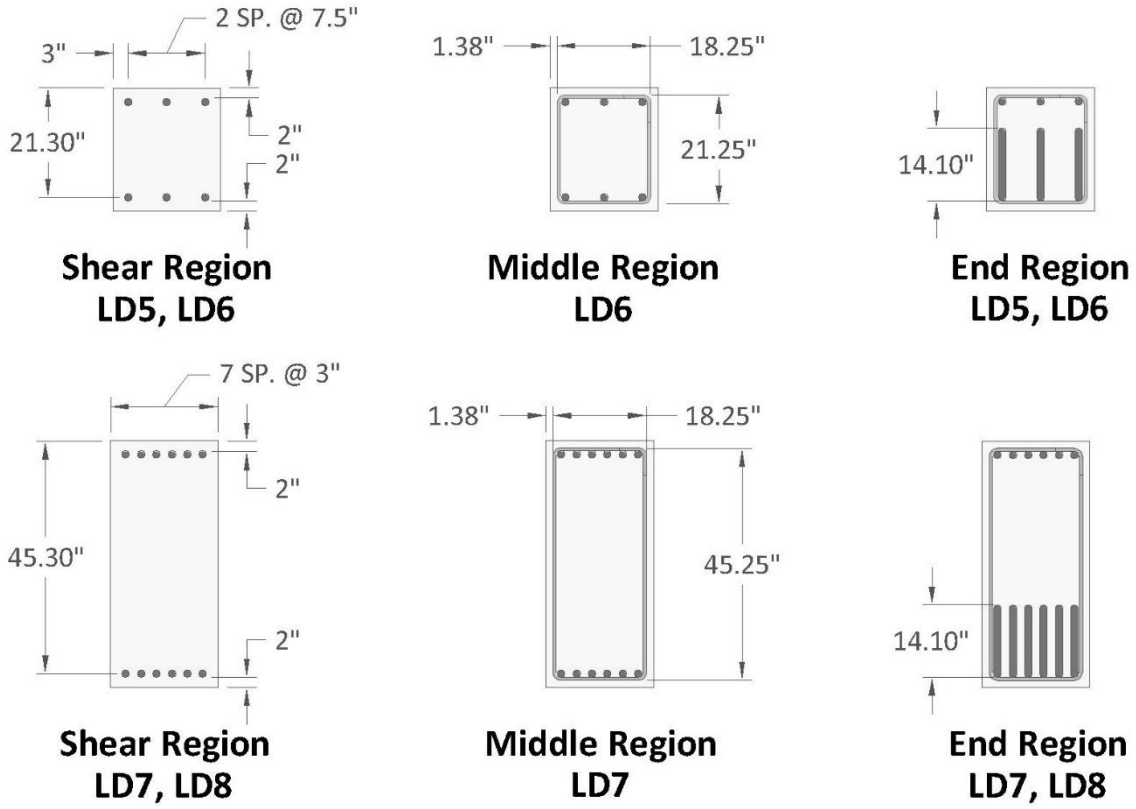

Figure 2-2: Specimen Section Cuts

2.2 MATERIAL PROPERTIES

One batch of concrete was used in the placement of each of the smaller specimens, and two batches of concrete were used in the placement of each of the larger specimens. Mixture proportions were identical for all four specimens: 28-day design strength of 4,000 psi (27.6 MPa), water to cement ratio (w/c) of 0.59, cement content of 423 lb/yd^3 (251 kg/m^3), and crushed limestone coarse aggregate with a nominal maximum size (a_g) of 1 in. (25 mm). Concrete materials testing was conducted on cylinders measuring 8 in. (203 mm) long and 4 in. (102 mm) in diameter. For each

material test conducted, a minimum of three cylinders were tested to ensure precision in the reported values. In some cases, outliers were removed as detailed in Appendix B. At 28 days, compression tests, modulus of elasticity tests, and split cylinder tensile tests were performed to obtain f'_c, E_c, and f'_t, respectively. Table 2-1 summarizes the results of this testing. At the time of structural testing, cylinder compressive strength tests were performed to determine the average compressive strength of concrete for normalization of test data presented in Section 2.5. The average compressive strength of cylinders at time of structural testing as well as the age of each specimen at time of structural testing is shown in Table 2-2. For LD7 and LD8, the -1 and -2 in Tables 2-1 and 2-2 denote batch one and two, respectively. In LD7, batches one and two were of equal volume, while in LD8, batch one was approximately 10 yd^3 and batch two was approximately 3.2 yd^3. The relative amounts of each batch are accounted for in all subsequent reported numbers and calculations using f'_c of LD8 as a whole. Batch one was placed first and therefore corresponds to the tension side of LD7 and the compression side of LD8. The difference in the compressive strengths of the first and second batches for both LD7 and LD8 can be noted in Tables 2-1 and 2-2.

Table 2-1: Concrete Average Material Properties at 28 Days

Batch Designation	f'_c psi (MPa)	E_c ksi (GPa)	f'_t psi (MPa)
LD5	5,190 (35.8)	4,093 (28.2)	520 (3.6)
LD6	4,505 (31.1)	4,343 (30.0)	470 (3.2)
LD7-1	3,333 (23.0)	4,027 (27.8)	402 (2.8)
LD7-2	3,730 (25.7)	4,017 (27.7)	453 (3.1)
LD8-1	3,843 (26.5)	4,067 (28.0)	445 (3.1)
LD8-2	4,760 (32.8)	4,313 (29.7)	483 (3.3)

Two structural tests were performed five days apart on LD7, leading to four concrete compressive strength entries in Table 2-2: two batches tested on two different days. The two structural tests on LD6 took place on the same day so only one set of cylinders was tested.

Table 2-2: Concrete Average Compressive Strength at Test Day

Batch Designation	Age days	f'_c psi (MPa)
LD5	127	4,805 (33.1)
LD6	28	4,505 (31.1)
LD7-N-1	34	3,367 (23.2)
LD7-N-2	34	3,563 (24.6)
LD7-S-1	39	3,430 (23.7)
LD7-S-2	39	3,807 (26.3)
LD8-1	31	4,167 (28.7)
LD8-2	31	4,573 (31.5)

Flexural reinforcement for all specimens was specified as ASTM A615 Gr 60 deformed carbon-steel bars. Each tensile reinforcement bar was ordered with an extra 3 ft (0.91 m) of length on the hook to serve as a tensile testing sample. Three samples from each specimen were sent to an ISO/IEC 17025 accredited laboratory for tensile testing. Measured flexural reinforcement properties are summarized in Table 2-3. All values reported meet the requirements for ASTM A615 Gr 60 deformed carbon-steel reinforcement.

Table 2-3: Flexural Reinforcement Average Properties

Specimen ID	Yield Stress ksi (MPa)	Ultimate Stress ksi (MPa)	% Elongation in 8 in. (203 mm)
LD5	71.8 (495.2)	105.0 (724.1)	19.0
LD6	74.5 (513.8)	109.7 (756.6)	16.0
LD7	64.8 (446.9)	95.7 (660.0)	21.3
LD8	64.8 (446.9)	96.2 (663.4)	20.7

2.3 CONCENTRATED LOAD TEST SETUP

Besides specimen geometry, one of the most important parameters in directly comparing any concentrated and uniform load test is shear span-to-depth ratio (a/d). In a concentrated load test, the shear span is often thought of as the smallest distance between a load and a support. Using that definition, the shear span (a) in these concentrated load tests is approximately 3d, giving a shear span-to-depth ratio (a/d) of 3.01 for LD6, and a shear span-to-depth ratio (a/d) of 3.00 for LD7. The simplicity of this definition is lost when considering a uniform load, in which the load is applied over the entire member length. The implication is that for a uniform load, the shear span is zero, which cannot be. To provide a logical definition, Kani (1966) defines the shear span as the ratio between maximum bending moment and maximum shear force, which would have units of length. Using Kani's definition, concentrated load tests once again have a shear span equal to the shortest distance between a load and a support. Figure 2-3 depicts the derivation of this relationship.

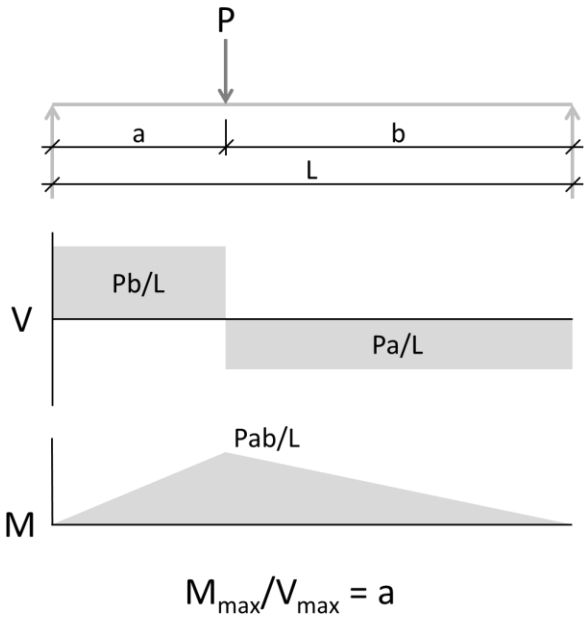

Figure 2-3: Relationship between Maximum Bending Moment and Maximum Shear Force for a Concentrated Load

Concentrated load was applied via a hydraulic ram attached to a loading frame that was connected to the laboratory strong floor. Force was measured using three load cells: two under the roller support and one under the tilt (pin) support. Steel bearing plates measuring 2 in. x 21 in. x 12 in. (51 mm x 533 mm x 305 mm) were used both at the supports and under the load, except for in testing of LD7-N, where a plate measuring 2 in. x 22 in. x 22 in. (51 mm x 559 mm x 559 mm) was used underneath the load. Figure 2-4 shows a schematic of the concentrated load test setup as well as photographs from LD6 and LD7. Self-weight was measured before structural testing and is included in the normalized results presented in Section 2.5. For all concentrated load tests, load was applied in 10 kip (44.5 kN) increments to track the progress of flexural cracking. LD6-N and LD6-S were both loaded incrementally to 80 kips (355.8 kN), LD7-N was loaded

incrementally to 90 kips (400.3 kN), and LD7-S was loaded incrementally to 60 kips (266.9 kN) prior to continuously loading to failure.

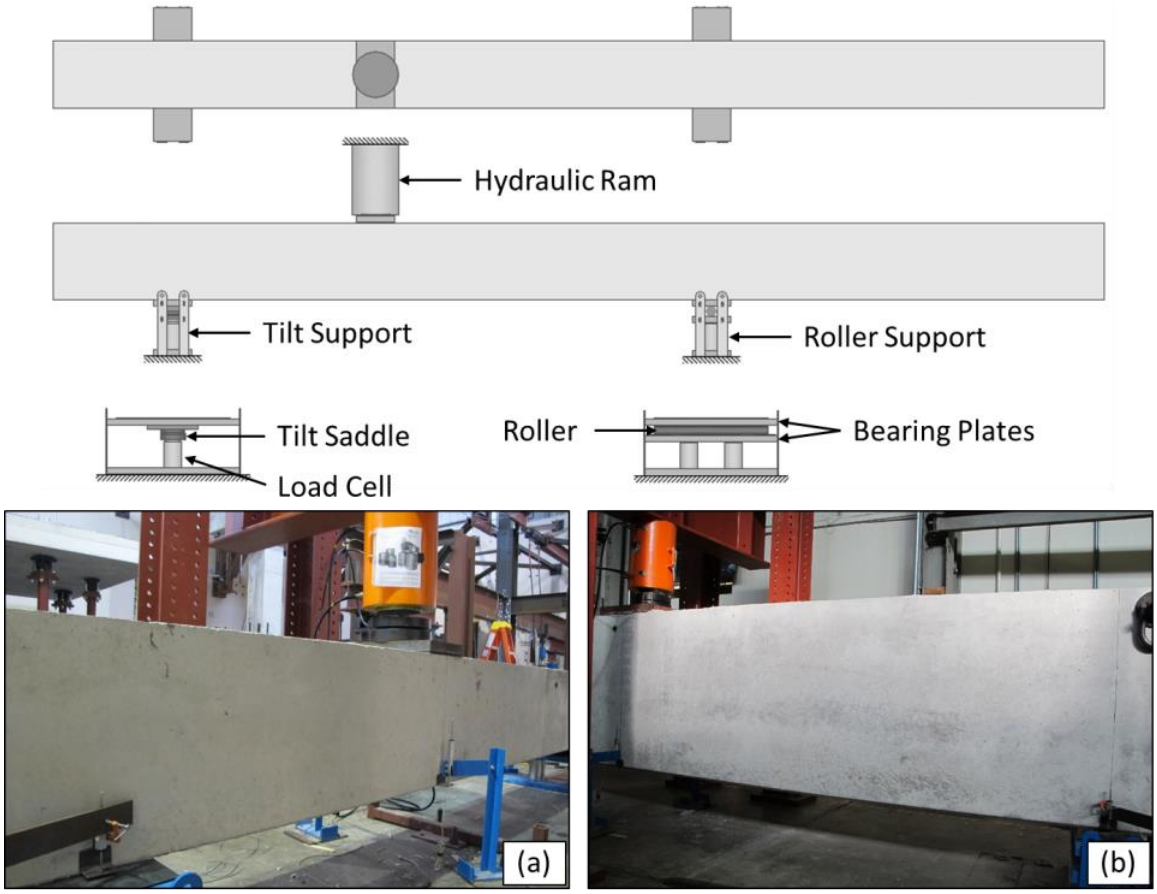

Figure 2-4: Concentrated Load Setup (top); LD6 Test Region Shown in (a), LD7 Test Region Shown in (b)

Displacements were measured using six linear potentiometers: two placed on either side of each support, and two placed on either side of the load point. The actual deflection at the load point was calculated using the average of all of the measured displacements according to the procedure detailed in Figure 2-5.

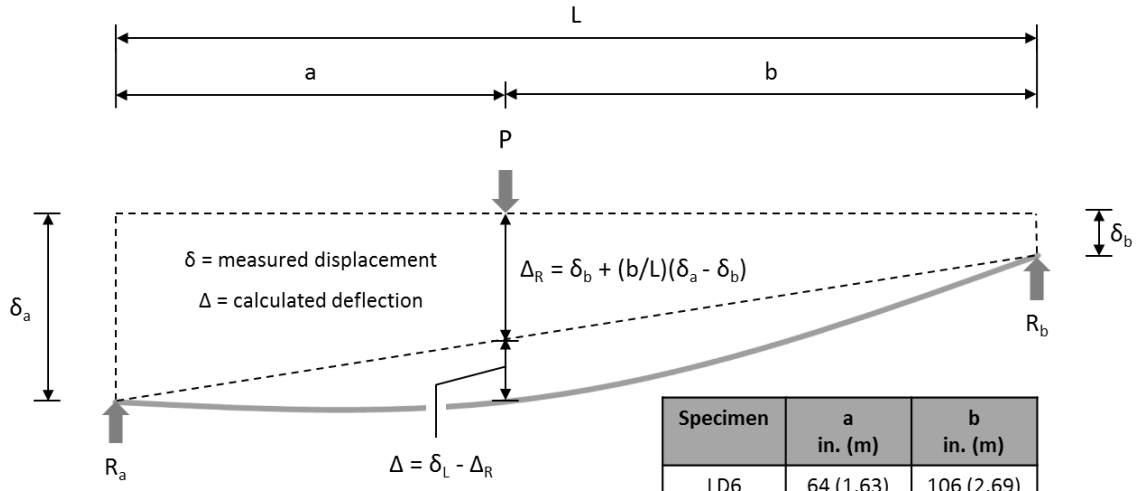

Specimen	a in. (m)	b in. (m)
LD6	64 (1.63)	106 (2.69)
LD7	136 (3.45)	226 (5.74)

Figure 2-5: Calculation of Deflection under the Load Point

2.4 UNIFORM LOAD TEST SETUP

The goal of the uniform load setup was to duplicate the shear span-to-depth ratio of the concentrated load setup to be able to compare directly the different loading configurations. Once again, Kani's (1966) definition of the shear span as the ratio between maximum moment and maximum shear was used, giving a shear span-to-depth ratio (a/d) of 3.01 for LD5, and a shear span-to-depth ratio (a/d) of 3.00 for LD8. These values are identical to their concentrated load counterparts. Figure 2-6 depicts the derivation of shear span for uniform loading.

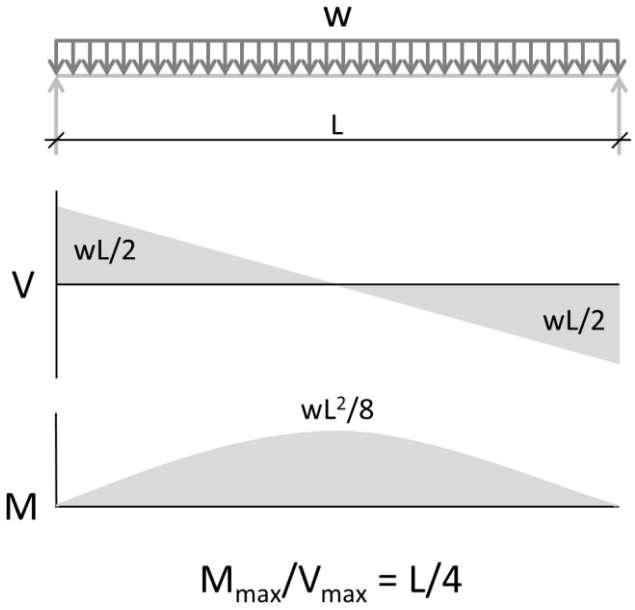

Figure 2-6: Relationship between Maximum Bending Moment and Maximum Shear Force for a Uniform Load

Uniform load was applied to the soffits of LD5 and LD8 using a Kevlar-reinforced air bladder placed across the entire test region and beam width. Force was measured using four load cells: two on top of the roller support and two on top of the pin support. Load was applied by pressurizing the air bladder and reacting against supports on top of the beam at each end. Steel bearing plates measuring 2 in. x 21 in. x 12 in. (51 mm x 533 mm x 305 mm) were used at the supports. Figure 2-7 shows a schematic of the uniform load test setup as well as photographs from LD5 and LD8. Self-weight was measured after structural testing and is included in the normalized results presented in Section 2.5. For LD5, load was applied in 10 kip (44.5 kN) increments to track the progress of flexural cracking, whereas in LD8, load was applied in 15 kip (44.5 kN) increments. LD5 was loaded incrementally to 60 kips (266.9 kN) and LD8 was loaded incrementally to 105 kips (467.0 kN) prior to continuously loading to failure.

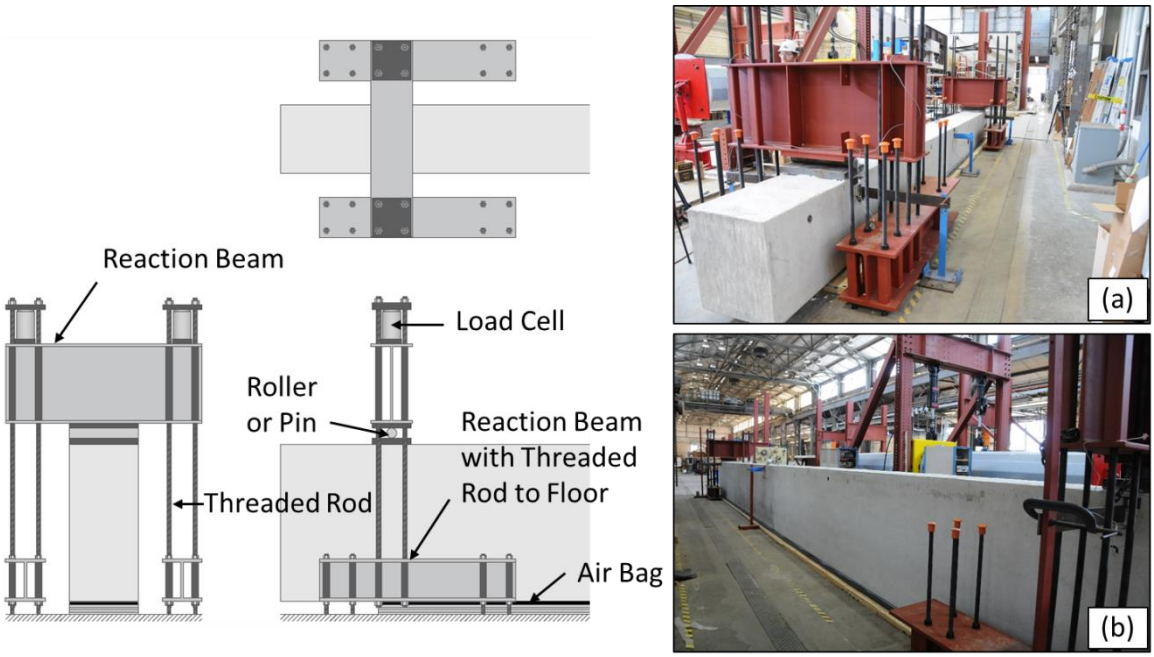

Figure 2-7: Uniform Load Setup (left); LD5 Shown in (a), LD8 Shown in (b)

Displacements were measured using six linear potentiometers: two placed on either side of each support, and two placed on either side of the midpoint, which is the theoretical location of maximum deflection. The actual deflection at the midpoint was calculated using the average of all of the measured displacements and the procedure detailed in Figure 2-5. Since (a) and (b) are equal for the uniform load tests, the calculated midpoint deflection becomes the average of the measured support displacements subtracted from the measured midpoint displacement.

2.5 TEST RESULTS

The failure criterion, as established by ACI 318-14, was the load at which each specimen exhibited first significant diagonal cracking. This load also happened to correspond with the ultimate load carried for every test in this study. A summary of the maximum shear force at various locations is shown in Table 2-4. The subscripts in Table

2-4 represent the sections at which shear force was calculated or measured: (ns) indicates the centerline of the support nearest to the failure location, (d) indicates a distance (d) away from the edge of the near support, (dv) indicates a distance (d_v) away from the edge of the near support (Note: d_v = 0.9d), and (xr) indicates the location where the critical shear crack crossed midheight of the specimen. For the concentrated load tests, LD6 and LD7, the shear force values differ only due to the self-weight of the specimens. The tabulated values are not normalized, but self-weights of both the specimen and of the loading apparatus are included.

Table 2-4: Maximum Shear Force at Various Sections

Test ID	V_{ns} kips (kN)	V_d kips (kN)	V_{dv} kips (kN)	V_{xr} kips (kN)
LD5	59.5 (264.8)	47.9 (212.9)	48.9 (217.5)	50.2 (223.2)
LD6-N	64.1 (285.0)	62.8 (279.4)	62.9 (279.8)	62.5 (278.0)
LD6-S	58.0 (258.0)	56.7 (252.4)	56.8 (252.8)	56.3 (250.3)
LD7-N	87.1 (387.4)	82.5 (367.2)	83.0 (369.0)	78.5 (349.4)
LD7-S	74.3 (330.6)	69.8 (310.4)	70.2 (312.2)	66.4 (295.2)
LD8	94.3 (419.2)	76.5 (340.5)	78.1 (347.4)	71.5 (317.9)

The sections presented in Table 2-4 were chosen because of what they represent: V_{ns} is the measured maximum shear force, V_d and V_{dv} are the calculated shear forces at the critical sections defined by ACI 318-14 and AASHTO LRFD 2014, respectively, and V_{xr} is the calculated shear force at the actual critical section. Figure 2-8 visually depicts

the sections described above for each test as well as shows the failure crack. The calculations performed to obtain shear forces at various distances from the support used the shear at the support (V_{ns}), the self-weight (w_b), and in the case of uniform load tests, the applied uniform load (w_a).

Though useful, the values in Table 2-4 cannot be directly compared to one another; normalization is required to gain an accurate picture of how each test compares to the others in the test program. The normalization scheme selected was that of normalized shear stress, in which shear force is divided by the square root of concrete compressive strength (f'_c), specimen width (b_w), and effective specimen depth (d in the case of v_d and $v_{xr,d}$ and d_v in the case of v_{dv} and $v_{xr,dv}$), as shown in Equations 2-1 and 2-2. This method allows for easy comparison with both ACI 318-14 Design Equation 22.5.5.1 and AASHTO LRFD 2014 Equation 5.8.3.3-3, which will be discussed in Chapter 3. Table 2-5 shows the normalized shear stress at failure for each test. Only sections at (d), (d_v), and (x_r) are presented in Table 2-5 because these sections are most easily compared both between tests and to code equations from ACI 318-14 and AASHTO LRFD 2014.

$$v = \frac{V}{b_w d \sqrt{f'_c}} \qquad \textit{Equation 2-1}$$

$$v = \frac{V}{b_w d_v \sqrt{f'_c}} \qquad \textit{Equation 2-2}$$

Table 2-5: Normalized Shear Stress and Maximum Deflection at Failure

Test ID	v_d √psi (√MPa)	$v_{xr,d}$ √psi (√MPa)	v_{dv} √psi (√MPa)	$v_{xr,dv}$ √psi (√MPa)	Deflection in. (mm)
LD5	1.54 (0.128)	1.62 (0.134)	1.75 (0.146)	1.80 (0.149)	0.78 (19.8)
LD6-N	2.09 (0.174)	2.08 (0.173)	2.33 (0.193)	2.31 (0.192)	0.26 (6.5)
LD6-S	1.89 (0.157)	1.88 (0.156)	2.10 (0.175)	2.08 (0.173)	0.22 (5.7)
LD7-N	1.47 (0.122)	1.40 (0.116)	1.65 (0.137)	1.56 (0.129)	0.32 (8.1)
LD7-S	1.22 (0.101)	1.16 (0.096)	1.36 (0.113)	1.29 (0.107)	0.26 (6.7)
LD8	1.23 (0.102)	1.15 (0.096)	1.40 (0.116)	1.28 (0.106)	1.12 (28.6)

Several observations can be made from Figure 2-8. First, the actual failure section (x_r) occurred further from the support than (d) or (d_v) away in every case except LD5. The further from the support a section is, the less the shear stress is at that section. In the case of every test except LD5, the location of the failure section equated to less shear stress at that section than at the location of the design sections of ACI 318-14 and AASHTO LRFD 2014. In terms of design, the implication is that designing for a failure section closer to the support than the actual failure section is conservative because a higher shear stress is being designed for. The second observation that can be made is that the approximate failure section methods of ACI 318-14 and AASHTO LRFD 2014 were closer approximations for the specimens with smaller overall height. Specimens of height 2 ft (0.61 m) had a failure section ranging from (0.8d to 1.5d) from the edge of the support, whereas specimens of height 4 ft (1.22 m) had a failure section ranging from (1.3d to 2.0d) away from the edge of the support.

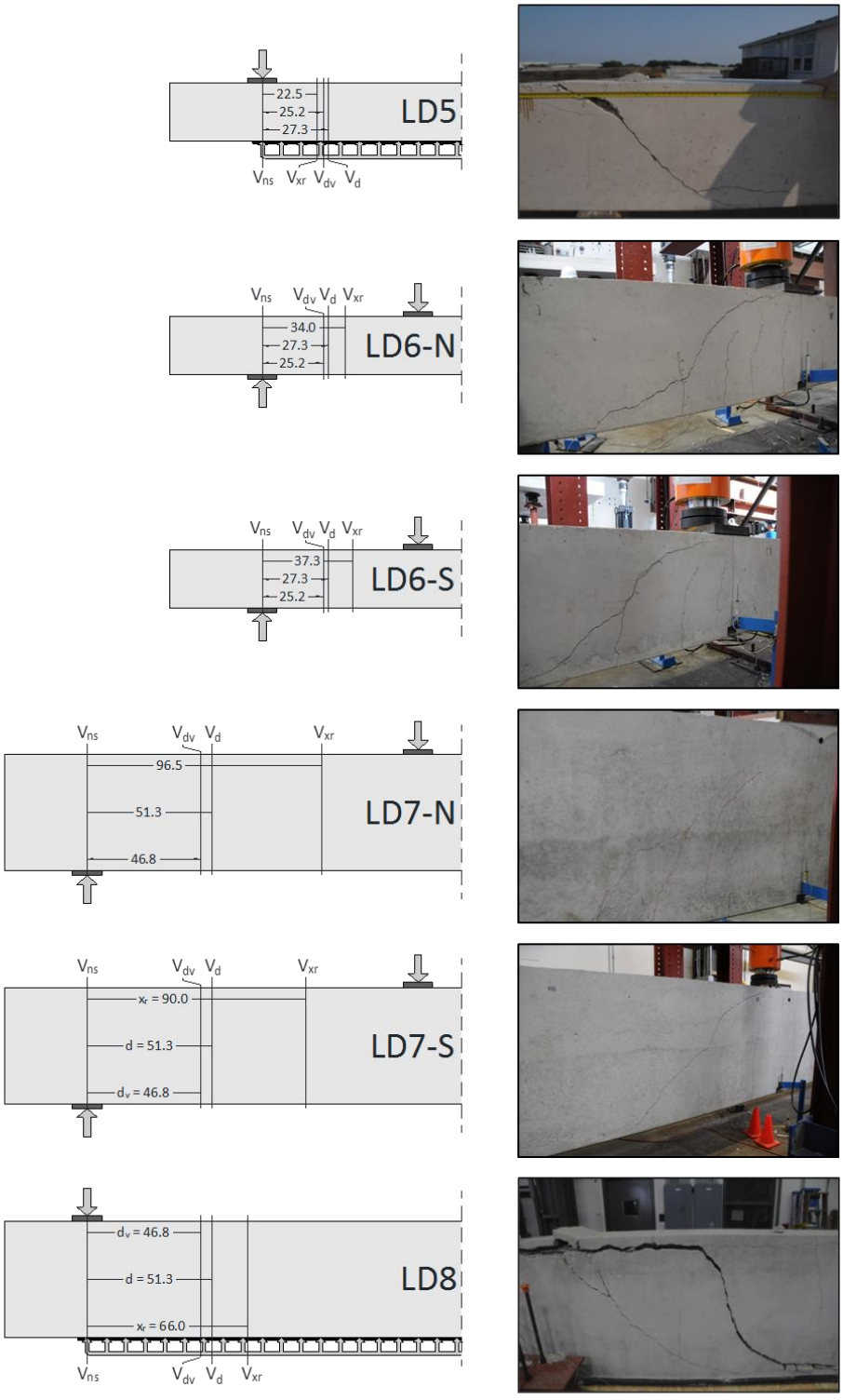

Figure 2-8: Shear Force Sections and Failure Crack Photo for Each Specimen

For uniform load tests, the observed failure section was much closer to the code approximations than those of concentrated load tests. This observation is significant in that shear stress varies much more under uniform loading as the section being considered moves along the length of the specimen. Though Figures 2-3 and 2-6 do not include self-weight, it can easily be seen that in a concentrated load test, the only change in shear stress along the length is due to the self-weight, as opposed to a uniform load test, where the change is due to the applied load and the self-weight.

A reasonable approximation for failure section becomes much more critical for a specimen subjected to uniform loading. The location of (x_r) was 23 percent less than (d) for LD5 and 32 percent greater for LD8. This difference between (x_r) and (d) leads to a change in the normalized shear stress by a 5 percent increase for LD5 and a 7 percent decrease for LD8, when comparing (v_{xr}) to (v_d). By contrast, if a similar comparison is made for concentrated load tests (LD6 and LD7), the range of difference between locations at (x_r) and (d) was 31 percent to 100 percent, leading to a range of difference in normalized shear stress at (x_r) and (d) of -5 percent to -1 percent. Though the actual failure sections were far less accurately estimated using (d) for concentrated load tests, the normalized shear stress showed less variance between sections than in uniform load tests.

The next observation that can be made is that the shear failure of LD8 consisted of two diagonal cracks, each formed nearly simultaneously upon failure as confirmed by video evidence. The value of (x_r) presented above is that of the crack closer to the support. This crack was chosen because it formed first (< 0.25 sec before the second crack), which is consistent with failure as defined by ACI 318-14. If the crack further from the edge of the support were to be considered the failure crack, the value of (x_r) for LD8 would become 93 in. (2.36 m). Thus, the failure crack is further from the

approximation of (d) away from the edge of the support, yet nearer to the failure crack locations seen in LD7 under concentrated loading. The shear force and normalized shear stress at the crack further from the support are 62.1 kips (276.4 kN) and 1.00 √psi (0.083 √MPa), respectively. Additionally, crack widths after unloading were visually greater for specimens subjected to uniform loading (LD5 and LD8).

Figures 2-9 through 2-12 depict the normalized shear stress, at a section (x_r) away from the edge of the support, versus maximum deflection (calculated as described previously) for specimens LD5 through LD8, respectively. The section at (x_r) was chosen to compare directly the failure stresses at the observed failure section between each test. The normalized shear stress at the approximate failure sections of (d) and (d_v) is more closely examined in Chapter 3. Specimens were plotted separately due to the wide variation in measured deflections. Theoretical deflections are a function of loading (P or w), modulus of elasticity (E), moment of inertia (I), and length (L). For each specimen, due to the differences in loading, depth, and concrete material properties, all four of these variables differed. Specific values of normalized shear stress and maximum deflection at failure can be found in Table 2-5.

Several important comparisons can be made using Figures 2-9 through 2-12 and Table 2-5. The proceeding discussion uses normalized shear stress at the failure section (x_r), and the values of percent increase and average increase were calculated according to Equations 2-3 and 2-4. In every case, tests with a height of 2 ft (0.61 m) had a greater normalized shear stress at failure than tests with a height of 4 ft (1.22 m), resulting in a range of increase in normalized shear stress of 31 percent to 68 percent and an average increase of 50 percent. If loading type is kept constant, LD5, the specimen of height 2 ft subjected to uniform loading, exhibited an increase in normalized shear stress of 41 percent over that of LD8, the specimen of height 4 ft subjected to uniform loading.

Specimens of height 2 ft and subjected to concentrated loading saw increases in normalized shear stress of 46 percent and 63 percent over their 4 ft counterparts. Overall, specimens subjected to concentrated loading had a greater normalized shear stress at failure than specimens subjected to uniform loading, resulting in a range of increase in normalized shear stress of -16 percent to 50 percent and an average increase of 18 percent. The same statement can be made when examining specimens with identical heights. Tests of the specimens with 2 ft height subjected to concentrated loading had a greater normalized shear stress at failure than the test of the specimen with 2 ft height subjected to uniform loading, resulting in percent increases in normalized shear stress of 16 percent and 29 percent. Tests of the specimen with height of 4 ft subjected to concentrated loading had a greater normalized shear stress at failure than the specimen of height 4 ft subjected to uniform loading, resulting in percent increases in normalized shear stress of 1 percent and 22 percent. In summary, the specimens with greater height exhibited decreased shear stress capacities relative to the shallower specimens, and uniform load tests exhibited decreased shear stress capacities relative to the concentrated load tests, with the difference due to load distribution decreased as height increased.

$$\boldsymbol{Percent\ increase} = \frac{v_{1,i} - v_{2,avg}}{v_{2,avg}} * 100 \qquad \textit{Equation 2-3}$$

$$\boldsymbol{Average\ increase} = \frac{v_{1,avg} - v_{2,avg}}{v_{2,avg}} * 100 \qquad \textit{Equation 2-4}$$

where:

Subscript 1 indicates the parameter with the greater average

Subscript i indicates an individual specimen within subset 1

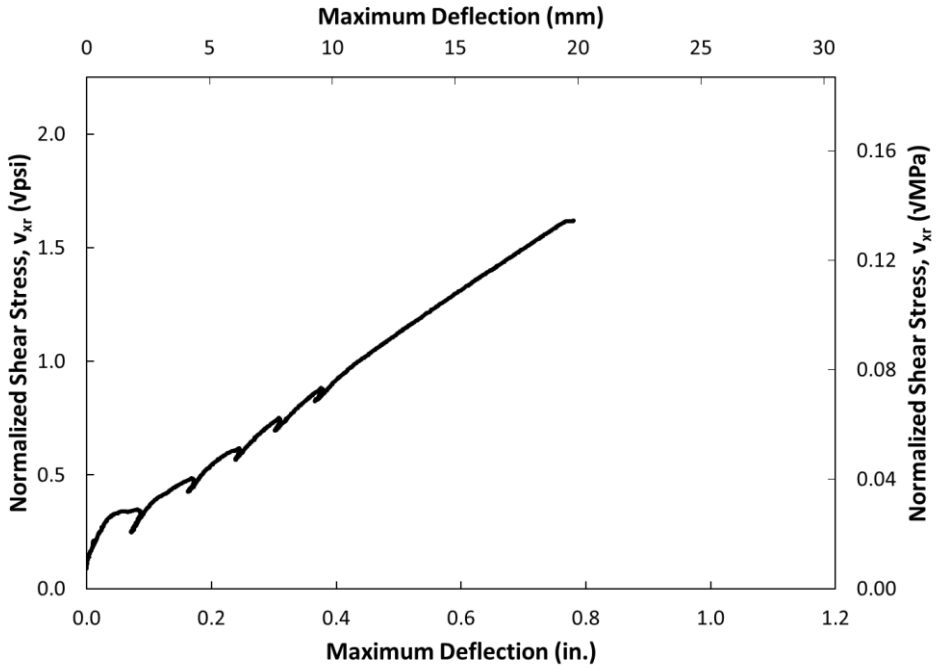

Figure 2-9: Stress versus Deflection for LD5 (h = 24 in.; Uniform Loading)

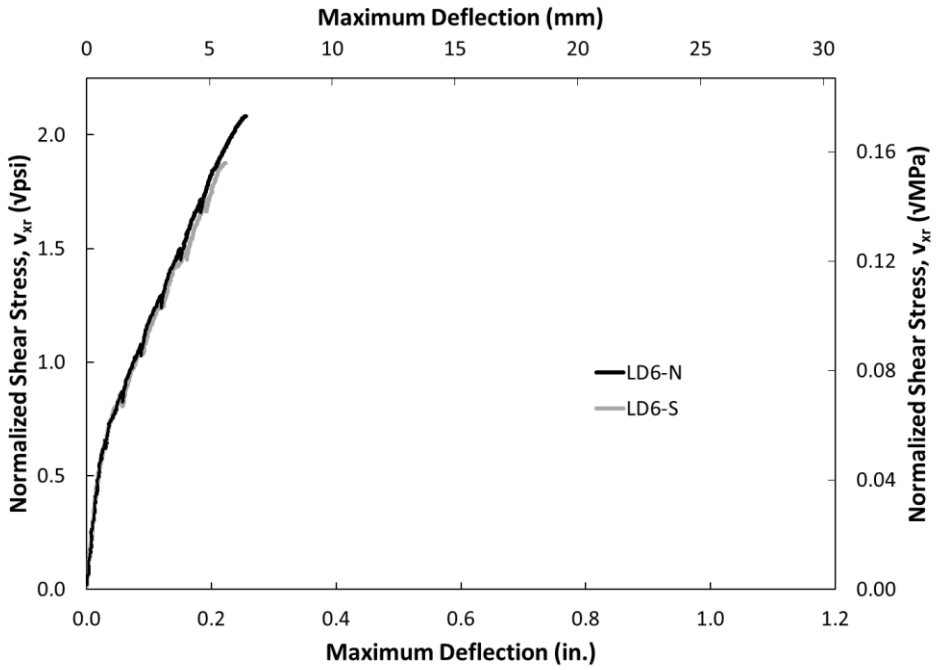

Figure 2-10: Stress versus Deflection for LD6 (h = 24 in.; Concentrated Loading)

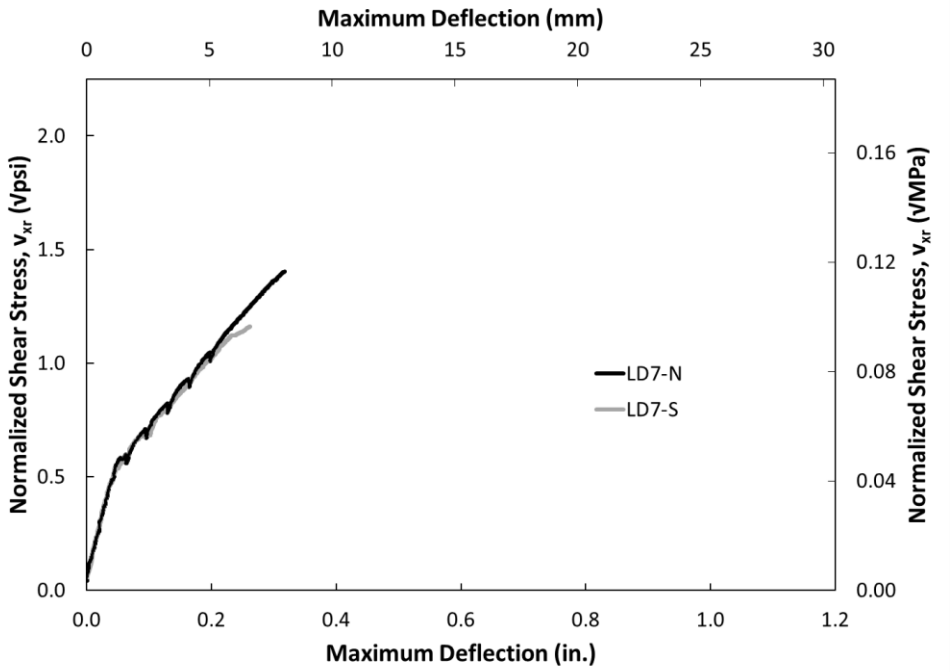

Figure 2-11: Stress versus Deflection for LD7 (h = 48 in.; Concentrated Loading)

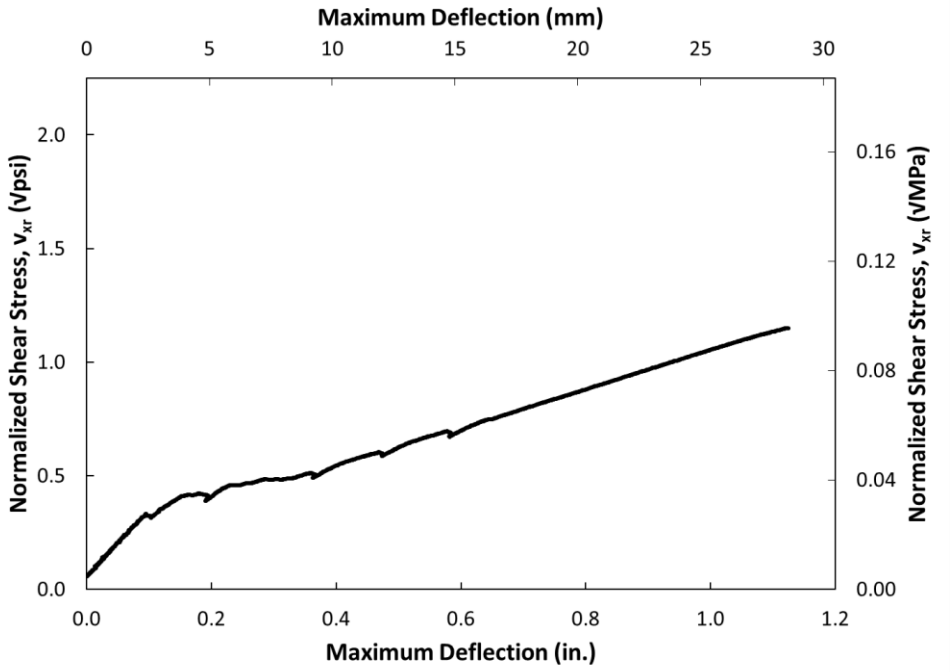

Figure 2-12: Stress versus Deflection for LD8 (h = 48 in.; Uniform Loading)

Chapter 3: Analytical Procedure

3.1 OVERVIEW

Three code equations were used to compare with tests results: two from ACI 318-14 and one from AASHTO LRFD 2014. Each method is a sectional design method, in which a critical section is defined, and the nominal strength of that section is calculated. Sectional design methods are thought to be most appropriate for slender members, or members in which the shear span-to-depth ratio is greater than approximately 2.5 (MacGregor and Wight, 2012). Methods such as strut-and-tie are more appropriate for deep members, which will not be discussed here.

All three of these equations are based upon the assumption that the contributions of concrete and steel to the shear strength of reinforced concrete members can be calculated separately and summed for total shear strength. Separate calculation implies that concrete provides similar shear resistance regardless of the presence or absence of shear reinforcement. Due to strict minimum shear reinforcement requirements, beams often contain stirrups. In contrast, slabs, footings, culverts and other members subjected to one-way shear are permitted to carry twice the factored shear stress as beams before requiring shear reinforcement. On the surface, this assumption appears reasonable: different members behave uniquely and should therefore be treated individually. The individual treatment of different members may not be accurate; testing by Sherwood et al. (2006) showed that member width has little effect on shear stress at failure for one-way members. Width is often the parameter used to differentiate between beam members and other one-way shear members such as slabs, footings, and culverts. Based on findings published by Sherwood et al. (2006), the research presented here is applicable to any member subjected to one-way shear.

3.2 ACI 318-14 EQUATION 22.5.5.1

ACI 318-14 Equation 22.5.5.1 is the most common method of providing a lower-bound estimate of one-way shear strength in practice. This equation was empirically formulated as a conservative simplification of the equations given in ACI 318-14 Table 22.5.5.1, as discussed in Section 3.3. It is a function of only three variables: concrete compressive strength (f'_c), web width (b_w), and effective specimen depth (d). The term λ is used as a modification factor for lightweight concrete in ACI 218-14. It is not shown because all concrete in this investigation was normal weight, making this factor equal to 1. Variables not considered in this equation include load distribution and overall member size, both of which are the focus of this investigation. The section at which this equation applies is located (d) away (or further) from the edge of the support and subject to the limitations of Sections 7.4.3.2 and 9.4.3.2 of ACI 318-14. ACI 318-14 Equation 22.5.5.1 is reproduced as Equation 3-1 below. For all ACI 318-14 calculations, f'_c is in units of psi.

$$V_c = 2\sqrt{f'_c}\, b_w d \qquad \textit{Equation 3-1}$$

3.3 ACI 318-14 TABLE 22.5.5.1

ACI 318-14 Table 22.5.5.1 presents three different equations and the minimum of these is to be taken as the nominal shear strength provided by concrete in a member, V_c. Like ACI 318-14 Equation 22.5.5.1, Table 22.5.5.1 is empirically derived from over 400 tests on beams without shear reinforcement, as presented in joint ASCE-ACI Committee 326 Report on Shear and Torsion (1962). It is a function of five variables: concrete compressive strength (f'_c), web width (b_w), effective specimen depth (d), longitudinal reinforcement ratio (ρ_w), and the ratio of factored shear demand multiplied by effective

depth to factored moment demand at a particular section ($V_u d/M_u$). This ratio indirectly includes the effects of load distribution; however, overall member size is not considered in this formulation. Like ACI 318-14 Equation 22.5.5.1, the section at which these equations apply is that of (d) away (or further) from the edge of the support subject to the limitations of Section 7.4.3.2 of ACI 318-14. ACI 318-14 Table 22.5.5.1 is reproduced as Table 3-1 below.

Table 3-1: ACI 318-14 Table 22.5.5.1

V_c = Least of (a), (b), and (c):	
(a)	$\left(1.9\sqrt{f_c'} + 2500\rho_w \frac{V_u d}{M_u}\right) b_w d$
(b)	$\left(1.9\sqrt{f_c'} + 2500\rho_w\right) b_w d$
(c)	$3.5\sqrt{f_c'} b_w d$

3.4 AASHTO LRFD 2014 SECTIONS 5.8.3.3 AND 5.8.3.4

The shear strength design procedure detailed in AASHTO LFRD 2014 is derived from the Modified Compression Field Theory (MCFT) presented by Vecchio and Collins (1986), based upon ultimate capacity, not first significant diagonal cracking as in ACI 318-14. The original implementation of MCFT into AASHTO LRFD was an iterative procedure, involving the use of design tables for several parameters. In 2008, these procedures were revised based on work done by Bentz et al. (2006), no longer requiring iteration and replacing design tables with algebraic equations. Section C5.8.3.4.2 of AASHTO LRFD 2014 notes that the equations provided are identical in function to those provided in the Canadian design code (CSA). The set of equations provided in AASHTO LRFD 2014 is a function of numerous variables; unlike ACI 318-14, AASHTO LRFD

2014 provides one set of shear equations that is also applicable to members subjected to axial force, prestressing forces, or both. For simplicity, the equations presented below do not include terms involving axial force or prestressing. Also unlike ACI 318-14, the AASHTO LRFD 2014 shear design procedure includes the effects of both load distribution in the equation for net longitudinal tensile steel strain (ε_s), and overall member size in the equation for the crack spacing parameter (s_{xe}). The section at which this procedure applies is that of (d_v) away (or further) from the edge of the support, where (d_v) = 0.9(d). AASHTO LRFD 2014 Equations 5.8.3.3-3, 5.8.3.4.2-2, 5.8.3.4.2-4, and 5.8.3.4.2-5 are presented below as Equations 3-2 through 3-5. For all AASHTO LRFD 2014 calculations, f'$_c$ is in units of ksi.

$$V_c = 0.0316\beta\sqrt{f'_c}\,b_v d_v \qquad \textit{Equation 3-2}$$

$$\beta = \frac{4.8}{(1+750\varepsilon_s)}\,\frac{51}{(39+s_{xe})} \qquad \textit{Equation 3-3}$$

$$\varepsilon_s = \frac{\left(\frac{|M_u|}{d_v} + |V_u|\right)}{E_s A_s} \qquad \textit{Equation 3-4}$$

$$s_{xe} = s_x \frac{1.38}{a_g+0.63} \qquad \textit{Equation 3-5}$$

where:

A_s = area of tensile longitudinal steel (in.^{2})

a_g = maximum aggregate size (in.)

b_v = effective web width (in.)

d_v = effective shear depth (in.)

E_s = modulus of elasticity of steel (ksi)

M_u	=	moment at section d_v (kip-in.)
s_x	=	the lesser of either d_v or the maximum distance between longitudinal crack control reinforcement (in.)
s_{xe}	=	crack spacing parameter, 12.0 in. $\leq s_{xe} \leq$ 80.0 in.
V_u	=	shear force at section d_v (kip)
β	=	factor indicating ability of diagonally cracked concrete to transmit tension and shear
ε_s	=	net longitudinal tensile steel strain at section d_v

3.5 COMPARISON OF ANALYTICAL AND EXPERIMENTAL RESULTS

Tables 3-2 through 3-4 show the design shear stress lower-bound estimates obtained for ACI 318-14 Equation 22.5.5.1, ACI 318-14 Table 22.5.5.1, and AASHTO LRFD 2014 Sections 5.8.3.3 and 5.8.3.4, respectively, versus the experimental results. Self-weight was considered in calculating applied shear force for all specimens. Note, in normalization for AASHTO LRFD 2014, the coefficient of 0.0316 in Equation 3-2 is approximately equal to $1/\sqrt{1000}$, making the $\sqrt{f'_c}$ term in units of $\sqrt{ksi}$ equivalent to that of $\sqrt{f'_c}$ in units of $\sqrt{psi}$. As such, the normalized shear stress is equivalent to the value of β given by Equation 3-3 when units of $\sqrt{psi}$ are used. The magnitudes of the estimations provided by AASHTO LRFD 2014 are much greater than those of ACI 318-14 procedures. The magnitude differences are due to the AASHTO LRFD 2014 use of (d_v) instead of (d), both as the failure section and in normalization, causing an increase in the magnitude of the design shear strength.

Table 3-2: Comparison of Test Results to ACI Equation 22.5.5.1

Test ID	Test Result, v_d √psi	Equation 22.5.5.1, v_d √psi	Test Result/Equation 22.5.5.1
LD5	1.54	2.00	0.77
LD6-N	2.09	2.00	1.05
LD6-S	1.89	2.00	0.95
LD7-N	1.47	2.00	0.74
LD7-S	1.22	2.00	0.61
LD8	1.23	2.00	0.62

Table 3-3: Comparison of Test Results to ACI Table 22.5.5.1

Test ID	Test Result, v_d √psi	Table 22.5.5.1, v_d √psi	Test Result/Table 22.5.5.1
LD5	1.54	2.16	0.72
LD6-N	2.09	2.21	0.95
LD6-S	1.89	2.21	0.86
LD7-N	1.47	2.26	0.65
LD7-S	1.22	2.25	0.54
LD8	1.23	2.20	0.56

Table 3-4: Comparison of Test Results to AASHTO LRFD 2014 Sections 5.8.3.3 and 5.8.3.4

Test ID	Test Result, v_{dv} √psi	AASHTO LRFD 2014, v_{dv} √psi	Test Result/AASHTO LRFD 2014
LD5	1.75	2.34	0.75
LD6-N	2.33	2.42	0.96
LD6-S	2.10	2.42	0.87
LD7-N	1.65	2.06	0.80
LD7-S	1.36	2.04	0.67
LD8	1.40	1.97	0.71

In every case but the ACI 318-14 Equation 22.5.5.1 calculation for LD6-N, the codes overestimated shear strength, meaning that the test result was less than the nominal design capacity. Of the three code procedures, ACI 318-14 Table 22.5.5.1 provided the least accurate and least safe estimation for every test. Also important to note is the fact that both ACI 318-14 Table 22.5.5.1 and AASHTO LRFD 2014 Sections 5.8.3.3 and 5.8.3.4 predict a higher normalized shear stress at failure for specimens subjected to concentrated load, despite the conclusion of existing technical literature that uniformly loaded specimens should exhibit higher shear strength.

Table 3-5 summarizes how each code procedure performed for the primary variables investigated in this testing program: size and load distribution. When averaging all tests together, AASHTO LRFD 2014 and ACI 318-14 Equation 22.5.5.1 were equally conservative. Once again, ACI 318-14 Table 22.5.5.1 provided the least conservative results for each category. Surprisingly, this included the categories involving load distribution, which is considered in ACI 318-14 Table 22.5.5.1 but not included in Equation 22.5.5.1. Subsequent comparisons will involve ACI 318-14 Equation 22.5.5.1 and AASHTO LRFD 2014 only.

Table 3-5: Performance of Code Estimates for Specific Variables

	Average Value of (Test Result, v_d or v_{dv})/(Code Procedure, v_d or v_{dv})		
Test Type	**ACI 318-14 Equation 22.5.5.1**	**ACI 318-14 Table 22.5.5.1**	**AASHTO LRFD 2014**
All Tests (n = 6)	0.79	0.71	0.79
24" Height (n = 3)	0.92	0.84	0.86
48" Height (n = 3)	0.65	0.58	0.73
Uniform Load (n = 2)	0.69	0.64	0.73
Concentrated Load (n = 4)	0.83	0.75	0.82

Though shear strength estimated per ACI 318-14 Equation 22.5.5.1 was somewhat better than AASHTO LRFD 2014 for specimens of height 24 in. (0.61 m), the opposite is true for 48 in. specimens. The performance of AASHTO LFRD 2014 at greater effective depths (d) is not surprising as it is the only procedure of the three that includes size effect. Conversely, when using ACI 318-14 the ratio of tested strength to design strength for members subjected to concentrated loads is marginally greater than when using AASHTO LRFD 2014, with the difference slightly more in favor of AASHTO for the strength of specimens subjected to uniform loading. Overall, the specimen height had a much more significant effect than load distribution. For every specimen of height 24 in. (0.61 m), ACI 318-14 Equation 22.5.5.1 was the least unconservative, and for every specimen of height 48 in. (1.22 m), AASHTO LRFD 2014 was the least unconservative; a similar statement cannot be made for load distribution.

Chapter 4: Directly Comparable Concentrated and Uniform Load Datasets

4.1 OVERVIEW

To provide context for the six tests performed as part of this investigation, the results were compared with test results from other experimental investigations. As ACI 318-14 Equation 22.5.5.1 is the most commonly used shear design procedure in the U.S., all comparisons were made in terms of that equation. The ACI-DAfStb Database of Shear Tests on Slender Reinforced Concrete Beams without Stirrups (Reineck et al. 2013) provides guidance on the scope of testing performed in the past, with an unfiltered total of over 1,000 shear tests. The database criterion for slenderness is any member with a shear span-to-depth (a/d) ratio no less than 2.4.

As useful as the shear database is for examining the scope of shear research performed, it cannot be directly used to assess the efficacy of ACI code equations for two important reasons. First, the shear force values reported in the database are based on ultimate load only, while ACI 318-14 considers shear failure for a member without transverse reinforcement to be the load at which first significant diagonal cracking occurs. Any comparison between first diagonal cracking load and ultimate load is inherently flawed. Load carrying capacity beyond first diagonal cracking cannot be relied upon, as demonstrated later in this thesis. Second, the method of calculating critical shear within the ACI-DAfStb database is inconsistent with ACI design procedures. As shown in Figure 4-1, loads considered for critical shear are only those acting on the shaded portion of each figure. The remainder of the load is assumed to travel directly into the support. While this assumption may be valid when describing observed behavior, ACI 318-14 design procedures would consider the shear acting on the critical section as shown in Figure 4-2. Furthermore, the shear database takes the critical section as the

location where the failure crack crosses midheight (x_r). Once again, though this might be a good practice for describing observed behavior, in design the location (x_r) is unknown, which is why ACI 318-14 approximates the failure section at (d) away from the face of the support as shown in Figure 4-2. In summary, both the load reported in the shear database and the method by which it was calculated are inconsistent with current ACI 318 design practice.

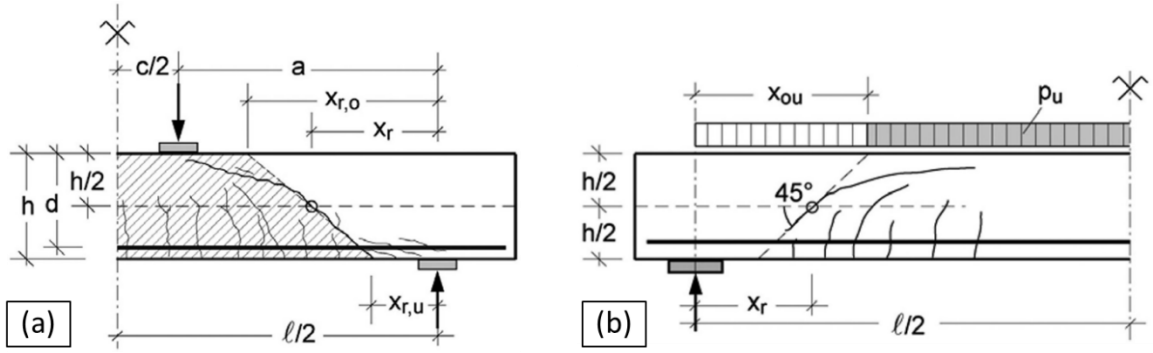

Figure 4-1: ACI-DAfStb Shear Database Calculation of Critical Shear Stress for (a) Concentrated Loading and (b) Uniform Loading

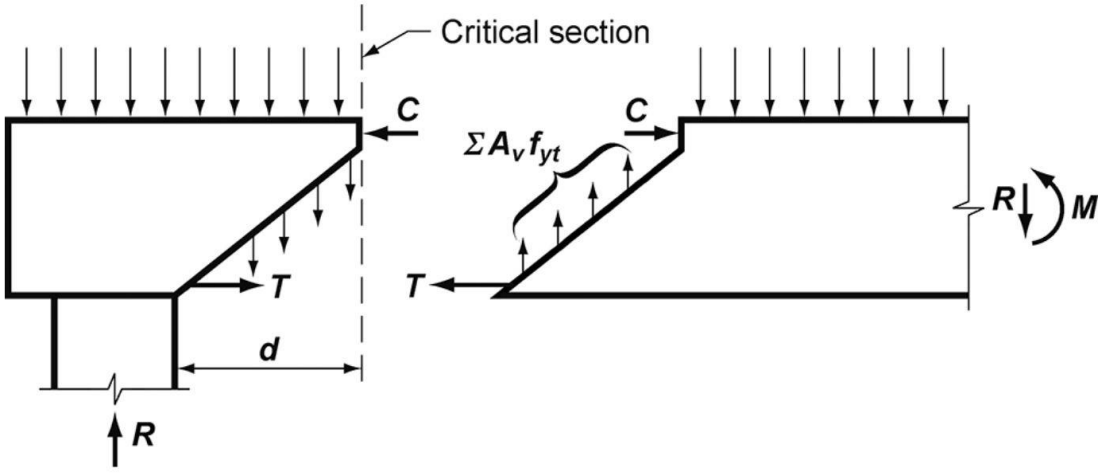

Figure 4-2: Calculation of Critical Shear Stress, Figure R9.4.3.2a from ACI 318-14

Due to the inconsistencies between the ACI-DAfStb Shear Database and ACI 318-14 design practices, any conclusions drawn about shear strength presented in this thesis were based on the test results reported in the originally published research. The original source material of the shear database was used to find diagonal cracking loads. To draw conclusions on the differences in shear strength between uniform and concentrated loading, this research was limited to specimens with identical geometry tested under both types of loading. Of the five different sources of uniform load testing presented in the shear database (Feldman and Siess 1955, Leonhardt and Walther 1962, Krefeld and Thurston 1966, Regan 1971, and Shioya 1989), the above criterion narrowed the potential sources to Feldman and Siess (1955), Leonhardt and Walther (1962), and Krefeld and Thurston (1966). Of those three, only Leonhardt and Walther (1962) did not report first diagonal cracking load. In addition to Feldman and Siess (1955) and Krefeld and Thurston (1966), results from testing performed at The University of Texas at Austin in 2014 by Dassow are also presented in this chapter.

Further filtering on the results from the literature was done to ensure their applicability to the reinforced concrete members being used in practice. The filtering parameters considered were:

- shear span-to-depth ratio (a/d) greater than or equal to 2.4,
- no other failure modes such as flexure,
- concrete compressive strength (f'_c) greater than or equal to 2,500 psi (per ACI 318-14 Table 19.2.1.1),
- net tensile strain in the extreme layer of longitudinal steel (ε_t) greater than or equal to 0.004 when shear is neglected (per ACI 318-14 Section 9.3.3.1), and
- area of longitudinal tensile steel greater than or equal to the minimum area ($A_{s,min}$) (per ACI 318-14 Section 9.6.1.2 and Table 7.6.1.1).

Furthermore, once all of these filtering parameters were met, an additional requirement was added that, for a given specimen geometry, more than one concentrated load test and more than one uniform load test must be remaining. Though the testing program herein does not meet that requirement, it was used for literature tests so that reasonable comparisons could be made, especially since factors such as reinforcement ratio (ρ) and effective depth (d) vary so widely between results presented herein and tests reported in the literature.

The minimum required area of flexural reinforcement ($A_{s,min}$) was calculated as if the members were both beams and slabs as per ACI 318-14 Section 9.6.1.2 and Table 7.6.1.1, respectively. Of the filtering parameters listed, ($A_{s,min}$) was the only requirement that every specimen met, regardless of whether ($A_{s,min}$) was calculated as if the specimen was a beam or a slab.

The requirement that the net tensile strain in the extreme layer of longitudinal steel (ε_t) was greater than or equal to 0.004 when ignoring shear was by far the parameter that excluded the most test results. When investigating shear behavior, often researchers choose to increase the longitudinal reinforcement ratio to avoid flexural failure during tests, which results in little net tensile strain at the onset of concrete crushing. Though avoiding flexural failure is an understandable research philosophy, it often leads to specimens that cannot be used in practice and, therefore, should not be used to evaluate code provisions. Of the 75 tests that met every other requirement, only 28 tests also met the net tensile strain requirement. The summary of the individual requirements for each different source is presented in its dedicated section. Of the 28 tests that met every requirement, six were from the tests presented in this thesis. With only 22 tests from the literature, the net tensile strain requirement was relaxed to obtain a larger dataset for more meaningful evaluation. The intent of the 0.004 limit for net tensile strain is to

ensure that beams display ductility by acting as tension-controlled members, that is, reaching yield in the steel before concrete crushes. Any member that does not reach the 0.004 limit cannot be considered a beam and must satisfy the column provisions in Chapter 10 of ACI 318-14. The reasoning behind this provision is sound, especially due to the uncertainty in material properties. For this review of literature, however, the beams being investigated here are likely neither compression- nor tension-controlled flexural members but instead are shear-controlled. Furthermore, the actual concrete compressive strength and steel yield strength are known, and the specimens were known not to have exhibited crushing in the flexural compression zone. As such, it was decided to relax the requirement of net tensile strain in the extreme layer of longitudinal steel (ε_t). Tests were included in this thesis if the calculated strain in the extreme layer of reinforcement was greater than or equal to the yield strain (ε_y). In that way, the original intention of the code is met, while still having enough data points to draw reasonable conclusions. With the relaxed requirement of net tensile strain (ε_t) greater than or equal to yield strain (ε_y), a potential set of 62 tests could be used for comparison.

4.2 CONTEXT WITHIN ACI-DAFSTB SHEAR DATABASE

When the geometry of the specimens presented herein was being developed, the 69 uniform load tests presented in the shear database were closely examined. Shear span-to-depth ratio (a/d), longitudinal reinforcement ratio (ρ), effective depth (d), and axial load are the four most important parameters when determining the shear capacity of specimens without shear reinforcement (ACI Committee 445 report 1999). As such, the examination of existing testing was limited to these variables, excluding axial force.

Figure 4-3 depicts the number of uniform load tests versus shear span-to-depth ratio (a/d) from the shear database along with tests reported in this thesis and by Dassow

(2014). Shear strength is inversely proportional to the (a/d) ratio, with shear behavior markedly changing when transitioning from deep to slender beam behavior. Though MacGregor and Wight (2012) define the transition at an (a/d) of 2.5, the shear database takes the limit as 2.4. For simplicity with literature comparisons, the 2.4 convention of the shear database was followed. As seen in Figure 4-3, the shear database represents a large number of different shear span-to-depth ratios. There is a slight skew towards (a/d) ratios between 2.5 and 3.0 due to the concern of flexural failure. The ratio of flexural capacity to shear capacity decreases as (a/d) increases, leading many researchers to choose smaller (a/d) values to ensure shear failure.

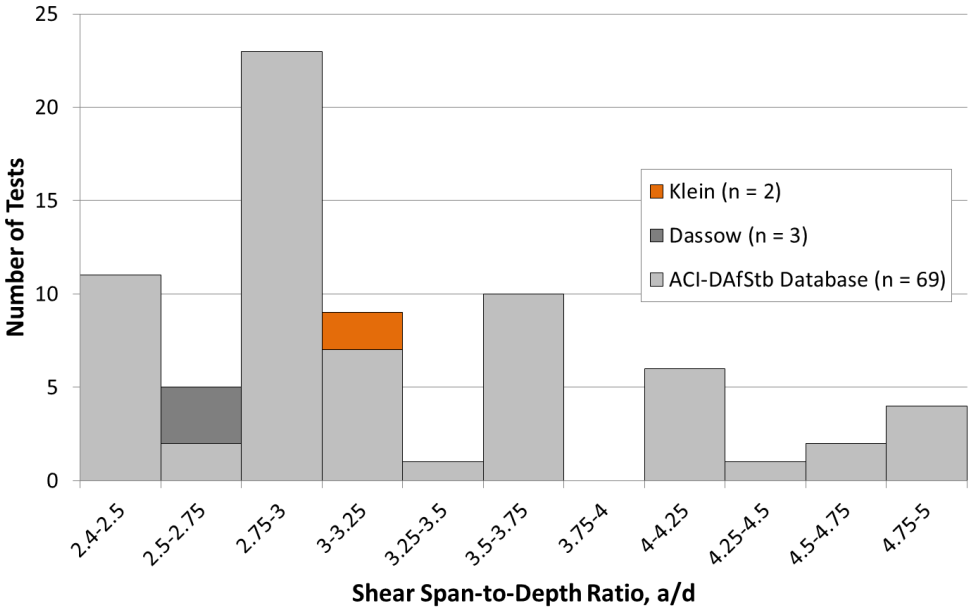

Figure 4-3: Number of Uniform Load Tests in the ACI-DAfStb Shear Database versus Shear Span-to-Depth Ratio (a/d)

As discussed previously, shear testing programs are well known for having large reinforcement ratios (ρ) to avoid flexural failure. This trend is easily seen in Figure 4-5.

Increasing the longitudinal reinforcement ratio (ρ) not only leads to specimens that could not be used in practice, but it also changes the shear strength of the specimens. Bentz and Collins (2006) note that crack width growth is limited as (ρ) increases. As ACI 318-14 R22.5.1.1 explains, the shear carried across a crack is due to aggregate interlock, dowel action in the longitudinal steel, and shear resistance of the concrete compression zone. Each of these phenomena contribute less shear resistance as crack width increases (MacGregor and Wight 2012), leading to a known relationship between reinforcement ratio and shear strength, depicted in Figure 4-4.

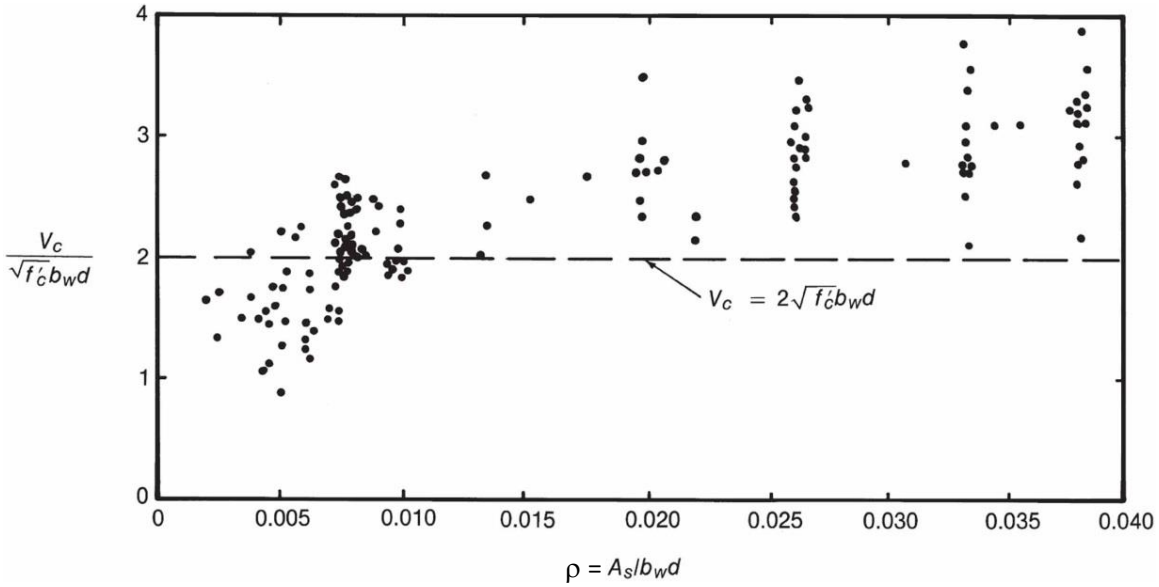

Figure 4-4: Relationship between Longitudinal Reinforcement Ratio (ρ) and Shear Strength (MacGregor and Wight 2012)

Figure 4-5 shows a substantial gap in the literature at reinforcement ratios (ρ) that are typically seen in beams. As such, the specimens described herein include a (ρ) of approximately 1 percent, which is recommended as a starting point in beam design by MacGregor and Wight (2012).

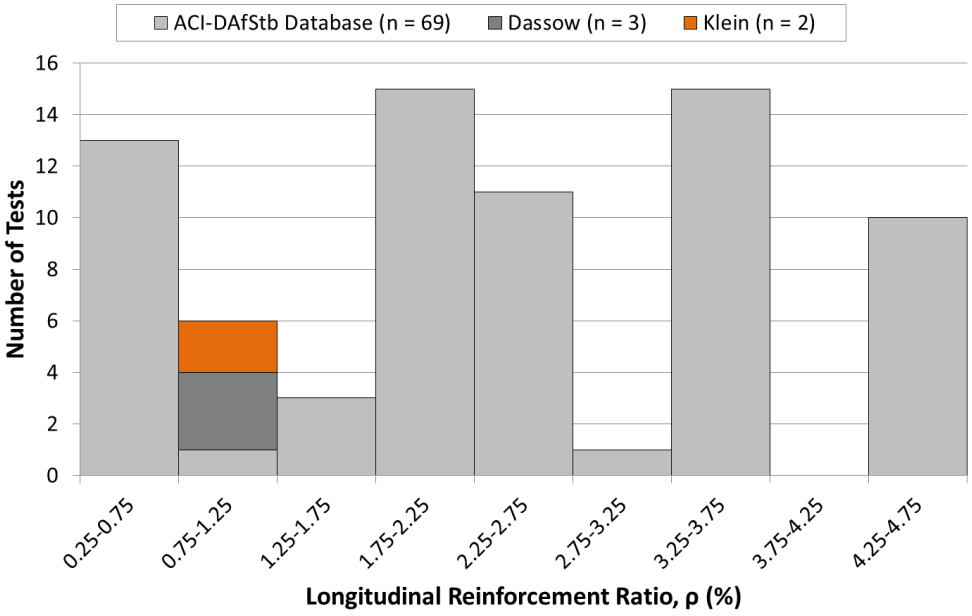

Figure 4-5: Number of Uniform Load Tests in the ACI-DAfStb Shear Database versus Longitudinal Reinforcement Ratio (ρ)

Perhaps an even greater gap in the literature exists for effective depths (d) greater than 12 in. (305 mm). Of the 69 uniform load tests presented in the ACI-DAfStb shear database, only eight tests (Shioya 1989) have an effective depth (d) greater than 12 in. (305 mm), as shown in Figure 4-6. All eight of these tests have a reinforcement ratio less than 0.5 percent, somewhat low for a specimen that might be used in practice. Similar to the behavior observed with small reinforcement ratios (ρ), a larger effective depth (d) increases crack width, which can adversely affect shear strength. This effect was first noted by Kani (1967) and termed "size effect."

To not only fill gaps in existing literature, but also to represent members typical of those used in practice, effective depths (d) of both 21 in. (533 mm) and 45 in. (1143 mm) along with reinforcement ratios of approximately 1 percent were chosen for the specimens described in this thesis. By examining the existing literature and determining

voids in testing, the dual research objectives of new knowledge and field-applicable specimens were met.

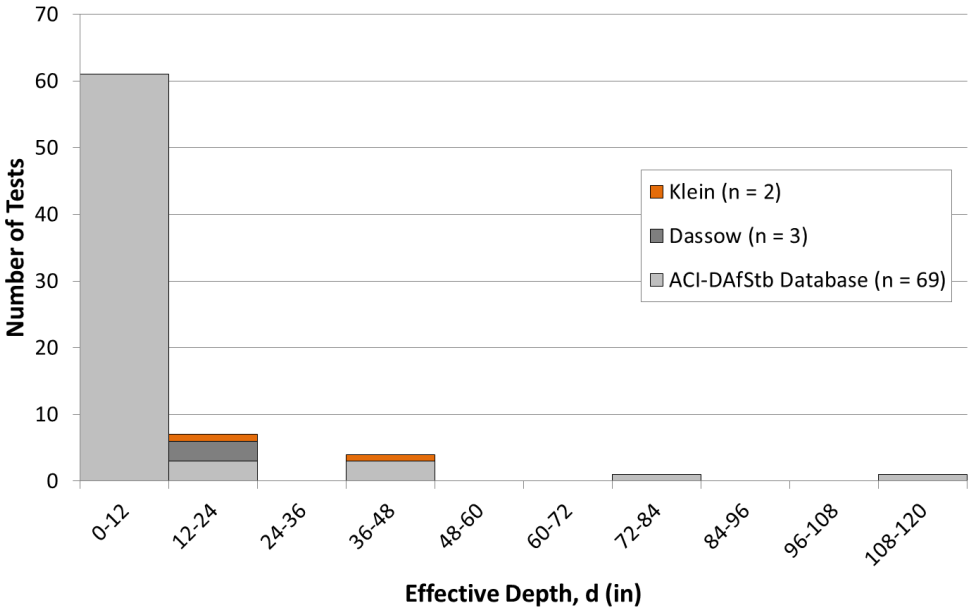

Figure 4-6: Number of Uniform Load Tests in the ACI-DAfStb Shear Database versus Effective Depth (d)

4.3 DISCUSSION OF TESTS REPORTED IN LITERATURE

Select test results from the sources described above are discussed in the following sections.

4.3.1 Feldman and Siess (1955)

Testing by Feldman and Siess in 1955 consisted of 13 nominally identical specimens, with a total of 11 concentrated load tests (four specimens were tested twice) and 6 uniform load tests. The testing method for the first concentrated load test on each specimen consisted of two symmetrically placed loads located 36 in. (914 mm) apart and spaced (a) away from either support. The second concentrated load test occurred on the

side of the specimen that did not exhibit shear failure and consisted of one concentrated load symmetrically placed (a) away from two supports, with a variable overhang off of one support. The uniform load tests consisted of ten individual loads placed on wide bearing surfaces equally spaced to mimic a uniform load distribution.

Tests were filtered using the parameters described above; results of filtering are summarized in Table 4-1. After all filtering operations, a usable dataset of 12 tests was formed: 8 concentrated load tests and 4 uniform load tests. Feldman and Siess (1955) reported total load on each specimen. For the uniform load tests, the reported load also included dead load from the specimen and the loading apparatus. The concentrated load tests did not include dead load so for consistency between different datasets, a self-weight of 150 pcf (23.6 kN/m^3) was assumed for all concentrated load tests. With reported load and assumed or reported self-weight, normalized shear stress at a section (d) away from the edge of the support was calculated.

Table 4-1: Filtering Results from Feldman and Siess (1955)

Filtering Parameter	Remaining of 17
Shear failure	15
$a/d \geq 2.4$	12
$A_{s,min}$ (for beams or slabs)	12
$f'c \geq 2500$ psi	12
$*\varepsilon_t \geq 0.004$	5
$\varepsilon_t \geq \varepsilon_y$	12
Identical specimens, Concentrated load tests > 1 and Uniform load tests >1	12

*Relaxed as described in Section 4.1

As all specimens were identical in construction, the 12 data points were used as one dataset. Figure 4-7 depicts the relationship between normalized shear stress (v_d) and shear span-to-depth ratio (a/d) for this dataset. Every test, with an average normalized

shear stress (v_d) of 3.82, failed well above the ACI 318-14 Equation 22.5.5.1 calculated value of 2. The difference between ACI 318-14 calculations and test results is not surprising due to the high reinforcement ratio (3.35 percent) and the small effective depth (9.94 in.). For uniform load tests, the average normalized shear stress (v_d) was 3.88, and for concentrated load tests, it was 3.78, amounting to an increase of only 3 percent in normalized shear stress (v_d) when comparing uniform load tests to concentrated load tests. Not only is this difference too small to note any trends between the different loading types, but the uniform load tests had an average shear span-to-depth ratio (a/d) about 0.75 times that of their concentrated load counterparts. As such, the uniform load tests should exhibit greater average normalized shear stress (v_d) at first diagonal cracking, all other variables being equal.

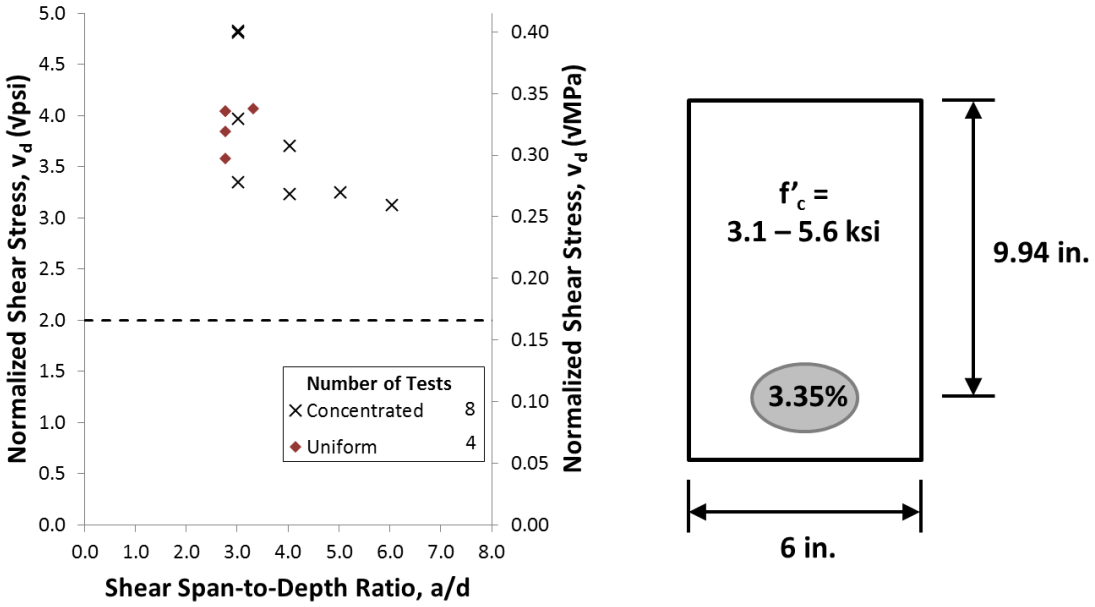

Figure 4-7: Select Results from Feldman and Siess (1955)

Another point to note about the results presented in Feldman and Siess (1955) is the post-cracking behavior. Of the 12 tests discussed here, all four uniform load tests and three of eight concentrated load tests had an ultimate load greater than the first diagonal cracking load. For these seven tests, the ultimate load was on average 20 percent greater than the diagonal cracking load.

4.3.2 Krefeld and Thurston (1966)

Testing by Krefeld and Thurston in 1966 consisted of 152 tests of various geometries, with a total of 78 concentrated load tests and 74 uniform load tests. The testing method for the concentrated load test consisted of a load symmetrically placed (a) away from two supports. The uniform load tests consisted of eight individual loads placed on wide bearing surfaces equally spaced to mimic a uniform load distribution.

Tests were filtered using the parameters described above; results of filtering are summarized in Table 4-2. After all filtering operations, a usable dataset of 31 tests was formed: 15 concentrated load tests and 16 uniform load tests. Krefeld and Thurston (1955) reported shear force values at the support for each test. Self-weight information was not given so a self-weight of 150 pcf (23.6 kN/m^3) was assumed for all specimens. With reported load and assumed self-weight, normalized shear stress at a section (d) away from the edge of the support was calculated.

Table 4-2: Filtering Results from Krefeld and Thurston (1966)

Filtering Parameter	Remaining of 152
Shear failure	122
$a/d \geq 2.4$	95
$A_{s,min}$ (for beams or slabs)	95
$f'c \geq 2500$ psi	69
$*\varepsilon_t \geq 0.004$	20
$\varepsilon_t \geq \varepsilon_y$	47
Identical specimens, Concentrated load tests > 1 and Uniform load tests >1	31

*Relaxed as described in Section 4.1

The 31 different tests represented three geometries, separating the tests into three different datasets, called Series I, II, and III.

4.3.2.1 Krefeld and Thurston Series I Tests

Figure 4-8 depicts the relationship between normalized shear stress (v_d) and shear span-to-depth ratio (a/d) for Series I. Every test in Series I, with an average normalized shear stress (v_d) of 2.99, failed well above the ACI 318-14 Equation 22.5.5.1 calculated value of 2. The difference between ACI 318-14 calculations and test results is not surprising due to the high reinforcement ratio (2.63 percent) and the small effective depth (10 in.). For uniform load tests, the average normalized shear stress (v_d) was 3.22, and for concentrated load tests, it was 2.71, amounting to an increase of 19 percent in normalized shear stress (v_d) when comparing uniform load tests to concentrated load tests. This difference would support the trend that uniform loading results in greater shear strength at failure, but the uniform load tests had an average shear span-to-depth ratio (a/d) about 0.6 times that of their concentrated load counterparts. From Series I only, it is uncertain whether the difference between the shear span-to-depth ratios is fully the cause of the discrepancy between shear strengths or if load distribution is also a factor.

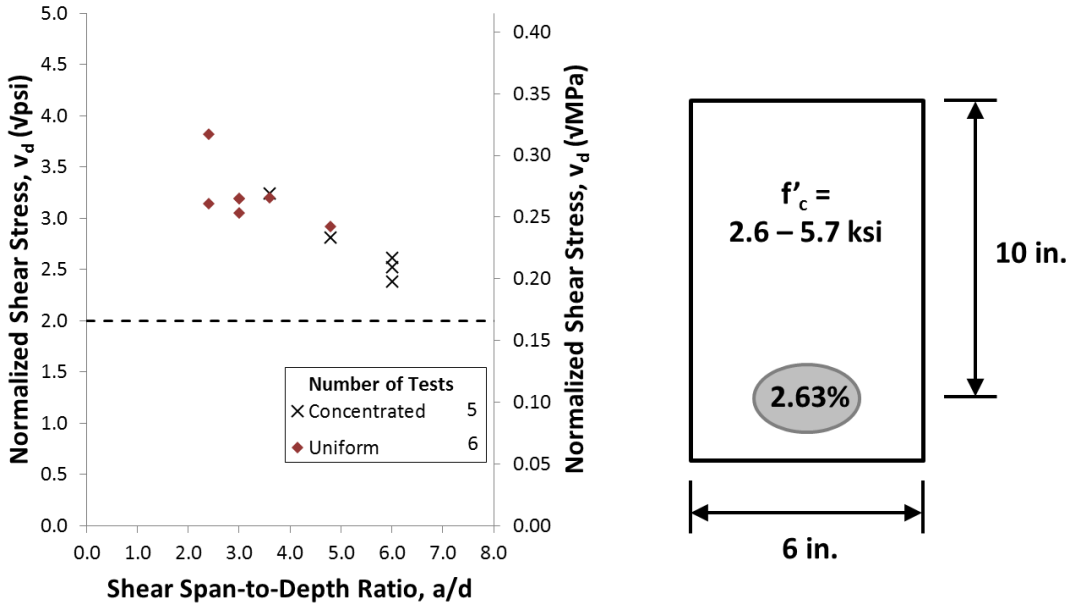

Figure 4-8: Select Results for Series I from Krefeld and Thurston (1966)

4.3.2.2 Krefeld and Thurston Series II Tests

Figure 4-9 depicts the relationship between normalized shear stress (v_d) and shear span-to-depth ratio (a/d) for Series II. Every test in Series II, with an average normalized shear stress (v_d) of 3.20, failed well above the ACI 318-14 Equation 22.5.5.1 calculated value of 2, and was moderately above the average for Series I. The difference between ACI 318-14 calculations and test results is not surprising due to the high reinforcement ratio (3.35 percent) and the low effective depth (9.94 in.). For uniform load tests, the average normalized shear stress (v_d) was 3.57, and for concentrated load tests, it was 2.65, amounting to an increase of 35 percent in normalized shear stress (v_d) when comparing uniform load tests to concentrated load tests. This difference would support the trend that uniform loading results in greater shear strength at failure, especially since

the uniform load tests had an average shear span-to-depth ratio (a/d) about 0.6 times that of their concentrated load counterparts.

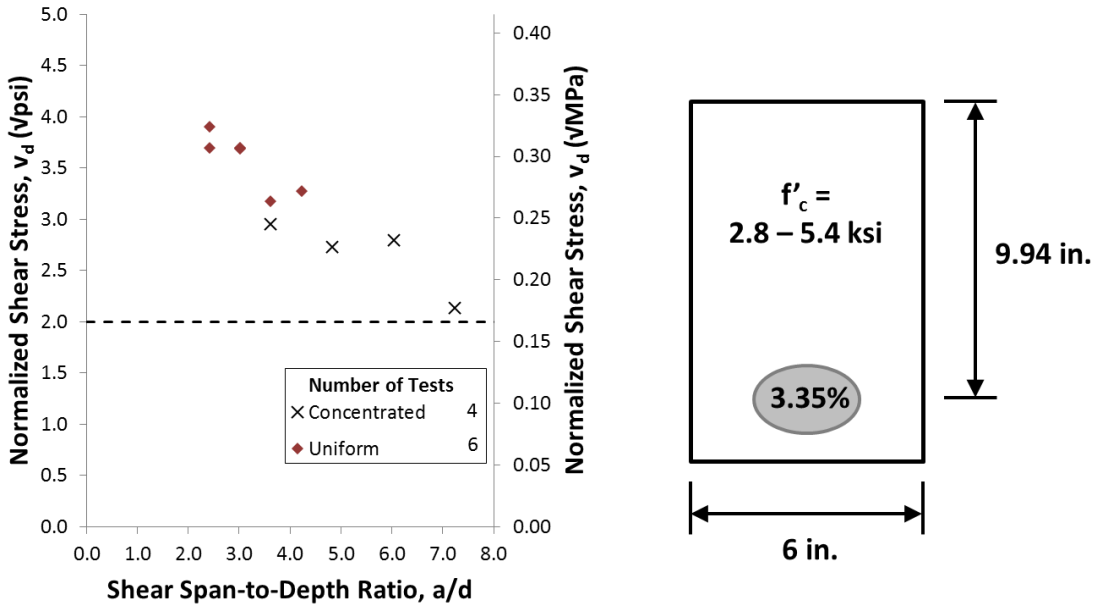

Figure 4-9: Select Results for Series II from Krefeld and Thurston (1966)

Since the ratio between shear span-to-depth ratio for uniform and concentrated loading was approximately equal for both Series I and II, the argument becomes better that uniform loading results in greater shear strength rather than that the difference is just because of the lower (a/d) ratios of the uniform load tests. The only major variable between Series I and II is reinforcement ratio (ρ), leading to the potential hypothesis that load distribution and reinforcement ratio (ρ) are related in terms of shear strength.

4.3.2.3 Krefeld and Thurston Series III Tests

Figure 4-10 depicts the relationship between normalized shear stress (v_d) and shear span-to-depth ratio (a/d) for Series III. Every test in Series III, with an average normalized shear stress (v_d) of 3.19, failed well above the ACI 318-14 Equation 22.5.5.1

calculated value of 2, was moderately above the average for Series I, and was nearly identical to the average for Series II. The difference between Series III and Series I is not surprising due to the high reinforcement ratio (4.29 percent) and the smaller effective depth (9.86 in.), yet it would be expected that Series III yielded slightly greater strength results than Series II. For uniform load tests, the average normalized shear stress (v_d) was 3.78, and for concentrated load tests, it was 2.80, amounting to an increase of 35 percent in normalized shear stress (v_d) when comparing uniform load tests to concentrated load tests. This difference would support the trend that uniform loading results in greater shear strength at failure, but the uniform load tests had an average shear span-to-depth ratio (a/d) 0.5 times that of their concentrated load counterparts, similar to the differences in Series I and II. As such, the uniform load tests should exhibit greater average normalized shear stress (v_d) at first diagonal cracking, all other variables being equal.

It is uncertain the relationship between shear span-to-depth ratio (a/d), reinforcement ratio (ρ), and load distribution based on Krefeld and Thurston (1966). The trend that uniform load results in a greater shear strength can be noted in Series I, II, and III; this difference was similar at very high reinforcement ratios (ρ) of 4.29 percent and 3.35 percent, and was smaller at the moderately high reinforcement ratio of 2.63 percent. The relationship between shear span-to-depth ratio (a/d) and load distribution is unclear based on these data.

Another point to note about the results presented in Krefeld and Thurston (1966) is the post-cracking behavior. Before the filtering parameter that identical geometries with more than one concentrated load test and more than one uniform load test was applied, there were 47 potential tests. Of those 47 tests, 44 (or 94 percent) had an ultimate load greater than the first diagonal cracking load. For these 44 tests, the ultimate load was on average 20 percent greater than the diagonal cracking load. The other three tests were

all without exception concentrated load tests. This behavior starkly contrasts with the results from the larger, more lightly-reinforced beams presented in this thesis.

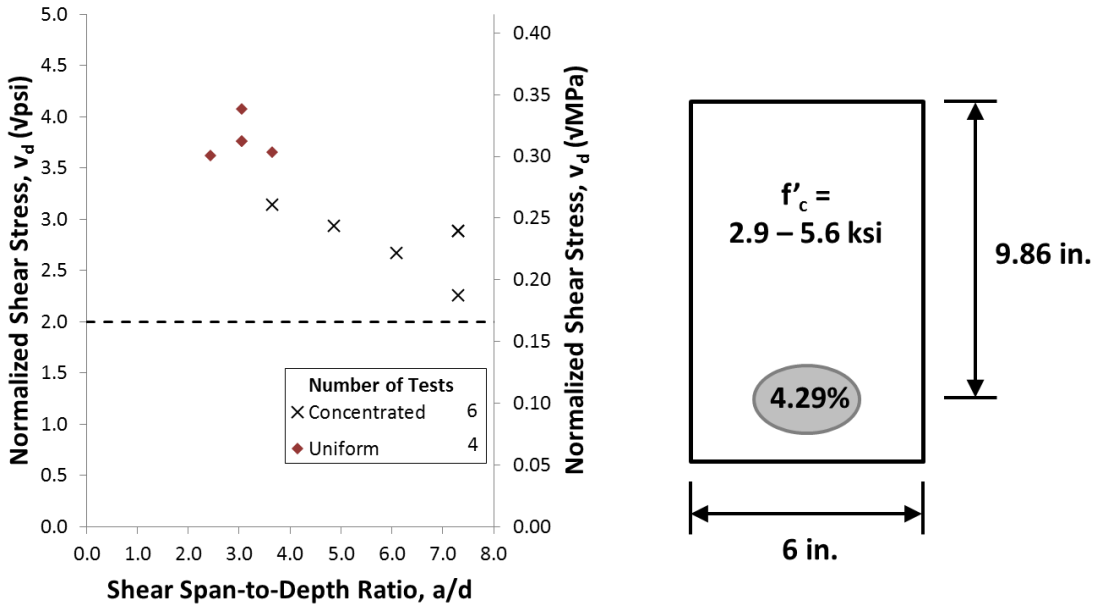

Figure 4-10: Select Results for Series III from Krefeld and Thurston (1966)

4.3.3 Dassow (2014)

Testing by Dassow in 2014 comprised of five specimens of identical geometries, with a total of 3 concentrated load tests and 3 uniform load tests. The testing method for the concentrated load test consisted of a load asymmetrically placed between two supports. The load and test span were placed in such a way as to permit a second concentrated load test on the opposite end as described in Chapter 2. Two tests were performed on both concentrated load beams; however, one specimen had a retrofit test conducted on one end that was not presented by Dassow (2014). The uniform load tests were performed identically to the method described in Chapter 2, i.e. using a Kevlar-reinforced air bladder and loading from the underside. Tests were filtered using the

parameters described above; each test met every requirement, including the requirement that net tensile steel strain (ε_t) is greater than or equal to 0.004. Dassow (2014) reported shear force values at (d) away from the edge of the support for consistency with ACI 318-14, as well as presenting shear-force values at other sections. Self-weight was included in the reported shear force values for all tests. With reported load and self-weight, normalized shear stress at a section (d) away from the edge of the support was calculated.

Figure 4-11 depicts the relationship between normalized shear stress (v_d) and shear span-to-depth ratio (a/d) for this dataset. The shear span-to-depth ratio was kept constant at 2.5. The reinforcement ratio (ρ) of 1.02 percent and the effective depth (d) of 21.3 in (541 mm) are much different from the specimen geometries presented in the other literature sources. The average normalized shear stress (v_d) was 1.97, slightly less than the ACI 318-14 Equation 22.5.5.1 calculated value of 2. ACI 38-14 Equation 22.5.5.1 is meant to be a conservative, lower-bound equation, reflecting the relatively small specimens used in formulation of that equation. It is interesting to note that the code equation tends to be less conservative as the specimen geometry becomes larger and more representative of members seen in practice, with a low to medium reinforcement ratio (ρ) and a medium to high effective depth (d).

For uniform load tests, the average normalized shear stress (v_d) was 2.05, and for concentrated load tests, it was 1.89, amounting to an increase of about 9 percent in normalized shear stress (v_d) when comparing uniform load tests to concentrated load tests. This difference is relatively small; the conjecture that uniform loading shows increased shear strength over concentrated loading is unclear with such a small difference, especially when considering the scatter of data.

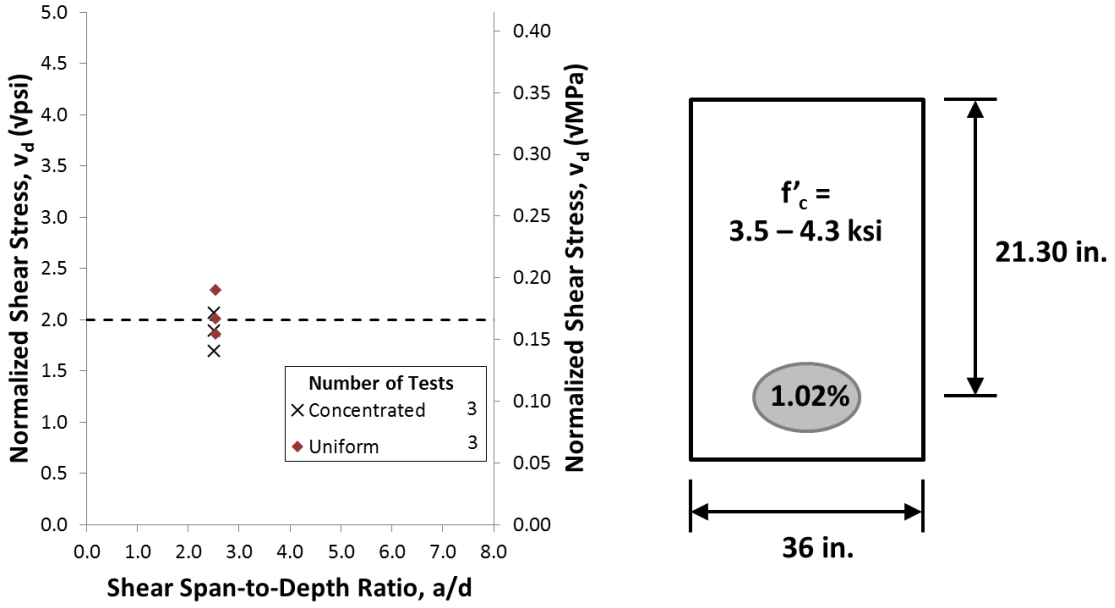

Figure 4-11: Results from Dassow (2014)

Another point to note about the results presented in Dassow (2014) is the post-cracking behavior. Of the six tests, three tests had an ultimate load greater than the first diagonal cracking load. For these three tests, the ultimate load was on average 27 percent greater than the diagonal cracking load. Of the three tests that achieved ultimate load and diagonal cracking load simultaneously, two were concentrated load tests and one was a uniform load test.

4.4 DISCUSSION OF PREVIOUS AND CURRENT TESTING

Figure 4-12 summarizes all of the literature data presented in this chapter, as well as data from this report. The current testing program shows disagreement with the literature on the difference between uniform and concentrated loading. It was noted for the research presented in this thesis, uniformly loaded beams exhibited on average less shear strength at failure than their concentrated load counterparts, whereas in the literature, the opposite was noted. It is uncertain what the overall trend may be for two

reasons: the current testing program only included two uniform load tests, and the increase noted in the literature was negligible in two of the three testing programs presented, Feldman and Siess (1955) and Dassow (2014).

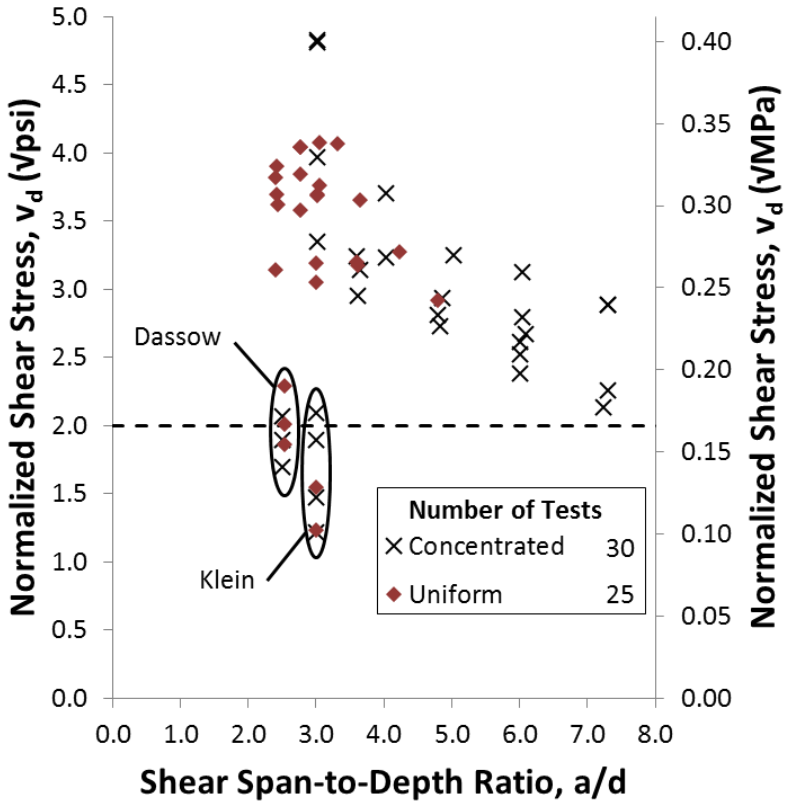

Figure 4-12: Results from All Tests Presented Herein

It must be noted that the testing program with the largest dataset, Krefeld and Thurston (1966), consistently had the greatest increase between uniform and concentrated load tests. At the same time, it also had the greatest, and hence least realistic, reinforcement ratios (ρ) of any of the datasets examined. Therein lies the true problem with the existing research: it consists of specimens that are inconsistent with members

typically used in practice. Though trends can be noted from existing literature, any observations made must keep the inconsistencies between research and practice in mind.

Both the research program presented herein and the literature agree on the existence of a size effect in shear behavior. Research done by Dassow (2014) presented specimens approximately double the effective depth (d) of the research presented in both Feldman and Siess (1955) and Krefeld and Thurston (1966), and the author has presented specimens approximately double the effective depth (d) of Dassow's specimens. In each case, with critical variables such as shear span-to-depth ratio (a/d) and reinforcement ratio (ρ) kept nearly constant, specimens with larger effective depths exhibited lower normalized shear stress (v_d) at first diagonal cracking. It must also be noted that the largest specimens failed at loads significantly less than the code calculated, lower-bound shear strengths.

Finally, post-diagonal cracking behavior showed moderate agreement between current and past research. The current testing program did not exhibit any load carrying capacity after first diagonal cracking, Feldman and Siess (1955) and Dassow (2014) only exhibited additional load carrying capacity in about half of their tests, and Krefeld and Thurston (1966) observed additional capacity in almost all of their tests. In general, concentrated load tests were more susceptible to loss of load carrying capacity after first diagonal cracking, with only three of 25 uniform load tests exhibiting such behavior. Of the tests that saw additional capacity after first diagonal cracking, the gain was consistently between 20 and 30 percent of the first diagonal cracking load. Overall, the desire to have lower-bound code provisions is consistent with the assumption that strength beyond first diagonal cracking cannot be relied upon.

Chapter 5: Conclusions

Six shear tests were performed at The University of Texas on reinforced concrete beams, comprising two different cross-sections, neither of which contained shear reinforcement. Based on this investigation, the following conclusions can be made:

- **The distinction in shear capacity between load distributions vanishes as effective depth (d) increases, and size effect begins to dominate behavior.** It is quite clear that the general trend in Figure 5-1 leads to the conclusion that any extra strength based on load distribution should be not be relied upon for design purposes when dealing with large specimens, which are more representative of members in practice.

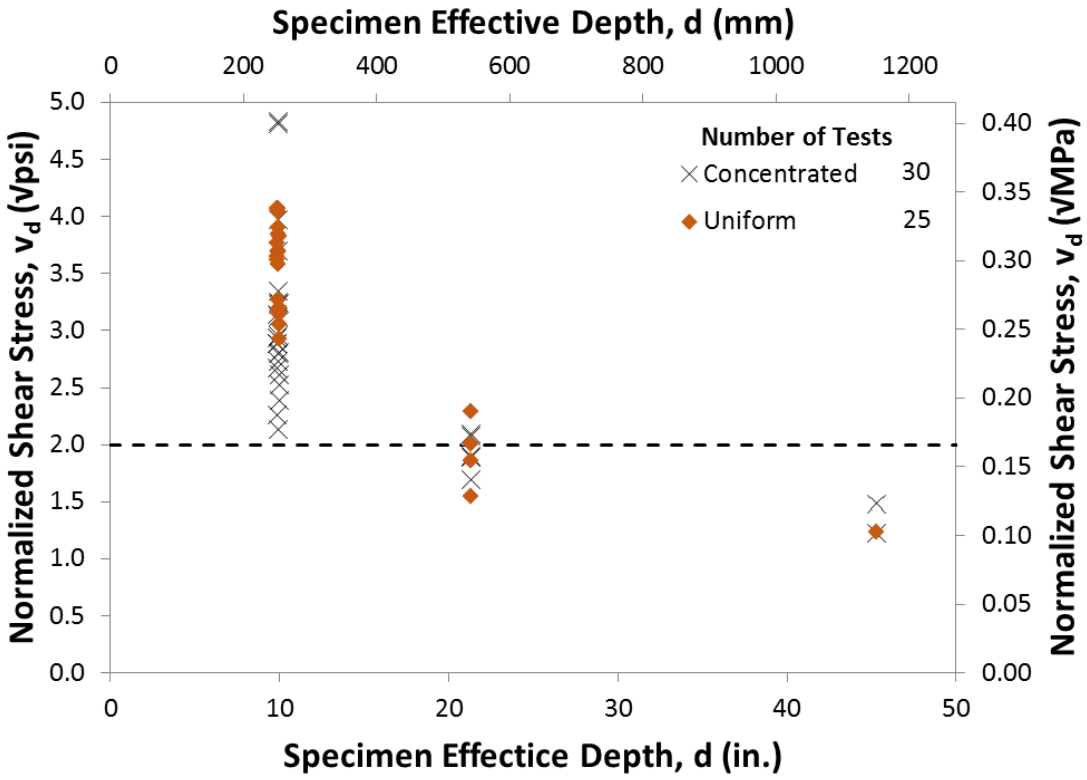

Figure 5-1: Normalized Shear Stress (v_d) versus Effective Depth (d) for All Tests Presented Herein

- **Approximating the failure at (d) or (d_v) away from the edge of a support is reasonable.** The distance to the failure section was often underestimated, which is conservative for design. The underestimation was more pronounced for the specimens with greater effective depths (d), where the need for conservatism is apparent. Each approximate failure section provided a much better estimate for members subjected to uniform loading, the more critical case due to the shear distribution. The observed failure section varied widely, yet (d) or (d_v) provide a simple and reasonable assumption for the failure section.
- **The size effect in shear strength was observed both in the literature and in this investigation.** The variation in shear strengths of specimens with different effective depths (d) was much more pronounced than any effects observed from differences in load distribution. Furthermore, the overestimation of shear strength from code provisions was much more pronounced as effective depth (d) increased. In general, ACI 318-14 more accurately and conservatively estimated the strength of specimens with medium to high effective depths (d = 21.3 in. or 541 mm), and AASHTO LRFD 2014 more accurately and conservatively estimated the strength of specimens with high effective depths (d = 45.3 in. or 1151 mm), though both produced unconservative values of design strength.
- **Shear strength beyond first diagonal cracking is unreliable in specimens without shear reinforcement.** The ACI 318-14 procedure of ignoring strength after first diagonal cracking is therefore appropriate. In general, specimens subjected to uniform loading are more likely to display increased

shear capacity after first diagonal cracking than their concentrated load counterparts.

- **The provisions of neither ACI 318-14 nor AASHTO LRFD 2014 produced safe design strengths of the specimens in this investigation.** Though the test results did not fall below the strength at which no minimum shear reinforcement ($A_{v,min}$) would be required in beams, they did fall below that value for slabs. As such, a slab similar to the test specimens, without stirrups, could be used in practice. If the assertion by Sherwood (2006) that one-way shear strength is largely independent of member width is true, there is cause for concern.
- **The ACI-DAfStb shear database, while a useful resource for examining the scope of testing performed, cannot be used to determine the efficacy of ACI 318-14 code provisions.** The test results presented in the database do not match the assumptions and requirements set forth in ACI 318-14.

The need for more full-scale testing on members with large effective depths (d) and realistic reinforcement ratios (ρ) is clear. Members with such properties have only begun to be investigated under various load distributions. Based on the findings presented herein, and the current state of the code provisions, two recommendations are presented. First, attempt to validate Sherwood (2006) with further research to determine if investigations such as the one presented here are truly applicable to all one-way shear members. If the conclusions reached by Sherwood (2006) are valid, minimum shear reinforcement provisions should not vary by member type. Second, code provisions for shear strength should account for member size, in the case of ACI 318-14, and should further reduce design strength for large members, in the case of AASHTO LRFD 2014.

Regardless of the action taken, code provisions and research should attempt to reflect the behavior and geometries of actual structures.

Appendix A: Specimen Construction and Instrumentation

Appendix A illustrates the methods by which specimens were constructed and instrumented for testing as follows:

- *Reinforcing Cage Construction, LD5 and LD6:* Figure A-1
- *Reinforcing Cage Construction, LD7:* Figure A-2
- *Reinforcing Cage Construction, LD8:* Figure A-3
- *Concrete Placement, LD5 and LD6:* Figure A-4
- *Concrete Placement, LD7 and LD8:* Figure A-5
- *Concentrated Load Test Instrumentation:* Figure A-6
- *Uniform Load Test Instrumentation:* Figure A-7
- *Concentrated Load Test Setup Photographs:* Figure A-8
- *Uniform Load Test Setup Photographs:* Figure A-9

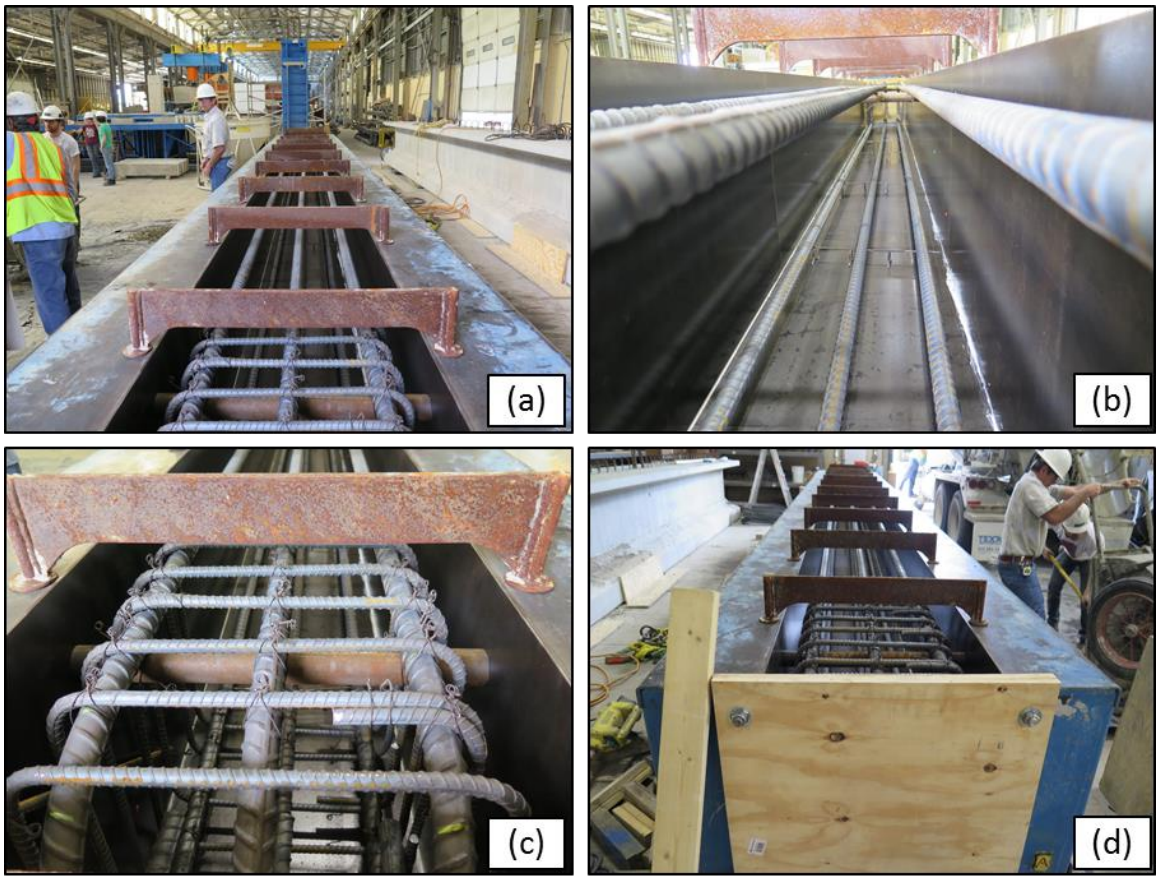

Figure A-1: Reinforcing Cage Construction for LD5 and LD6 Showing: (a) Completed Cage, (b) Test Region, (c) End Region, and (d) Formwork at End and Sides

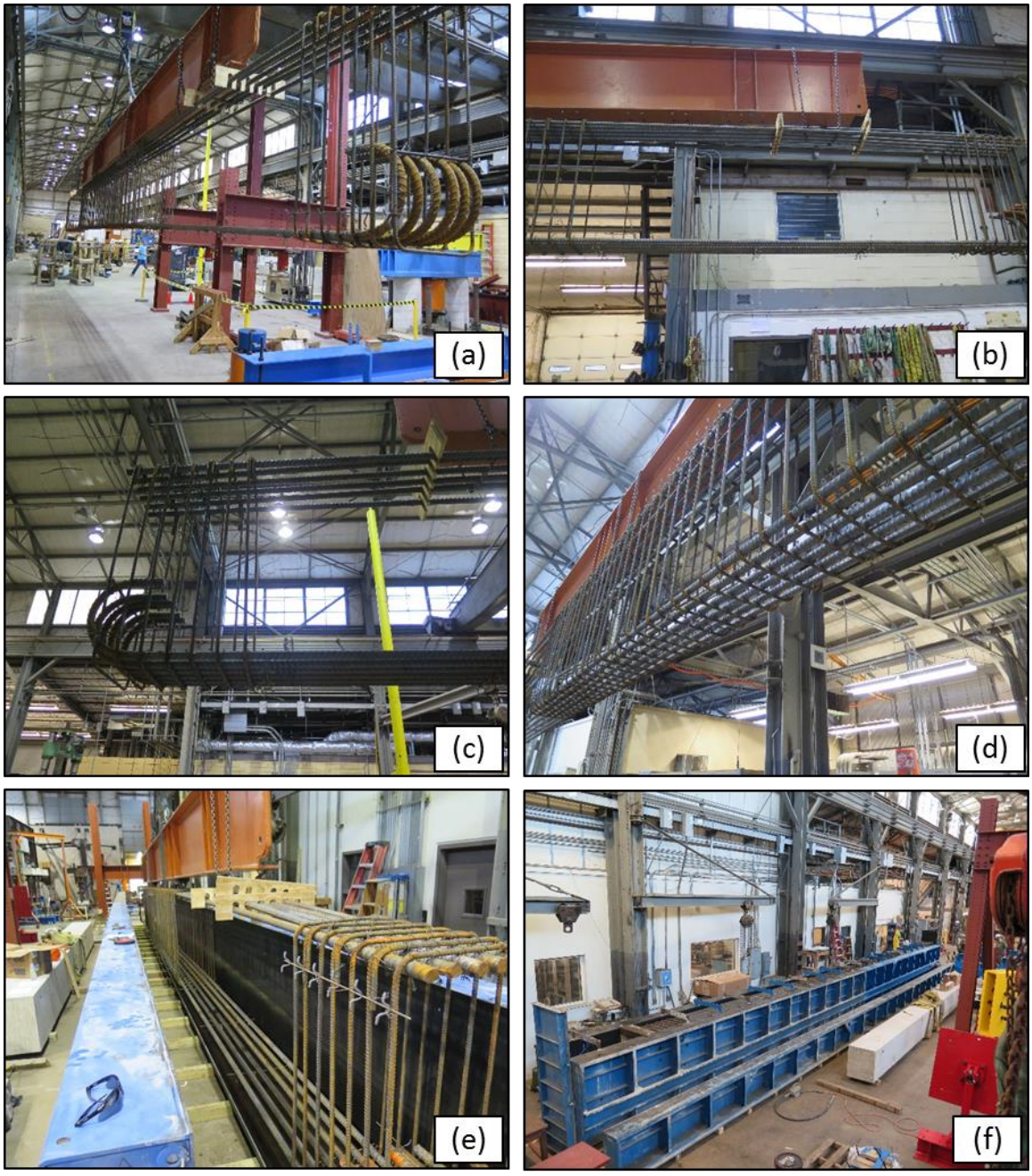

Figure A-2: Reinforcing Cage Construction for LD7 Showing: (a) Completed Cage being Transported, (b) Test Region, (c) End Region, (d) Middle Region, (e) Placement of Cage, and (f) Completed Cage in Formwork

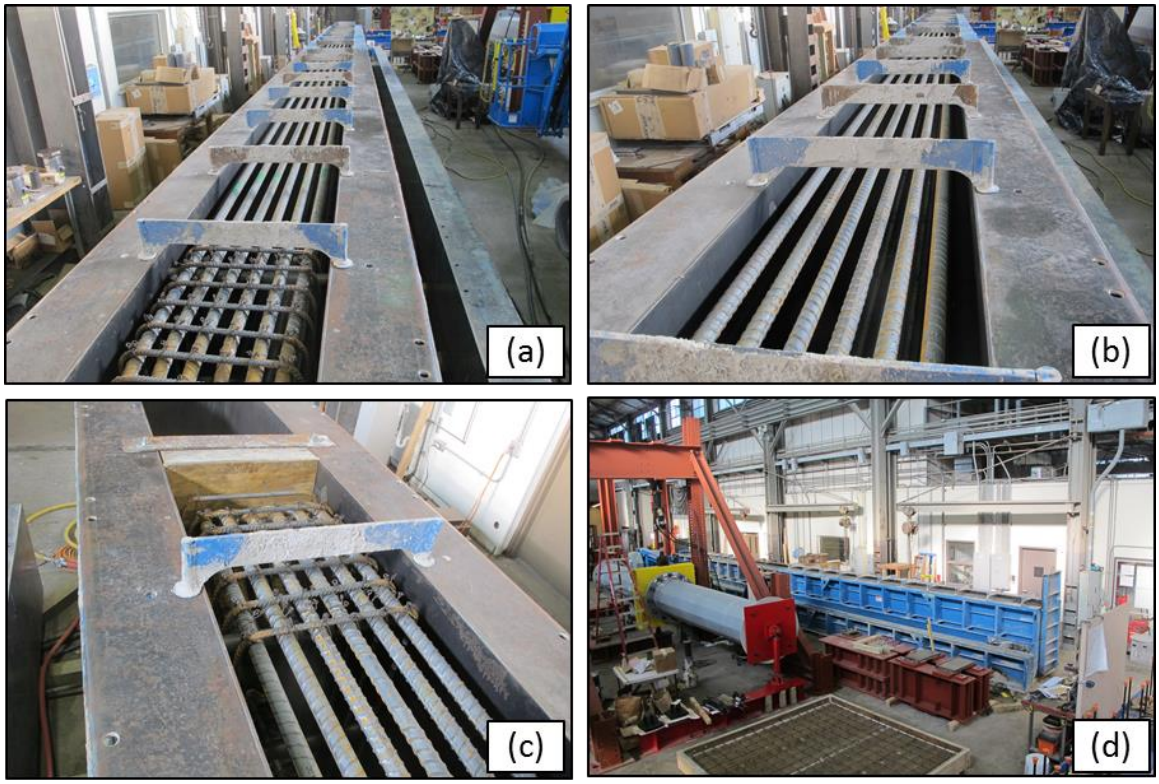

Figure A-3: Reinforcing Cage Construction for LD8 Showing: (a) Completed Cage, (b) Test Region, (c) End Region, and (d) Aerial View of Cage in Formwork

Figure A-4: Concrete Placement for LD5 and LD6 Showing: (a) Slump Test, (b) Cylinder Operations, (c) Specimen Concrete Placement, (d) Internal Vibrating and Leveling of Surface, (e) Surface Finishing, and (f) Completed Specimen

Figure A-5: Concrete Placement for LD7 and LD8 Showing: (a) Slump Test, (b) Cylinder Operations, (c) Specimen Concrete Placement, (d) Internal and External Vibrating, (e) Surface Finishing, and (f) Completed Specimen

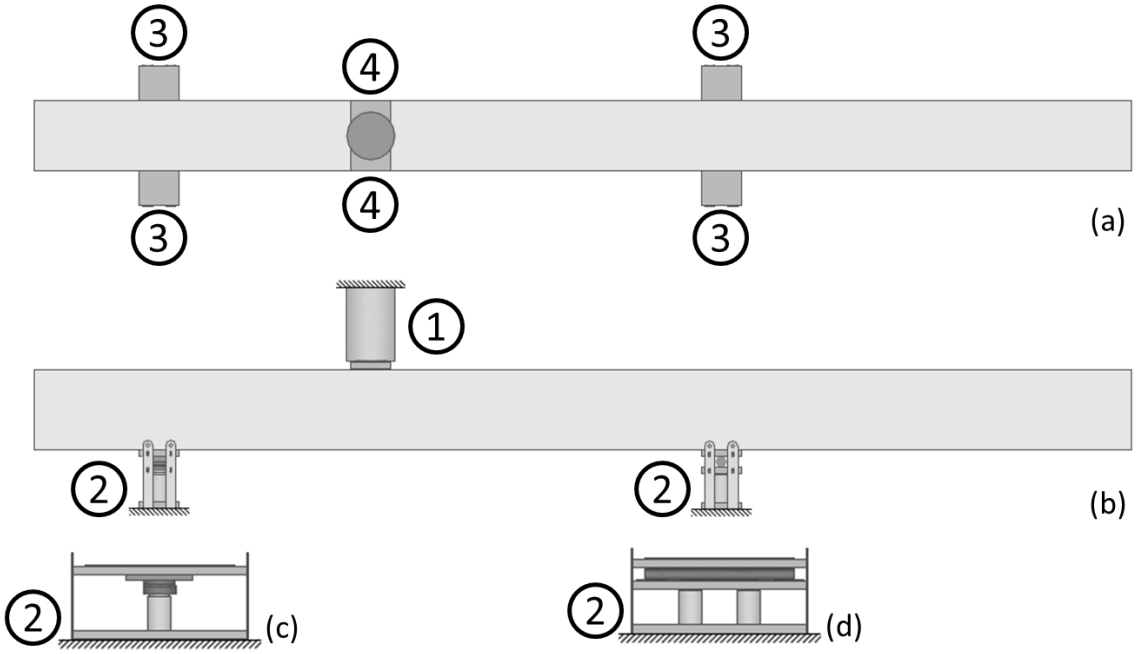

Location	Function	Manufacturer	Model	Capacity
1	Apply Load	Force-Pak	R400-12	400 tons
2	Measure Load	Strainsense	SSTS504C	250 tons
3	Measure Displacement	Novotechnik	TR-0050	2 in.
4	Measure Displacement	Novotechnik	TR-0100	4 in.

(e)

Figure A-6: Concentrated Load Test Instrumentation Showing the Following: (a) Plan View, (b) Elevation View, (c) Tilt Support, (d) Roller Support, and (e) Instrumentation Detailing

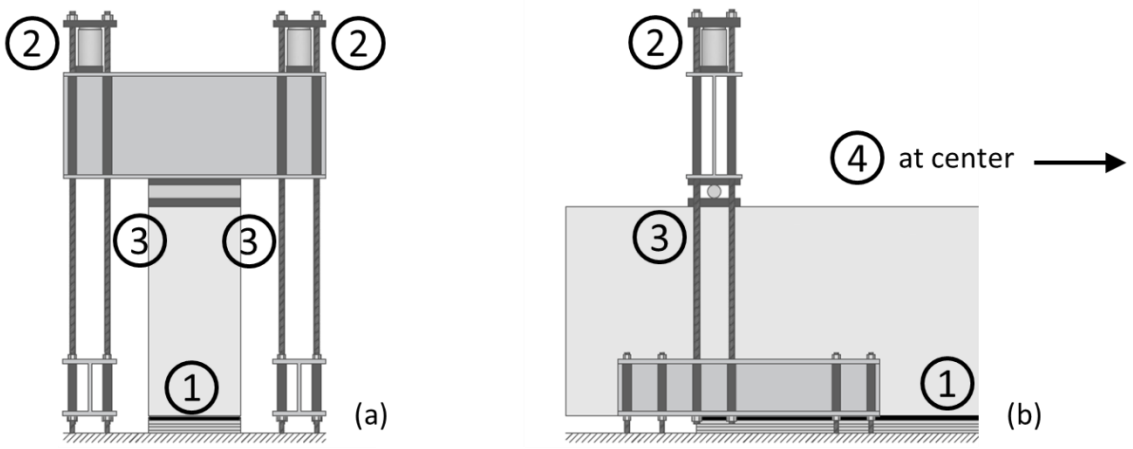

Location	Function	Manufacturer	Model	Capacity
1	Apply Load	Aero Tech	Kevlar Reinforced Bladder	50 psi
2	Measure Load	Strainsense	SSTS504C	250 tons
3	Measure Displacement	Novotechnik	TR-0050	2 in.
4	Measure Displacement	Novotechnik	TR-0100	4 in.

(c)

Figure A-7: Uniform Load Test Instrumentation Showing the Following: (a) End View, (b) Elevation View, and (c) Instrumentation Detailing

Figure A-8: Concentrated Load Test Setup Photographs Showing: (a) LD6-N, (b) LD6-S, (c) and (d) LD7-N, and (e) and (f) LD7-S

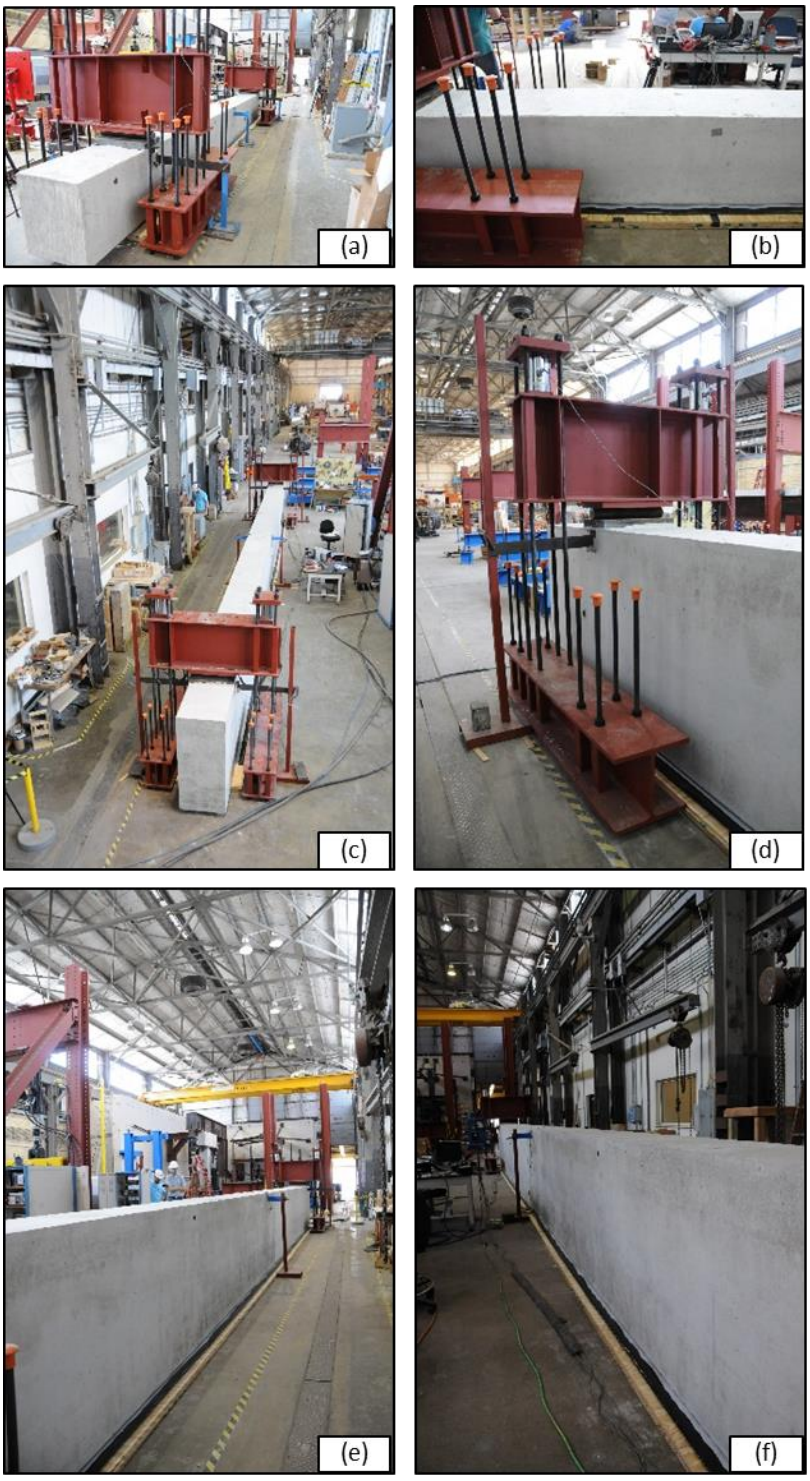

Figure A-9: Uniform Load Test Setup Photographs Showing: (a) and (b) LD5, and (c), (d), (e), and (f) LD8

Appendix B: Material Testing Records

Appendix B presents the results of materials testing for both concrete and steel as follows:

- *Concrete Mix Design Properties:* Figure B-1
- *Individual Concrete Batch Tickets:* Figures B-2 through B-7
- *Concrete Compressive Strength Data:* Tables B-1 through B-6
- *Concrete Compressive Strength Development:* Figures B-8 through B-13
- *Concrete Modulus of Elasticity Data:* Tables B-7
- *Concrete Tensile Strength Data:* Tables B-8
- *Steel Mill Certification Details:* Figures B-14 through B-16
- *Steel Tensile Testing Data:* Figures B-17 through B-18

TEXAS CONCRETE MATERIALS
apac Safety First Always

UT RESEARCH PROJECT

Date : **2/14/2014**
Mix Code : **4500727** Description : **4.5 SK NO FA, 3/4"LS, MRWR**

Revision Number : 4 Creation Date : 14 Feb 2014 Customer :
Plant : 973 PLANT Created By : cthomas2 Project :

Specifications

Consistence Class : 4.00 Air, % : 1.5
Strength Class : 3000 Max W/C : Max Agg Size : 1

Material Type	Material Code	Description	Supplier Source	Design Quantity	Specific Gravity	Volume ft3
Cement	CEMENT	CEMENT	ALAMO CEMENT CO-SANANTON	423 lb	3.15	2.15
Fine Aggregate	SAND	SAND	AUSTIN AGGREGATES-AUSTIN	1505 lb	2.62	9.20
Coarse Aggregate	57CLS	1" Limestone	COLORADO MATERIALS-SAN MA	1795 lb	2.57	11.19
Water	WATER	WATER	CITY-WATER	30.0 gal	1.00	4.01
Admixture	WREDUCER	WATER REDUCER	SIKA ADMIXTURES-DALLAS	7.0 /cwt	1.10	0.03
Admixture	WRRETARD	RETARDER/WATER REDUCER	SIKA ADMIXTURES-DALLAS	1.0 /cwt	1.20	0.00
			Yield	**3975 lb**	**27.00**	

Design Properties

Density : 147.2 lb/ft3 Grading Specification :
Cement Content : 423 lb Actual Dmax : 1 mm

Prepared By :

Corben Thomas

Figure B-1: Concrete Mix Design Properties

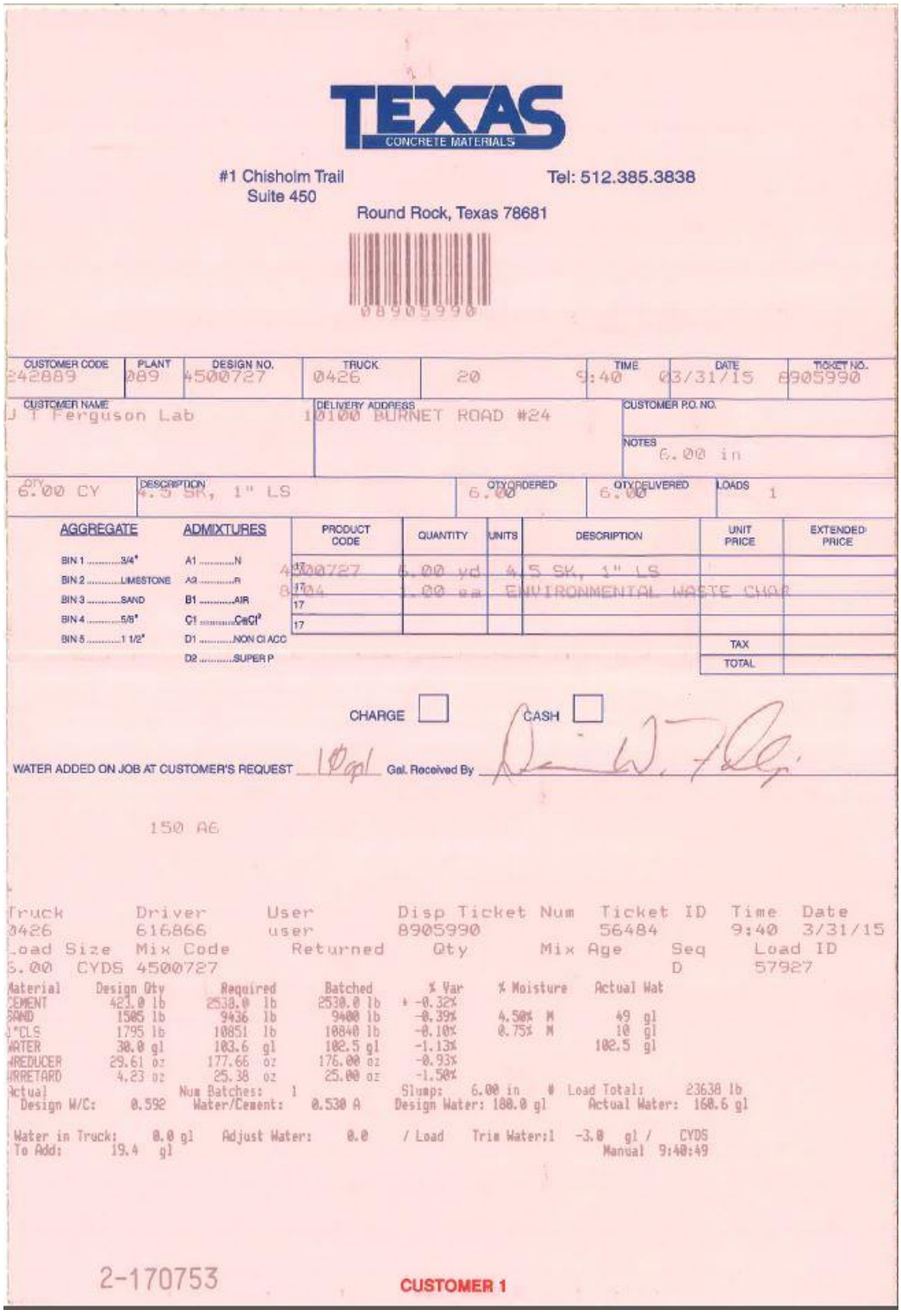

TEXAS
CONCRETE MATERIALS

#1 Chisholm Trail
Suite 450
Round Rock, Texas 78681

Tel: 512.385.3838

08905990

CUSTOMER CODE	PLANT	DESIGN NO.	TRUCK		TIME	DATE	TICKET NO.
242889	089	4500727	0426	20	9:40	03/31/15	8905990

CUSTOMER NAME: J T Ferguson Lab
DELIVERY ADDRESS: 10100 BURNET ROAD #24
CUSTOMER P.O. NO.:
NOTES: 6.00 in

QTY	DESCRIPTION	QTY ORDERED	QTY DELIVERED	LOADS
6.00 CY	4.5 SK, 1" LS	6.00	6.00	1

AGGREGATE
BIN 1 .....3/4"
BIN 2 .....LIMESTONE
BIN 3 .....SAND
BIN 4 .....5/8"
BIN 5 .....1 1/2"

ADMIXTURES
A1 .....N
A3 .....R
B1 .....AIR
C1 .....CaCl²
D1 .....NON CI ACC
D2 .....SUPER P

PRODUCT CODE	QUANTITY	UNITS	DESCRIPTION	UNIT PRICE	EXTENDED PRICE
17 4500727	6.00	yd	4.5 SK, 1" LS		
17 8004	1.00	ea	ENVIRONMENTAL WASTE CHAR		
17					
17					
				TAX	
				TOTAL	

CHARGE ☐ CASH ☐

WATER ADDED ON JOB AT CUSTOMER'S REQUEST 10 gal Gal. Received By

150 A6

Truck	Driver	User	Disp Ticket Num	Ticket ID	Time	Date
0426	616866	user	8905990	56484	9:40	3/31/15

Load Size	Mix Code	Returned	Qty	Mix Age	Seq	Load ID
6.00 CYDS	4500727				D	57927

Material	Design Qty	Required	Batched	% Var	% Moisture	Actual Wat
CEMENT	421.0 lb	2538.0 lb	2530.0 lb	+ -0.32%		
SAND	1565 lb	9436 lb	9400 lb	-0.39%	4.50% M	49 gl
1"CLS	1795 lb	10851 lb	10840 lb	-0.10%	0.75% M	10 gl
WATER	30.0 gl	183.6 gl	182.5 gl	-1.13%		182.5 gl
WREDUCER	29.61 oz	177.66 oz	176.00 oz	-0.93%		
WRETARD	4.23 oz	25.38 oz	25.00 oz	-1.50%		

Actual Num Batches: 1 Slump: 6.00 in # Load Total: 23638 lb
Design W/C: 0.592 Water/Cement: 0.530 A Design Water: 180.0 gl Actual Water: 160.6 gl

Water in Truck: 0.0 gl Adjust Water: 0.0 / Load Trim Water:1 -3.0 gl / CYDS
To Add: 19.4 gl Manual 9:40:49

2-170753

CUSTOMER 1

Figure B-2: LD5 Batch Ticket

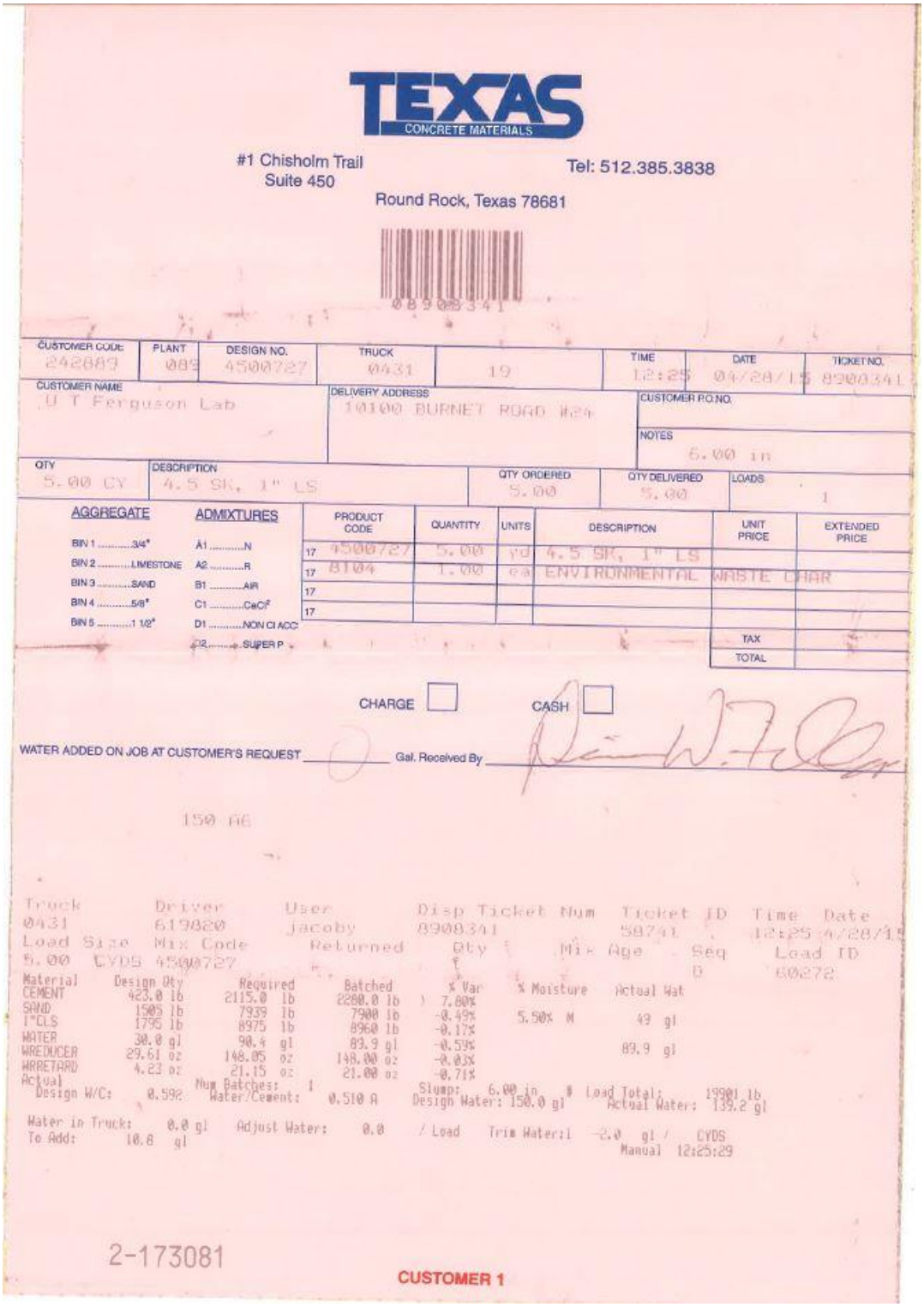

TEXAS
CONCRETE MATERIALS

#1 Chisholm Trail
Suite 450
Round Rock, Texas 78681

Tel: 512.385.3838

8900341

CUSTOMER CODE	PLANT	DESIGN NO.	TRUCK		TIME	DATE	TICKET NO.
242883	089	4500727	0431	19	12:25	04/28/15	8900341

CUSTOMER NAME: U T Ferguson Lab
DELIVERY ADDRESS: 10100 BURNET ROAD #24
CUSTOMER P.O.NO.:
NOTES: 6.00 in

QTY	DESCRIPTION	QTY ORDERED	QTY DELIVERED	LOADS
5.00 CY	4.5 SK, 1" LS	5.00	5.00	1

AGGREGATE
BIN 1 .....3/4"
BIN 2 .....LIMESTONE
BIN 3 .....SAND
BIN 4 .....5/8"
BIN 5 .....1 1/2"

ADMIXTURES
A1 .....N
A2 .....R
B1 .....AIR
C1 .....CaCl2
D1 .....NON CI ACC
D2 .....SUPER P

PRODUCT CODE	QUANTITY	UNITS	DESCRIPTION	UNIT PRICE	EXTENDED PRICE
17 4500727	5.00	yd	4.5 SK, 1" LS		
17 BT04	1.00	ea	ENVIRONMENTAL WASTE CHAR		
17					
17					
				TAX	
				TOTAL	

CHARGE ☐ CASH ☐

WATER ADDED ON JOB AT CUSTOMER'S REQUEST 0 Gal. Received By

150 66

Truck	Driver	User	Disp Ticket Num	Ticket ID	Time	Date
0431	619820	jacoby	8900341	58741	12:25	4/28/15

Load Size	Mix Code	Returned	Qty	Mix Age	Seq	Load ID
5.00 CYDS	4500727				0	60272

Material	Design Qty	Required	Batched	% Var	% Moisture	Actual Wat
CEMENT	423.0 lb	2115.0 lb	2280.0 lb	7.80%		
SAND	1585 lb	7939 lb	7900 lb	-0.49%	5.50% M	43 gl
1"CLS	1795 lb	8975 lb	8960 lb	-0.17%		
WATER	30.0 gl	90.4 gl	89.9 gl	-0.59%		89.9 gl
WREDUCER	29.61 oz	148.05 oz	148.00 oz	-0.03%		
WRRETARD	4.22 oz	21.15 oz	21.00 oz	-0.71%		

Actual Design W/C: 0.592 Num Batches: 1 Water/Cement: 0.510 A Slump: 6.00 in # Load Total: 19901 lb Design Water: 150.0 gl Actual Water: 139.2 gl

Water in Truck: 0.0 gl Adjust Water: 0.0 / Load Trim Water:1 -2.0 gl / CYDS
To Add: 10.8 gl Manual 12:25:29

2-173081

CUSTOMER 1

Figure B-3: LD6 Batch Ticket

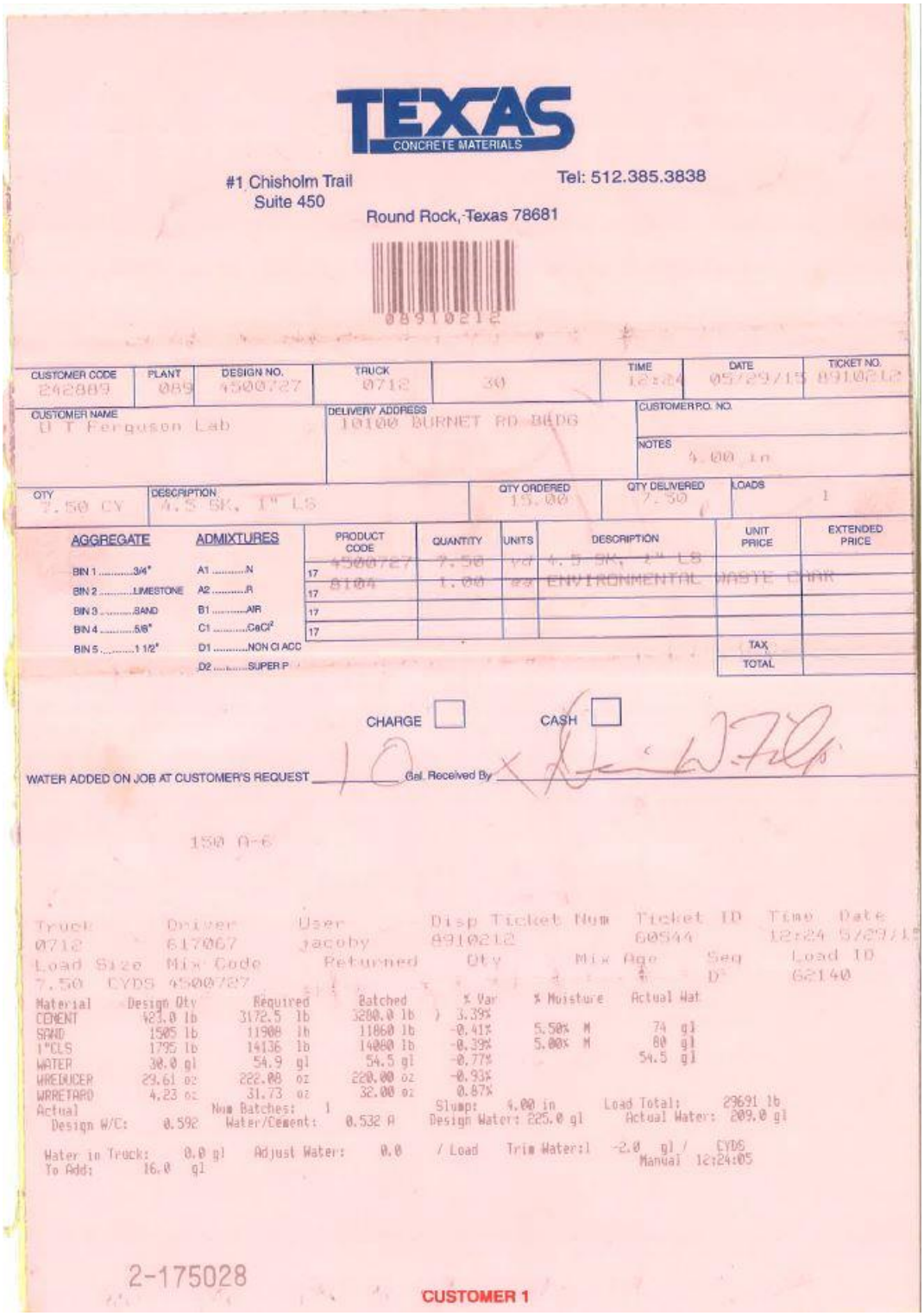

TEXAS
CONCRETE MATERIALS

#1 Chisholm Trail
Suite 450
Round Rock, Texas 78681

Tel: 512.385.3838

8891021?

CUSTOMER CODE	PLANT	DESIGN NO.	TRUCK		TIME	DATE	TICKET NO.
242889	089	4500727	0712	30	12:24	05/29/15	8910212

CUSTOMER NAME	DELIVERY ADDRESS	CUSTOMER P.O. NO.
U T Ferguson Lab	10100 BURNET RD BLDG	
		NOTES: 4.00 in

QTY	DESCRIPTION	QTY ORDERED	QTY DELIVERED	LOADS
7.50 CY	4.5 SK, 1" LS	15.00	7.50	1

AGGREGATE
BIN 1 .....3/4"
BIN 2 .....LIMESTONE
BIN 3 .....SAND
BIN 4 .....5/8"
BIN 5 .....1 1/2"

ADMIXTURES
A1 .....N
A2 .....R
B1 .....AIR
C1 .....$CaCl^2$
D1 .....NON CI ACC
D2 .....SUPER P

PRODUCT CODE	QUANTITY	UNITS	DESCRIPTION	UNIT PRICE	EXTENDED PRICE
17 4500727	7.50	yd	4.5 SK, 1" LS		
17 8104	1.00	ea	ENVIRONMENTAL WASTE DISP		
17					
17					
				TAX	
				TOTAL	

CHARGE ☐ CASH ☐

WATER ADDED ON JOB AT CUSTOMER'S REQUEST 10 Gal. Received By X

150 A-6

Truck	Driver	User	Disp Ticket Num	Ticket ID	Time	Date
0712	617067	jacoby	8910212	60544	12:24	5/29/15

Load Size	Mix Code	Returned	Qty	Mix Age	Seq	Load ID
7.50 CYDS	4500727				D	62140

Material	Design Qty	Required	Batched	% Var	% Moisture	Actual Wat
CEMENT	423.0 lb	3172.5 lb	3200.0 lb	3.39%		
SAND	1505 lb	11908 lb	11860 lb	-0.41%	5.50% M	74 gl
1"CLS	1795 lb	14136 lb	14080 lb	-0.39%	5.00% M	80 gl
WATER	30.0 gl	54.9 gl	54.5 gl	-0.77%		54.5 gl
WREDUCER	29.61 oz	222.08 oz	220.00 oz	-0.93%		
WRRETARD	4.23 oz	31.73 oz	32.00 oz	0.87%		

Actual Num Batches: 1 Slump: 4.00 in Load Total: 29691 lb
Design W/C: 0.592 Water/Cement: 0.532 A Design Water: 225.0 gl Actual Water: 209.0 gl

Water in Truck: 0.0 gl Adjust Water: 0.0 / Load Trim Water: -2.0 gl / CYDS
To Add: 16.0 gl Manual 12:24:05

2-175028

CUSTOMER 1

Figure B-4: LD7-1 Batch Ticket

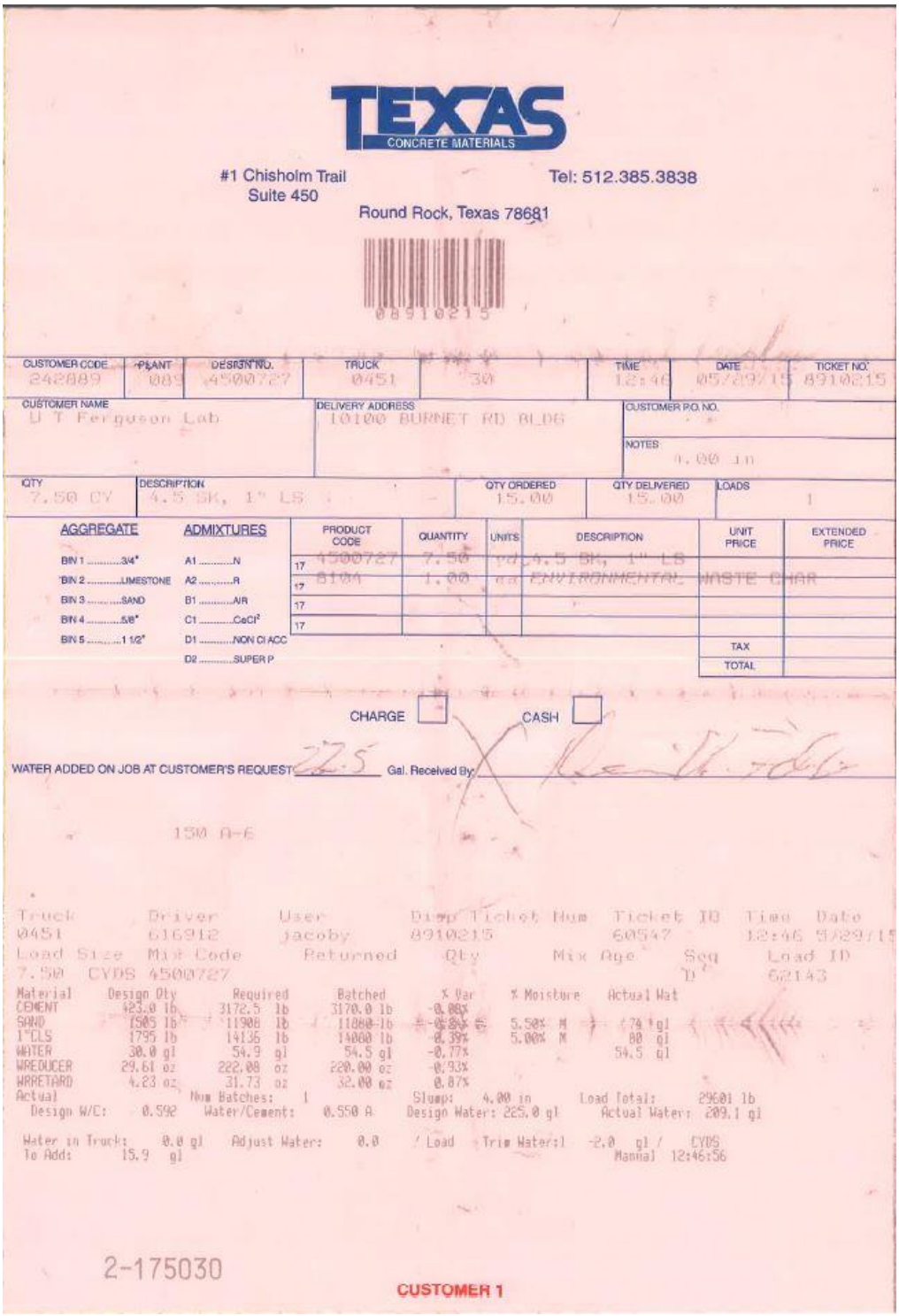

TEXAS
CONCRETE MATERIALS

#1 Chisholm Trail
Suite 450
Round Rock, Texas 78681

Tel: 512.385.3838

08910215

CUSTOMER CODE	PLANT	DESIGN NO.	TRUCK		TIME	DATE	TICKET NO.
242889	089	4500727	0451	30	12:46	05/29/15	8910215

CUSTOMER NAME	DELIVERY ADDRESS	CUSTOMER P.O. NO.
U T Ferguson Lab	10100 BURNET RD BLDG	NOTES 1.00 in

QTY	DESCRIPTION	QTY ORDERED	QTY DELIVERED	LOADS
7.50 CY	4.5 SK, 1" LS	15.00	15.00	1

AGGREGATE	ADMIXTURES
BIN 1 .....3/4"	A1 .....N
BIN 2 .....LIMESTONE	A2 .....R
BIN 3 .....SAND	B1 .....A/R
BIN 4 .....5/8"	C1 .....$CaCl^2$
BIN 5 .....1 1/2"	D1 .....NON CI ACC
	D2 .....SUPER P

	PRODUCT CODE	QUANTITY	UNITS	DESCRIPTION	UNIT PRICE	EXTENDED PRICE
17	4500727	7.50	yd	4.5 SK, 1" LS		
17	B10A	1.00	ea	ENVIRONMENTAL WASTE CHAR		
17						
17						
					TAX	
					TOTAL	

CHARGE ☐ CASH ☐

WATER ADDED ON JOB AT CUSTOMER'S REQUEST 22.5 Gal. Received By:

150 A-E

Truck	Driver	User	Dump Ticket Num	Ticket ID	Time	Date
0451	616912	jacoby	8910215	60547	12:46	5/29/15

Load Size	Mix Code	Returned	Qty	Mix Age	Seq	Load ID
7.50 CYDS	4500727				D	62143

Material	Design Qty	Required	Batched	% Var	% Moisture	Actual Wat
CEMENT	423.0 lb	3172.5 lb	3170.0 lb	-0.08%		
SAND	1585 lb	11908 lb	11080 lb	-6.96%	5.50% M	674 gl
1"CLS	1795 lb	14136 lb	14000 lb	-0.39%	5.00% M	80 gl
WATER	30.0 gl	54.9 gl	54.5 gl	-0.77%		54.5 gl
WRREDUCER	29.61 oz	222.08 oz	220.00 oz	-0.93%		
WRRETARD	4.23 oz	31.73 oz	32.00 oz	0.87%		

Actual Num Batches: 1 Slump: 4.00 in Load Total: 29601 lb
Design W/C: 0.592 Water/Cement: 0.550 A Design Water: 225.0 gl Actual Water: 209.1 gl

Water in Truck: 0.0 gl Adjust Water: 0.0 / Load Trim Water:1 -2.0 gl / CYDS
To Add: 15.9 gl Manual 12:46:56

2-175030

CUSTOMER 1

Figure B-5: LD7-2 Batch Ticket

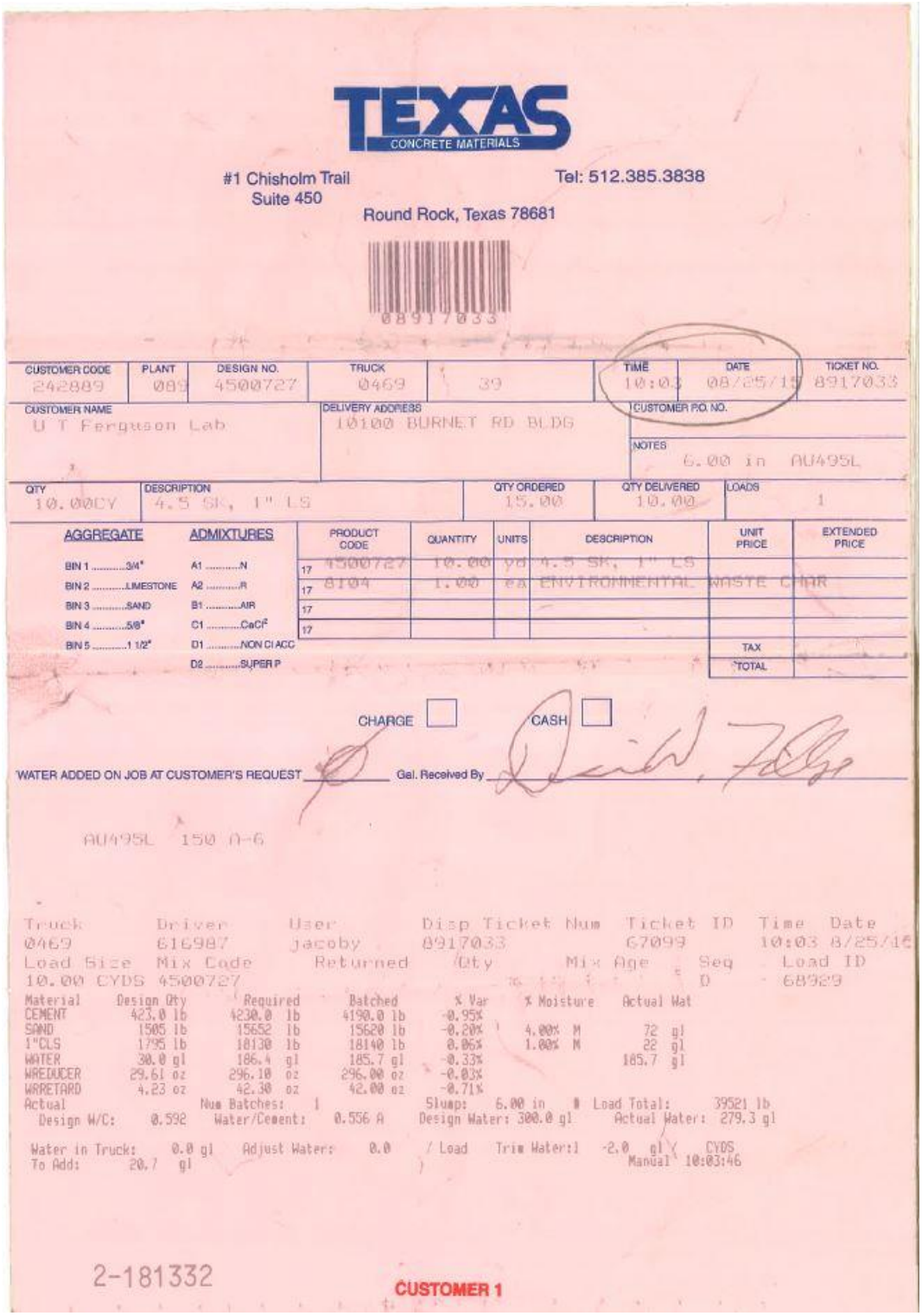

TEXAS
CONCRETE MATERIALS

#1 Chisholm Trail
Suite 450
Round Rock, Texas 78681

Tel: 512.385.3838

08917033

CUSTOMER CODE	PLANT	DESIGN NO.	TRUCK		TIME	DATE	TICKET NO.
242889	089	4500727	0469	39	10:03	08/25/15	8917033

CUSTOMER NAME: U T Ferguson Lab
DELIVERY ADDRESS: 10100 BURNET RD BLDG
CUSTOMER PO NO.:
NOTES: 6.00 in AU495L

QTY	DESCRIPTION	QTY ORDERED	QTY DELIVERED	LOADS
10.00CY	4.5 SK, 1" LS	15.00	10.00	1

AGGREGATE
BIN 1 .....3/4"
BIN 2 .....LIMESTONE
BIN 3 .....SAND
BIN 4 .....5/8"
BIN 5 .....1 1/2"

ADMIXTURES
A1 .....N
A2 .....R
B1 .....AIR
C1 .....$CaCl^2$
D1 .....NON CI ACC
D2 .....SUPER P

PRODUCT CODE	QUANTITY	UNITS	DESCRIPTION	UNIT PRICE	EXTENDED PRICE
17 4500727	10.00	yd	4.5 SK, 1" LS		
17 8104	1.00	ea	ENVIRONMENTAL WASTE CHAR		
17					
17					
				TAX	
				TOTAL	

CHARGE ☐ CASH ☐

WATER ADDED ON JOB AT CUSTOMER'S REQUEST _____ Gal. Received By _____

AU495L 150 A-6

Truck	Driver	User	Disp Ticket Num	Ticket ID	Time	Date
0469	616987	jacoby	8917033	67099	10:03	8/25/15

Load Size	Mix Code	Returned	Qty	Mix Age	Seq	Load ID
10.00 CYDS	4500727				D	68929

Material	Design Qty	Required	Batched	% Var	% Moisture	Actual Wat
CEMENT	423.0 lb	4230.0 lb	4190.0 lb	-0.95%		
SAND	1505 lb	15652 lb	15620 lb	-0.20%	4.00% M	72 gl
1"CLS	1795 lb	18130 lb	18140 lb	0.06%	1.00% M	22 gl
WATER	30.0 gl	186.4 gl	185.7 gl	-0.33%		185.7 gl
WREDUCER	29.61 oz	296.10 oz	296.00 oz	-0.03%		
WRRETARD	4.23 oz	42.30 oz	42.00 oz	-0.71%		

Actual Num Batches: 1 Slump: 6.00 in B Load Total: 39521 lb
Design W/C: 0.592 Water/Cement: 0.556 A Design Water: 300.0 gl Actual Water: 279.3 gl

Water in Truck: 0.0 gl Adjust Water: 0.0 / Load Trim Water:1 -2.0 gl Y CYDS
To Add: 20.7 gl Manual 10:03:46

2-181332

CUSTOMER 1

Figure B-6: LD8-1 Batch Ticket

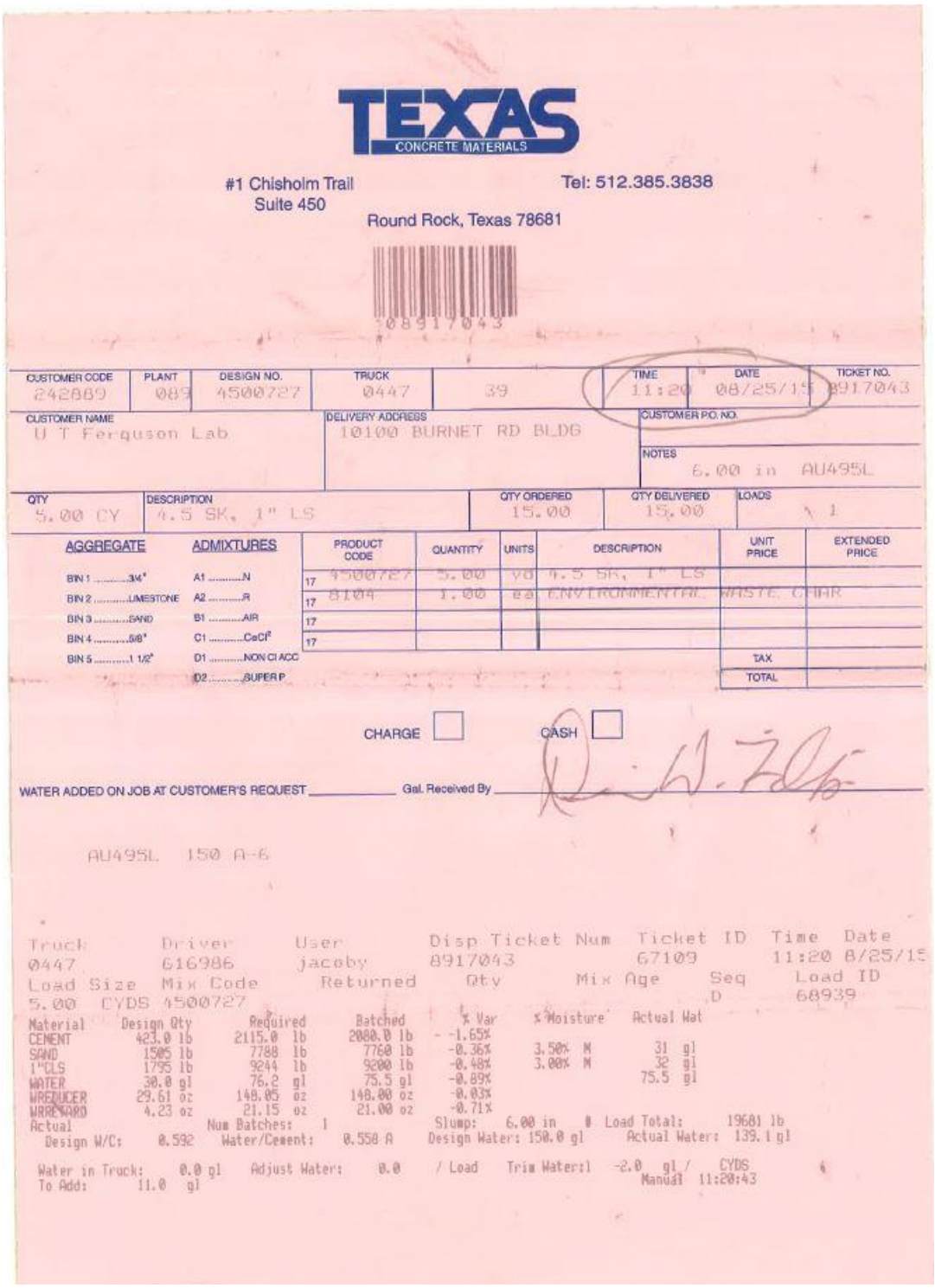

TEXAS
CONCRETE MATERIALS

#1 Chisholm Trail
Suite 450
Round Rock, Texas 78681

Tel: 512.385.3838

08917043

CUSTOMER CODE	PLANT	DESIGN NO.	TRUCK		TIME	DATE	TICKET NO.
242889	089	4500727	0447	39	11:20	08/25/15	8917043

CUSTOMER NAME: U T Ferguson Lab
DELIVERY ADDRESS: 10100 BURNET RD BLDG
CUSTOMER P.O. NO.:
NOTES: 6.00 in AU495L

QTY	DESCRIPTION	QTY ORDERED	QTY DELIVERED	LOADS
5.00 CY	4.5 SK, 1" LS	15.00	15.00	1

AGGREGATE
BIN 1 .....3/4"
BIN 2 .....LIMESTONE
BIN 3 .....SAND
BIN 4 .....5/8"
BIN 5 .....1 1/2"

ADMIXTURES
A1 .....N
A2 .....R
B1 .....AIR
C1 .....CaCl2
D1 .....NON CI ACC
D2 .....SUPER P

PRODUCT CODE	QUANTITY	UNITS	DESCRIPTION	UNIT PRICE	EXTENDED PRICE
17 4500727	5.00	yd	4.5 SK, 1" LS		
17 8104	1.00	ea	ENVIRONMENTAL WASTE CHAR		
17					
17					
				TAX	
				TOTAL	

CHARGE ☐ CASH ☐

WATER ADDED ON JOB AT CUSTOMER'S REQUEST _____ Gal. Received By _____

AU495L 150 A-6

Truck	Driver	User	Disp Ticket Num	Ticket ID	Time	Date
0447	616986	jacoby	8917043	67109	11:20	8/25/15

Load Size	Mix Code	Returned	Qty	Mix Age	Seq	Load ID
5.00 CYDS	4500727				D	68939

Material	Design Qty	Required	Batched	% Var	% Moisture	Actual Wat
CEMENT	423.0 lb	2115.0 lb	2080.0 lb	-1.65%		
SAND	1505 lb	7788 lb	7760 lb	-0.36%	3.50% M	31 gl
1"CLS	1795 lb	9244 lb	9200 lb	-0.48%	3.00% M	32 gl
WATER	30.0 gl	76.2 gl	75.5 gl	-0.89%		75.5 gl
WRREDUCER	29.61 oz	148.05 oz	148.00 oz	-0.03%		
WRRETARD	4.23 oz	21.15 oz	21.00 oz	-0.71%		

Actual Num Batches: 1 Slump: 6.00 in @ Load Total: 19681 lb
Design W/C: 0.592 Water/Cement: 0.550 A Design Water: 150.0 gl Actual Water: 139.1 gl

Water in Truck: 0.0 gl Adjust Water: 0.0 / Load Trim Water:1 -2.0 gl / CYDS
To Add: 11.0 gl Manual 11:20:43

Figure B-7: LD8-2 Batch Ticket

Table B-1: LD5 Concrete Compressive Strength Data

Age	Date	Time	D (in.)	L_1 (in.)	L_2 (in.)	L_3 (in.)	L_4 (in.)	L_{AVG} (in.)	L/D	Max. Load (lb)	Failure Type	f'_c (psi)
3	04/03/15	11:45 AM	4.012	7.8	7.8	7.8	7.8	7.8	1.95	41,416	III	3,280
3	04/03/15	11:48 AM	4.012	7.9	7.9	7.9	7.9	7.9	1.96	40,771	III	3,230
3	04/03/15	11:51 AM	4.011	7.9	7.9	7.9	7.9	7.9	1.96	42,044	III	3,330
7	04/07/15	1:47 PM	4.015	7.8	7.8	7.8	7.8	7.8	1.95	52,686	III	4,160
7	04/07/15	1:53 PM	4.012	7.8	7.8	7.8	7.8	7.8	1.95	50,778	III	4,020
7	04/07/15	1:57 PM	4.012	7.8	7.8	7.8	7.8	7.8	1.95	50,277	III	3,980
28	04/28/15	10:41 AM	4.010	7.8	7.8	7.8	7.8	7.8	1.96	64,481	III	5,110
28	04/28/15	10:46 AM	4.010	7.9	7.9	7.9	7.9	7.9	1.96	65,483	III	5,190
28	04/28/15	10:51 AM	4.010	7.8	7.8	7.8	7.8	7.8	1.96	66,556	III	5,270
127	08/05/15	2:47 PM	4.018	7.8	7.8	7.8	7.8	7.8	1.95	60,637	III	4,780
127	08/05/15	2:52 PM	4.011	7.8	7.8	7.8	7.8	7.8	1.94	61,034	III	4,830
127	08/05/15	2:59 PM	4.011	7.9	7.9	7.9	7.9	7.9	1.96	53,538	III	4,240*
127	08/05/15	3:04 PM	4.009	7.8	7.8	7.8	7.9	7.8	1.96	53,728	III	4,260*

*Discarded because of inconsistencies with 28-day strength due to field-curing conditions

Table B-2: LD6 Concrete Compressive Strength Data

Age	Date	Time	D (in.)	L_1 (in.)	L_2 (in.)	L_3 (in.)	L_4 (in.)	L_{AVG} (in.)	L/D	Max. Load (lb)	Failure Type	f'_c (psi)
3	05/01/15	11:13 AM	4.011	7.9	7.9	7.9	7.9	7.9	1.96	37,098	III	2,940
3	05/01/15	11:17 AM	4.011	7.9	7.9	7.9	7.9	7.9	1.96	37,640	III	2,980
3	05/01/15	11:22 AM	4.008	7.9	7.9	7.9	7.9	7.9	1.97	36,462	III	2,890
7	05/05/15	10:27 AM	4.010	7.9	7.9	7.9	7.9	7.9	1.97	45,424	III	3,600
7	05/05/15	10:49 AM	4.011	7.8	7.9	7.9	7.8	7.8	1.96	46,147	III	3,650
7	05/05/15	10:56 AM	4.010	7.9	7.9	7.9	7.9	7.9	1.96	37,692	III	2,980
28	05/26/15	5:50 PM	4.011	7.9	7.9	7.9	7.9	7.9	1.98	54,940	III	4,350
28	05/26/15	5:54 PM	4.008	7.9	7.9	7.9	7.9	7.9	1.97	48,590	III	3,850
28	05/26/15	5:59 PM	4.009	7.9	7.9	7.9	7.9	7.9	1.96	58,878	III	4,660

Table B-3: LD7-1 Concrete Compressive Strength Data

Age	Date	Time	D (in.)	L_1 (in.)	L_2 (in.)	L_3 (in.)	L_4 (in.)	L_{AVG} (in.)	L/D	Max. Load (lb)	Failure Type	f'_c (psi)
3	06/01/15	2:43 PM	4.015	7.9	7.9	7.9	7.9	7.9	1.97	23,972	III	1,890
3	06/01/15	2:46 PM	4.018	7.9	7.9	7.9	7.9	7.9	1.97	24,067	III	1,900
3	06/01/15	2:49 PM	4.016	7.9	7.9	7.9	7.9	7.9	1.96	24,273	III	1,920
28	06/26/15	11:16 AM	4.015	7.9	7.9	7.9	7.9	7.9	1.96	41,743	III	3,300
28	06/26/15	11:19 AM	4.020	7.9	7.9	7.9	7.9	7.9	1.96	41,321	III	3,260
28	06/26/15	11:22 AM	4.014	7.9	7.9	7.9	7.9	7.9	1.96	43,506	III	3,440
34	07/02/15	5:15 PM	4.013	7.9	7.9	7.9	7.9	7.9	1.97	39,713	III	3,140
34	07/02/15	5:19 PM	4.014	7.9	7.9	7.9	7.9	7.9	1.96	43,162	III	3,410
34	07/02/15	5:24 PM	4.011	7.9	7.9	7.9	7.9	7.9	1.96	44,917	III	3,550
39	07/07/15	4:10 PM	4.012	7.9	7.9	7.9	7.9	7.9	1.96	43,214	III	3,420
39	07/07/15	4:13 PM	4.012	7.9	7.9	7.9	7.9	7.9	1.96	43,420	III	3,430
39	07/07/15	4:17 PM	4.013	7.9	7.9	7.9	7.9	7.9	1.97	43,532	III	3,440

Table B-4: LD7-2 Concrete Compressive Strength Data

Age	Date	Time	D (in.)	L_1 (in.)	L_2 (in.)	L_3 (in.)	L_4 (in.)	L_{AVG} (in.)	L/D	Max. Load (lb)	Failure Type	f'_c (psi)
3	06/01/15	2:52 PM	4.016	7.8	7.8	7.8	7.8	7.8	1.95	29,555	III	2,330
3	06/01/15	2:55 PM	4.018	7.9	7.9	7.9	7.9	7.9	1.96	29,684	III	2,340
3	06/01/15	2:58 PM	4.019	7.9	7.9	7.9	7.9	7.9	1.96	27,869	III	2,200
28	06/26/15	11:25 AM	4.012	8.0	8.0	8.0	7.9	8.0	1.98	46,414	III	3,670
28	06/26/15	11:29 AM	4.013	7.9	7.9	7.9	7.9	7.9	1.98	48,409	III	3,830
28	06/26/15	11:32 AM	4.014	7.9	7.9	7.9	7.9	7.9	1.97	46,697	III	3,690
34	07/02/15	5:29 PM	4.011	7.9	7.9	7.9	7.9	7.9	1.96	44,521	III	3,520
34	07/02/15	5:32 PM	4.015	7.9	7.9	7.9	7.9	7.9	1.98	43,179	III	3,410
34	07/02/15	5:36 PM	4.011	7.9	7.9	7.9	7.9	7.9	1.97	47,566	III	3,760
39	07/07/15	4:21 PM	4.012	7.9	7.9	7.9	7.9	7.9	1.97	47,945	III	3,790
39	07/07/15	4:26 PM	4.013	7.9	7.9	7.9	7.9	7.9	1.96	48,409	III	3,830
39	07/07/15	4:31 PM	4.013	7.9	7.9	7.9	7.9	7.9	1.96	48,048	III	3,800

Table B-5: LD8-1 Concrete Compressive Strength Data

Age	Date	Time	D (in.)	L_1 (in.)	L_2 (in.)	L_3 (in.)	L_4 (in.)	L_{AVG} (in.)	L/D	Max. Load (lb)	Failure Type	f'_c (psi)
3	08/28/15	1:13 PM	4.015	7.8	7.8	7.8	7.8	7.8	1.95	31,920	III	2,520
3	08/28/15	1:16 PM	4.015	7.8	7.8	7.8	7.8	7.8	1.95	29,864	III	2,360
3	08/28/15	1:19 PM	4.018	7.8	7.8	7.8	7.8	7.8	1.94	31,903	III	2,520
23	09/17/15	2:02 PM	4.015	7.8	7.9	7.9	7.8	7.8	1.96	47,850	III	3,780
23	09/17/15	2:05 PM	4.015	7.8	7.8	7.8	7.8	7.8	1.95	49,699	III	3,930
23	09/17/15	2:08 PM	4.015	7.8	7.8	7.8	7.8	7.8	1.95	49,011	III	3,870
28	09/22/15	3:55 PM	4.013	7.9	7.9	7.8	7.8	7.8	1.96	48,831	III	3,860
28	09/22/15	4:00 PM	4.016	7.8	7.8	7.8	7.8	7.8	1.95	49,295	III	3,890
28	09/22/15	4:04 PM	4.014	7.9	7.9	7.9	7.9	7.9	1.96	47,807	III	3,780
31	09/25/15	9:06 AM	4.017	7.8	7.8	7.8	7.8	7.8	1.95	52,675	III	4,160
31	09/25/15	9:11 AM	4.019	7.8	7.8	7.8	7.8	7.8	1.95	52,874	III	4,170
31	09/25/15	9:15 AM	4.017	7.8	7.8	7.8	7.8	7.8	1.95	52,822	III	4,170

Table B-6: LD8-2 Concrete Compressive Strength Data

Age	Date	Time	D (in.)	L_1 (in.)	L_2 (in.)	L_3 (in.)	L_4 (in.)	L_{AVG} (in.)	L/D	Max. Load (lb)	Failure Type	f'_c (psi)
3	08/28/15	1:22 PM	4.019	7.8	7.8	7.8	7.9	7.8	1.95	39,317	III	3,100
3	08/28/15	1:25 PM	4.015	7.9	7.9	7.9	7.9	7.9	1.97	37,434	III	2,960
3	08/28/15	1:29 PM	4.020	7.9	7.9	7.9	7.9	7.9	1.95	39,154	III	3,080
23	09/17/15	2:14 PM	4.013	7.8	7.8	7.8	7.8	7.8	1.95	59,194	III	4,680
23	09/17/15	2:18 PM	4.015	7.9	7.9	7.9	7.9	7.9	1.96	58,530	III	4,620
23	09/17/15	2:23 PM	4.015	7.9	7.9	7.9	7.9	7.9	1.97	58,193	III	4,600
28	09/22/15	4:08 PM	4.015	7.9	7.9	7.9	7.9	7.9	1.96	61,017	III	4,820
28	09/22/15	4:12 PM	4.018	7.9	7.9	7.9	7.9	7.9	1.97	59,566	III	4,700
28	09/22/15	4:16 PM	4.016	7.9	7.9	7.9	7.9	7.9	1.97	60,300	III	4,760
31	09/25/15	11:40 AM	4.020	7.8	7.8	7.8	7.8	7.8	1.95	58,124	III	4,580
31	09/25/15	11:43 AM	4.017	7.9	7.9	7.9	7.9	7.9	1.97	59,152	III	4,670
31	09/25/15	11:46 AM	4.018	7.9	7.9	7.9	7.9	7.9	1.96	56,630	III	4,470

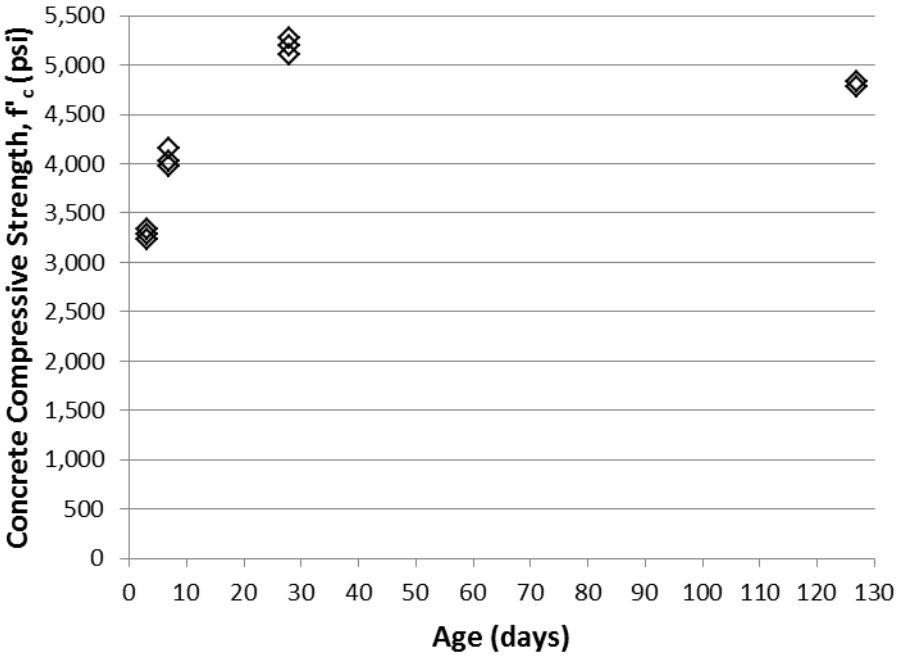

Figure B-8: LD5 Concrete Compressive Strength Development

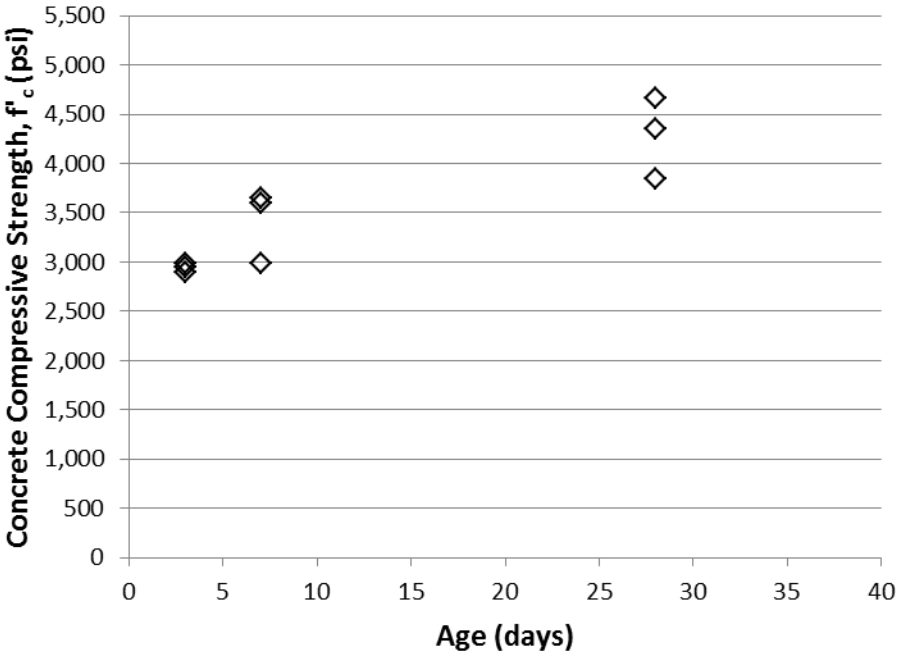

Figure B-9: LD6 Concrete Compressive Strength Development

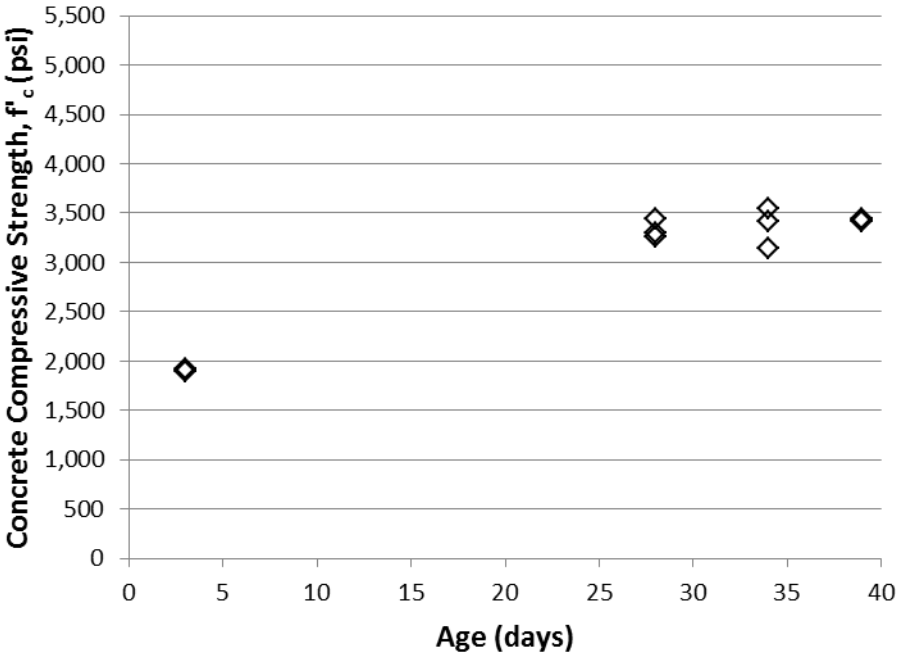

Figure B-10: LD7-1 Concrete Compressive Strength Development

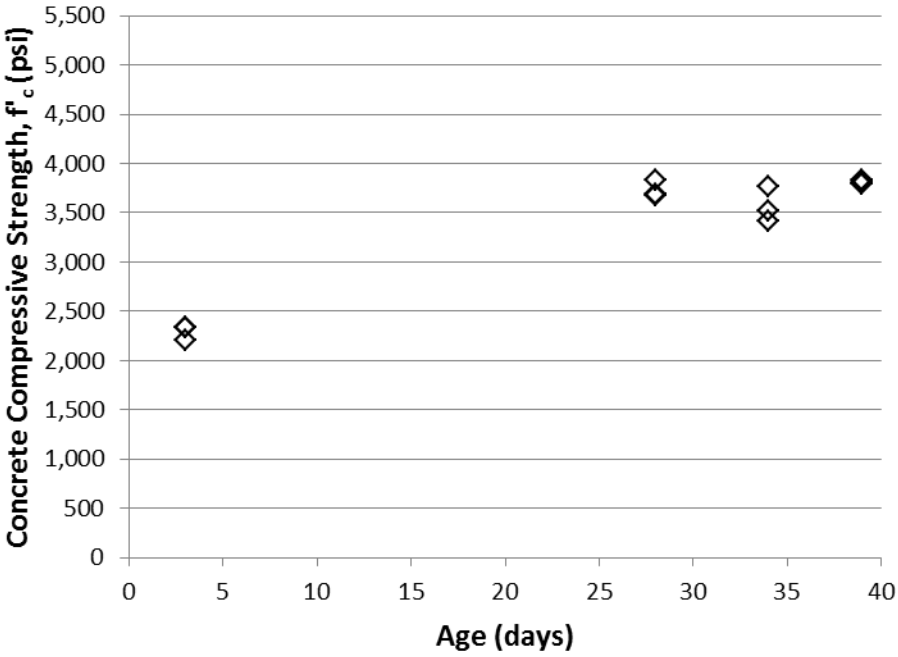

Figure B-11: LD7-2 Concrete Compressive Strength Development

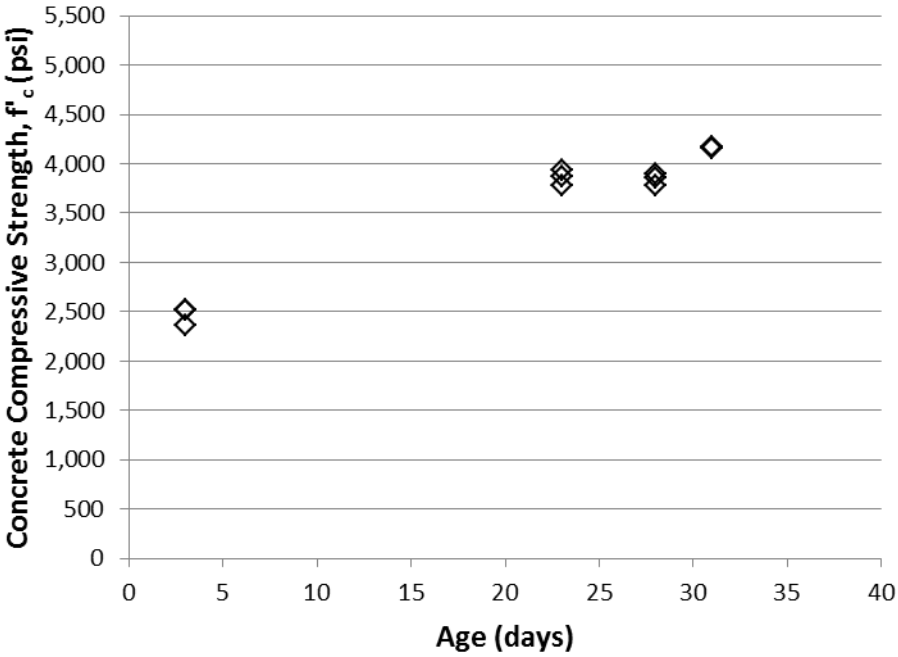

Figure B-12: LD8-1 Concrete Compressive Strength Development

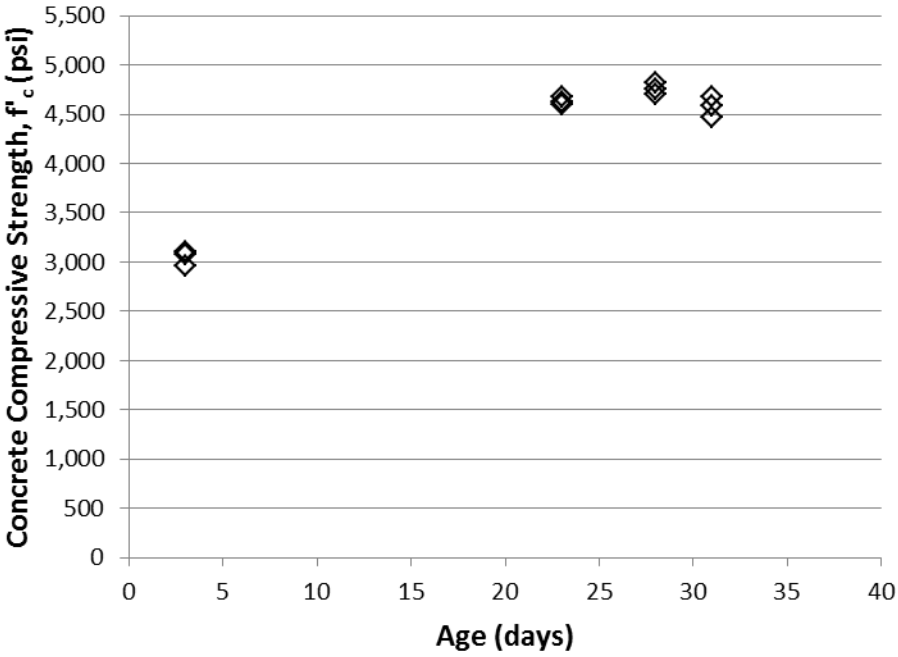

Figure B-13: LD8-2 Concrete Compressive Strength Development

Table B-7: Concrete Modulus of Elasticity Data

Batch ID	Date	Time	D (in.)	L_1 (in.)	L_2 (in.)	L_3 (in.)	L_4 (in.)	L_{AVG} (in.)	L/D	# of Cycles	E_c (ksi)
LD5	04/28/15	11:34 AM	4.008	7.8	7.8	7.8	7.8	7.8	1.96	2	4,470
LD5	04/28/15	11:45 AM	4.009	7.8	7.8	7.8	7.8	7.8	1.96	2	3,810
LD5	04/28/15	11:58 AM	4.009	7.9	7.9	7.9	7.9	7.9	1.97	2	3,790
LD6	05/26/15	6:12 PM	4.008	7.9	7.9	7.9	7.9	7.9	1.96	2	4,560
LD6	05/26/15	6:24 PM	4.008	7.9	7.9	7.9	7.9	7.9	1.97	2	3,910
LD6	05/26/15	6:38 PM	4.009	8.0	8.0	7.9	7.9	8.0	1.98	2	4,560
LD7-1	06/26/15	11:55 AM	4.014	7.9	7.9	7.9	7.9	7.9	1.97	2	4,180
LD7-1	06/26/15	1:24 PM	4.016	7.8	7.8	7.8	7.8	7.8	1.95	2	4,220
LD7-1	06/26/15	1:39 PM	4.016	7.9	7.9	7.9	7.9	7.9	1.97	2	3,680
LD7-2	06/26/15	2:00 PM	4.013	7.9	7.9	7.9	7.9	7.9	1.97	2	4,390
LD7-2	06/26/15	2:22 PM	4.019	7.9	7.9	7.9	7.9	7.9	1.96	2	3,950
LD7-2	06/26/15	2:43 PM	4.018	7.9	7.9	7.9	7.9	7.9	1.96	2	3,710
LD8-1	09/22/15	5:14 PM	4.013	7.9	7.9	7.9	7.8	7.9	1.96	2	4,650
LD8-1	09/22/15	5:24 PM	4.015	7.9	7.9	7.9	7.9	7.9	1.96	2	3,940
LD8-1	09/22/15	5:33 PM	4.020	7.8	7.8	7.8	7.8	7.8	1.95	2	3,610
LD8-2	09/22/15	4:23 PM	4.016	7.9	7.9	7.9	7.9	7.9	1.97	2	4,180
LD8-2	09/22/15	4:34 PM	4.018	7.9	7.9	7.9	7.9	7.9	1.96	2	4,590
LD8-2	09/22/15	4:46 PM	4.016	7.9	7.9	7.9	7.9	7.9	1.96	2	4,170

Table B-8: Concrete Tensile Strength Data

Batch ID	Date	Time	L_1 (in.)	L_2 (in.)	L_{AVG} (in.)	D_1 (in.)	D_2 (in.)	D_3 (in.)	D_{AVG} (in.)	Max. Load (lb)	f'_t (psi)
LD5	04/28/15	2:59 PM	7.8400	7.8490	7.8445	4.011	4.010	4.009	4.010	26,235	530
LD5	04/28/15	3:05 PM	7.8565	7.8455	7.8510	4.010	4.011	4.012	4.011	25,237	510
LD5	04/28/15	3:11 PM	7.8420	7.8430	7.8425	4.012	4.012	4.012	4.012	25,693	520
LD6	05/26/15	3:49 PM	7.9080	7.9100	7.9090	4.011	4.011	4.011	4.011	23,585	475
LD6	05/26/15	5:28 PM	7.8990	7.8920	7.8955	4.011	4.010	4.011	4.011	22,622	455
LD6	05/26/15	5:37 PM	7.8825	7.8850	7.8838	4.010	4.012	4.012	4.011	23,852	480
LD7-1	06/26/15	3:28 PM	7.9120	7.9005	7.9063	4.017	4.013	4.013	4.014	20,420	410
LD7-1	06/26/15	3:32 PM	7.8610	7.8665	7.8638	4.016	4.015	4.015	4.015	19,353	390
LD7-1	06/26/15	3:37 PM	7.8715	7.8770	7.8743	4.014	4.013	4.015	4.014	20,084	405
LD7-2	06/26/15	3:42 PM	7.8755	7.8815	7.8785	4.016	4.016	4.018	4.017	21,607	435
LD7-2	06/26/15	3:47 PM	7.9490	7.9415	7.9453	4.014	4.014	4.014	4.014	22,484	450
LD7-2	06/26/15	3:52 PM	7.9360	7.9435	7.9398	4.012	4.012	4.012	4.012	23,852	475
LD8-1	09/22/15	6:02 PM	7.8665	7.8720	7.8693	4.007	4.015	4.016	4.013	22,312	450
LD8-1	09/22/15	6:06 PM	7.8570	7.8545	7.8558	4.017	4.015	4.023	4.018	21,486	435
LD8-1	09/22/15	6:10 PM	7.8530	7.8430	7.8480	4.012	4.015	4.025	4.017	22,269	450
LD8-2	09/22/15	5:48 PM	7.8345	7.8380	7.8363	4.020	4.015	4.021	4.019	23,009	465
LD8-2	09/22/15	5:53 PM	7.8765	7.8800	7.8783	4.016	4.018	4.024	4.019	24,712	495
LD8-2	09/22/15	5:57 PM	7.8380	7.8305	7.8343	4.012	4.020	4.021	4.018	24,110	490

NUCOR

NUCOR CORPORATION
NUCOR STEEL TEXAS

Mill Certification
2/26/2015

MTR #: 0000085534
8812 Hwy 79 W
Jewett, TX 75846
(903) 626-4461
Fax: (903) 626-6290

Sold To: HARRIS REBAR NUFAB LLC
PO BOX 627
AUBURN, IN 46706
(936) 258-8221
Fax: (936) 258-9637

Ship To: HARRIS-SAN ANTONIO-CARRIER
N/A
NEW BRAUNFELS, TX 78130
(830) 387-2910

Customer P.O.	0000157619	Sales Order	215336.7
Product Group	Rebar	Part Number	900000366004200
Grade	ASTM A615/A615M-14 GR 60[420] AASHTO M31-07	Lot #	JW1510083002
Size	36/#11 Rebar	Heat #	JW15100830
Product	36/#11 Rebar 50' A615M GR420 (Gr60)	B.L. Number	J1-698724
Description	A615M GR 420 (Gr60)	Load Number	J1-301990
Customer Spec		Customer Part #	

I hereby certify that the material described herein has been manufactured in accordance with the specifications and standards listed above and that it satisfies those requirements.

Roll Date: 2/11/2015 Melt Date: 1/30/2015 Qty Shipped LBS: 16,205 Qty Shipped Pcs: 61

C	Mn	P	S	Si	Cu	Ni	Cr	Mo	V	Cb	CEA706
0.36%	0.98%	0.018%	0.027%	0.16%	0.29%	0.16%	0.26%	0.054%	0.0300%	0.001%	0.56%

CEA706: A706 CARBON EQUIVALENT

Yield 1: 75,700psi Tensile 1: 104,900psi Elongation: 16% in 8"(% in 203.3mm)

Bend OK

Specification Comments:

Comments: E-mail: websales@nstexas.com

1. All manufacturing processes of the steel, including melting, have been performed in the U.S.A.
2. Mercury in any form has not been used in the production or testing of this product.
3. Welding or weld repair was not performed on this material.
4. This material conforms to the specifications described on this document and may not be reproduced, except in full, without written approval of Nucor Corporation.
5. Results reported for ASTM E45 (Inclusion content) and ASTM E381 (Macro-etch) are provided as interpretation of ASTM procedures.

Bhargava R Vantari
Division Metallurgist

NBMG-10 January 1, 2012

Page 2 of 2

Figure B-14: LD5 Steel Mill Certification Test Report

NUCOR

NUCOR CORPORATION
NUCOR STEEL TEXAS

Mill Certification
4/6/2015

MTR #: 0000092015
8812 Hwy 79 W
Jewett, TX 75846
(903) 626-4461
Fax: (903) 626-6290

Sold To: HARRIS REBAR NUFAB LLC
PO BOX 627
AUBURN, IN 46706
(936) 258-8221
Fax: (936) 258-9637

Ship To: HARRIS-SAN ANTONIO-CARRIER
N/A
NEW BRAUNFELS, TX 78130
(830) 387-2910

Customer P.O.	0000159339	Sales Order	217015.9
Product Group	Rebar	Part Number	900000367204200
Grade	ASTM A615/A615M-14 GR 60[420] AASHTO M31-07	Lot #	JW1510083201
Size	36/#11 Rebar	Heat #	JW15100832
Product	36/#11 Rebar 60' A615M GR420 (Gr60)	B.L. Number	J1-701621
Description	A615M GR 420 (Gr60)	Load Number	J1-305122
Customer Spec		Customer Part #	

I hereby certify that the material described herein has been manufactured in accordance with the specifications and standards listed above and that it satisfies those requirements.

Roll Date: 2/11/2015 Melt Date: 1/30/2015 Qty Shipped LBS: 6,376 Qty Shipped Pcs: 20

C	Mn	P	S	Si	Cu	Ni	Cr	Mo	V	Cb	CEA706
0.36%	1.04%	0.012%	0.038%	0.19%	0.29%	0.20%	0.18%	0.062%	0.0278%	0.002%	0.56%

CEA706: A706 CARBON EQUIVALENT

Yield 1: 72,900psi Tensile 1: 103,100psi Elongation: 15% in 8"(% in 203.3mm)

Bend OK

Specification Comments:

Comments: E-mail: websales@nstexas.com

1. All manufacturing processes of the steel, including melting, have been performed in the U.S.A.
2. Mercury in any form has not been used in the production or testing of this product.
3. Welding or weld repair was not performed on this material.
4. This material conforms to the specifications described on this document and may not be reproduced, except in full, without written approval of Nucor Corporation.
5. Results reported for ASTM E45 (Inclusion content) and ASTM E381 (Macro-etch) are provided as interpretation of ASTM procedures.

Bhargava R Vantari
Division Metallurgist

NBMG-10 January 1, 2012

Page 2 of 2

Figure B-15: LD6 Steel Mill Certification Test Report

NUCOR
NUCOR CORPORATION
NUCOR STEEL TEXAS

Mill Certification
4/6/2015

MTR #: 0000092015
8812 Hwy 79 W
Jewett, TX 75846
(903) 626-4461
Fax: (903) 626-6290

Sold To: HARRIS REBAR NUFAB LLC
PO BOX 627
AUBURN, IN 46706
(936) 258-8221
Fax: (936) 258-9637

Ship To: HARRIS-SAN ANTONIO-CARRIER
N/A
NEW BRAUNFELS, TX 78130
(830) 387-2910

Customer P.O.	0000159339	Sales Order	217015.9
Product Group	Rebar	Part Number	900000367204200
Grade	ASTM A615/A615M-14 GR 60[420] AASHTO M31-07	Lot #	JW1510029101
Size	36/#11 Rebar	Heat #	JW15100291
Product	36/#11 Rebar 60' A615M GR420 (Gr60)	B.L. Number	J1-701621
Description	A615M GR 420 (Gr60)	Load Number	J1-305122
Customer Spec		Customer Part #	

I hereby certify that the material described herein has been manufactured in accordance with the specifications and standards listed above and that it satisfies those requirements.

Roll Date: 1/13/2015 Melt Date: 1/12/2015 Qty Shipped LBS: 38,256 Qty Shipped Pcs: 120

C	Mn	P	S	Si	Cu	Ni	Cr	Mo	V	Cb	CEA706
0.34%	0.97%	0.009%	0.040%	0.17%	0.32%	0.11%	0.12%	0.034%	0.0216%	0.001%	0.52%

CEA706: A706 CARBON EQUIVALENT

Yield 1: 65,500psi Tensile 1: 93,100psi Elongation: 12% in 8"(% in 203.3mm)

Bend OK

Specification Comments:

Comments: E-mail: websales@nstexas.com

1. All manufacturing processes of the steel, including melting, have been performed in the U.S.A.
2. Mercury in any form has not been used in the production or testing of this product.
3. Welding or weld repair was not performed on this material.
4. This material conforms to the specifications described on this document and may not be reproduced, except in full, without written approval of Nucor Corporation.
5. Results reported for ASTM E45 (Inclusion content) and ASTM E381 (Macro-etch) are provided as interpretation of ASTM procedures.

Bhargava R Vantari
Division Metallurgist

NBMG-10 January 1, 2012

Figure B-16: LD7 and LD8 Steel Mill Certification Test Report

LABORATORY TESTING INC.

2331 Topaz Drive, Hatfield, PA 19440
TEL: 800-219-9095 • FAX: 800-219-9096

Certified Test Report

UTA001-15-04-13456-1

Accredited Nadcap
Materials Testing Laboratory
Nondestructive Testing

SOLD TO
University of Texas at Austin
Ferguson Structural Engineering
10100 Burnet Road, Building 177
Austin, TX 78758

SHIP TO
University of Texas at Austin
Ferguson Structural Engineering
10100 Burnet Road, Building 177
Austin, TX 78758
ATTN: Joseph Klein

CUSTOMER P.O.	CERTIFICATION DATE	SHIP VIA
CREDIT-CARD	4/15/2015	EMAIL

DESCRIPTION

Quantity:	3	**Quantity:**	3
Description:	GR 60 No. 11 Rebar	**Description:**	GR 60 No. 11 Rebar
Project:	MPR 0326-0063	**Project:**	MPR 0326-0063
Identified as:	LD5-1, LD5-2 and LD5-3	**Identified as:**	48SR-1, 48SR-2 and 48SR-3
Reference:	ASTM A615-09	**Reference:**	ASTM A615-09

TENSILE TEST:
APPLICABLE SPECIFICATIONS: ASTM A615-09, Grade 60
KEY: C - Conforms NC - Non-Conformance R-Report for Information

SAMPLE ID	(psi) TENSILE STRENGTH	(psi) YIELD POINT STRESS	(%) ELONGATION IN 8" (MANUAL)	KEY C/NC/R
REQUIRED	Min	Min	Min	
	90,000	60,000	7	
LD5				
1	105,000	72,000	19	C
2	105,000	72,000	20	C
3	105,000	71,500	18	C
48SR				
1	104,000	71,500	19	C
2	104,000	71,500	20	C
3	104,000	71,500	18	C

Procedures/Methods: 86-TT-2, Rev. 14, Room Temp. Tensile Testing for Metallic Materials

The services performed above were done in accordance with LTI's Quality System Program Manual Revision 20 dated 12/12/12 and ISO/IEC 17025. These results relate only to the items tested and this report shall not be reproduced, except in full, without the written approval of Laboratory Testing, Inc. L.T.I. is accredited by Nadcap for NDT and Materials Testing for the test methods and specific services as listed in the Scopes of Accreditation available at www.labtesting.com and www.eAuditNet.com. The results reported on this test report represent the actual attributes of the material tested and indicate full compliance with all applicable specification and contract requirements.

MERCURY CONTAMINATION: During the testing and inspection, the product did not come in direct contact with mercury or any of its compounds nor with any mercury containing devices employing a single boundary of containment.

NOTE: The recording of false, fictitious or fraudulent statements or entries on this document may be punishable as a felony under Federal Statutes.

Frank Peszka
Director of Quality
Frank Peszka
Authorized Signature (ES)

Figure B-17: LD5 Steel Tensile Testing Report

LABORATORY TESTING INC.

2331 Topaz Drive, Hatfield, PA 19440
TEL: 800-219-9095 • FAX: 800-219-9096

Certified Test Report

UTA001-15-07-28641-1

Accredited Nadcap
Materials Testing Laboratory
Nondestructive Testing

SOLD TO
University of Texas at Austin
Ferguson Structural Engineering
10100 Burnet Road, Building 17
Austin, TX 78758

SHIP TO
University of Texas at Austin
Ferguson Structural Engineering
10100 Burnet Road, Building 17
Austin, TX 78758
ATTN: Joseph Klein

CUSTOMER P.O.	CERTIFICATION DATE	SHIP VIA
MPR-07/23/15	8/3/2015	EMAIL

DESCRIPTION

Quantity: 9
Description: GR. 60 No. 11 Rebar
Project: MPR 0326-0063
Identified as: LD6 1, LD6 2, LD6 3, LD7 1, LD7 2, LD7 3, LD8 1, LD8 2, LD8 3
Reference: ASTM A615-09

TENSILE TEST:
APPLICABLE SPECIFICATIONS: ASTM A615-09, Grade 60
KEY: C - Conforms NC - Non-Conformance R-Report for Information

SAMPLE ID	(psi) TENSILE STRENGTH	(psi) YIELD POINT STRESS	(%) ELONGATION IN 8" (MANUAL)	KEY C/NC/R
REQUIRED	Min	Min	Min	
	90,000	60,000	7	
LD6-1	110,000	75,000	16	C
LD6-2	109,000	74,500	14	C
LD6-3	110,000	74,000	18	C
LD7-1	95,500	65,000	22	C
LD7-2	95,500	64,500	21	C
LD7-3	96,000	65,000	21	C
LD8-1	96,000	64,500	20	C
LD8-2	96,000	64,500	23	C
LD8-3	96,500	65,500	19	C

Procedures/Methods: 86-TT-2, Rev. 15, Room Temp. Tensile Testing for Metallic Materials

The services performed above were done in accordance with LTI's Quality System Program Manual Revision 20 dated 12/12/12 and ISO/IEC 17025. These results relate only to the items tested and this report shall not be reproduced, except in full, without the written approval of Laboratory Testing, Inc. L.T.I. is accredited by Nadcap for NDT and Materials Testing for the test methods and specific services as listed in the Scopes of Accreditation available at www.labtesting.com and www.eAuditNet.com. The results reported on this test report represent the actual attributes of the material tested and indicate full compliance with all applicable specification and contract requirements.

MERCURY CONTAMINATION: During the testing and inspection, the product did not come in direct contact with mercury or any of its compounds nor with any mercury containing devices employing a single boundary of containment.

NOTE: The recording of false, fictitious or fraudulent statements or entries on this document may be punishable as a felony under Federal Statutes.

Sherri L. Scheifele
QA Specialist
Sherri L Scheifele
Authorized Signature

Figure B-18: LD6, LD7, and LD8 Steel Tensile Testing Report

Appendix C: Experimental Methods

Appendix C describes the testing procedure for both uniform and concentrated load tests as follows:

- *Test Matrices Showing Investigated and Constant Parameters:* Table C-1 and Table C-2
- *Additional Details of Testing Process*

Table C-1: Test Matrix Showing Investigated Parameters

Test ID	Type of Loading	d (in.)	f'_c (psi)
LD5	Uniform	21.295	4,805
LD6-N	Concentrated	21.295	4,505
LD6-S	Concentrated	21.295	4,505
LD7-N	Concentrated	45.295	3,465
LD7-S	Concentrated	45.295	3,618
LD8	Uniform	45.295	4,266

Table C-2: Test Matrix Showing Constant Parameters

b (in.)	a/d	ρ
21	3.0	1.0%

C.1 ADDITIONAL DETAILS OF TESTING PROCESS

Additional details of the testing process not included in Chapter 2 are as follows:

- A load rate of 200-300 lb/sec was used for all specimens except for LD7-S, where a load rate of 100-200 lb/sec was used.
- Flexural cracking was marked at the end of each load increment, and pictures were taken afterwards so as to have a crack pattern record.
- Load and displacement measurements were recorded every half second.
- Uniform load tests began by pressurizing the air bladder until the specimens made firm contact with the supports. Displacement measurements were corrected for the displacement that took place before loading occurred.
- Uniform load specimens were initially loaded to 10 kips at which point the load was balanced between the supports by adjusting the reaction bolts at the top of each support.

Appendix D: Experimental Results

Appendix D presents detailed experimental results from each structural test as follows:

- *Load-Deflection Summaries:* Figure D-1 through Figure D-6
- *Summary of Dataset and Equations for Converting Shear*
- *Shortened Dataset:* Table D-1 through Table D-8
- *Crack Pattern Monitoring:* Figure D-7 through Figure D-12
- *Uniform Load Failure Photographs:* Figure D-13 through Figure D-14
- *Observations Records:* Figure D-15 through Figure D-20

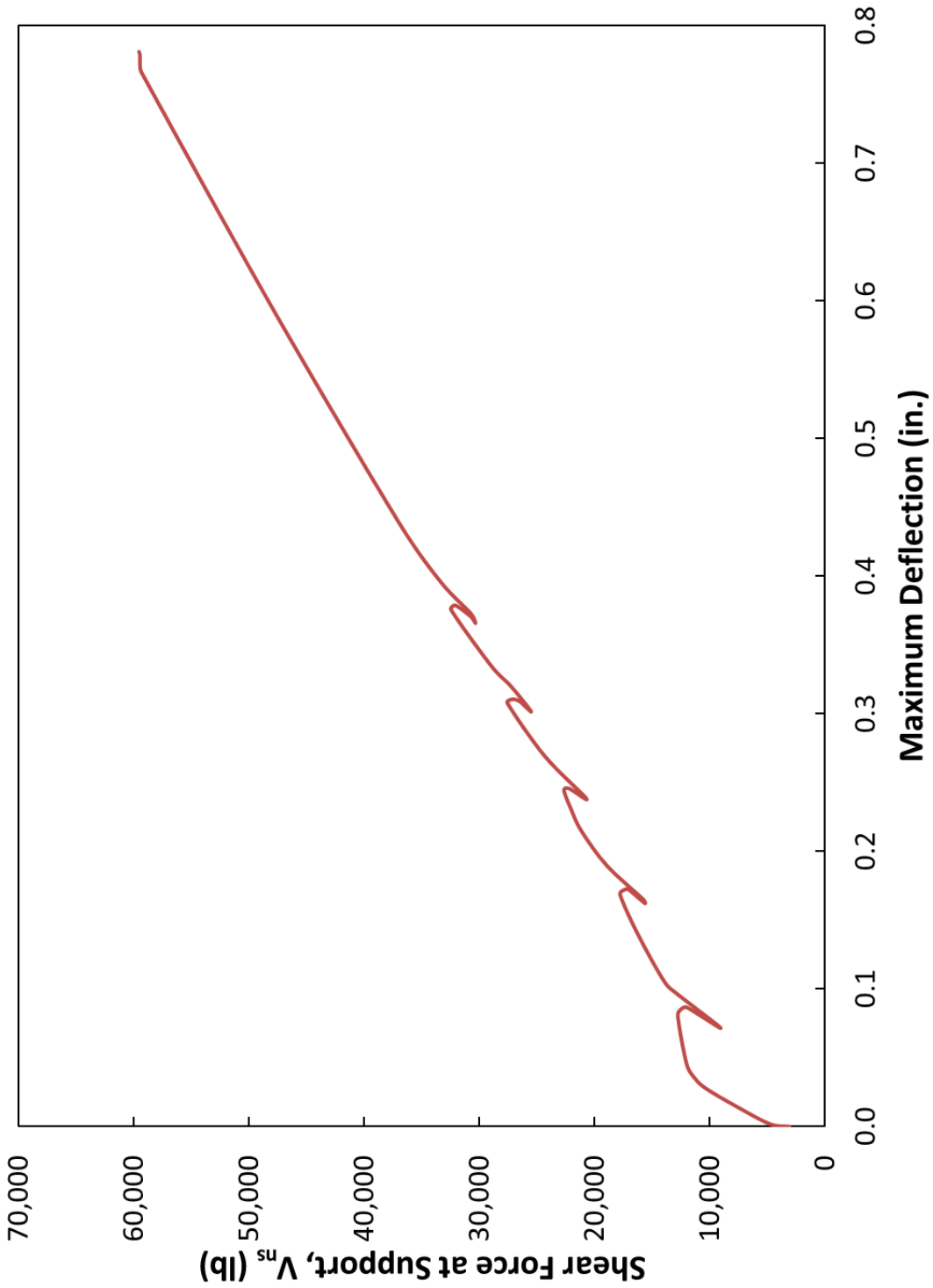

Figure D-1: LD5 Load-Deflection Summary

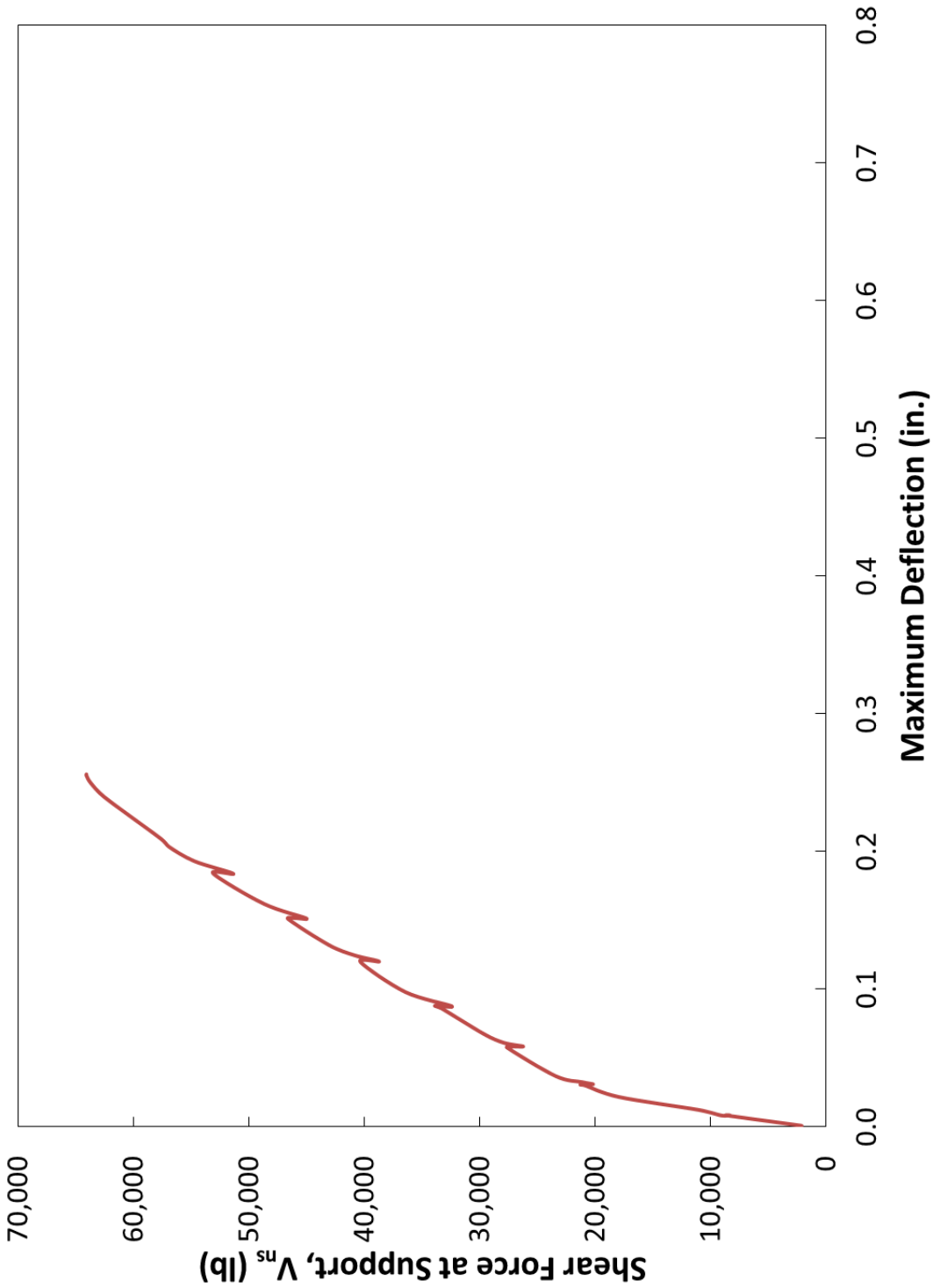

Figure D-2: LD6-N Load-Deflection Summary

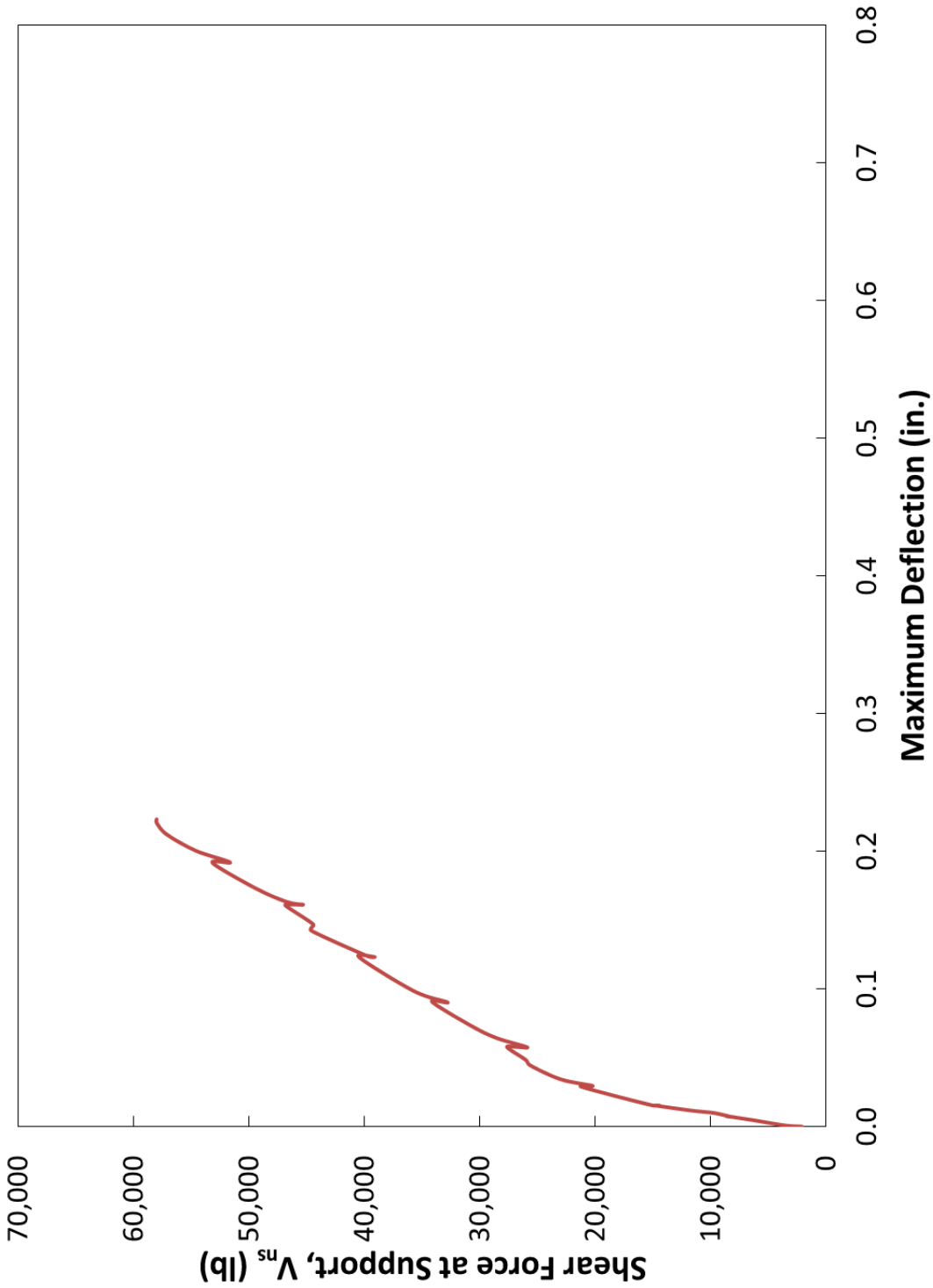

Figure D-3: LD6-S Load-Deflection Summary

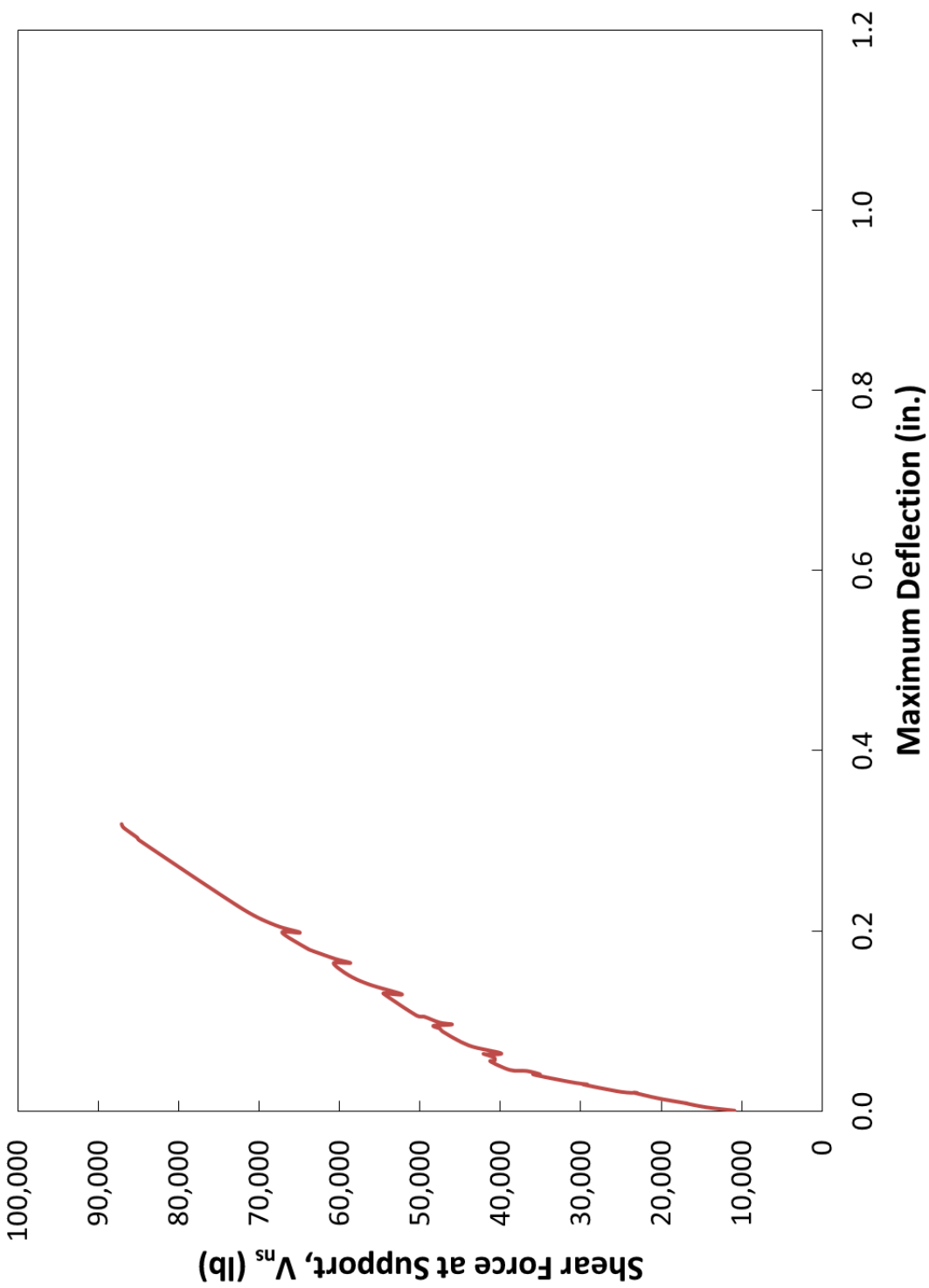

Figure D-4: LD7-N Load-Deflection Summary

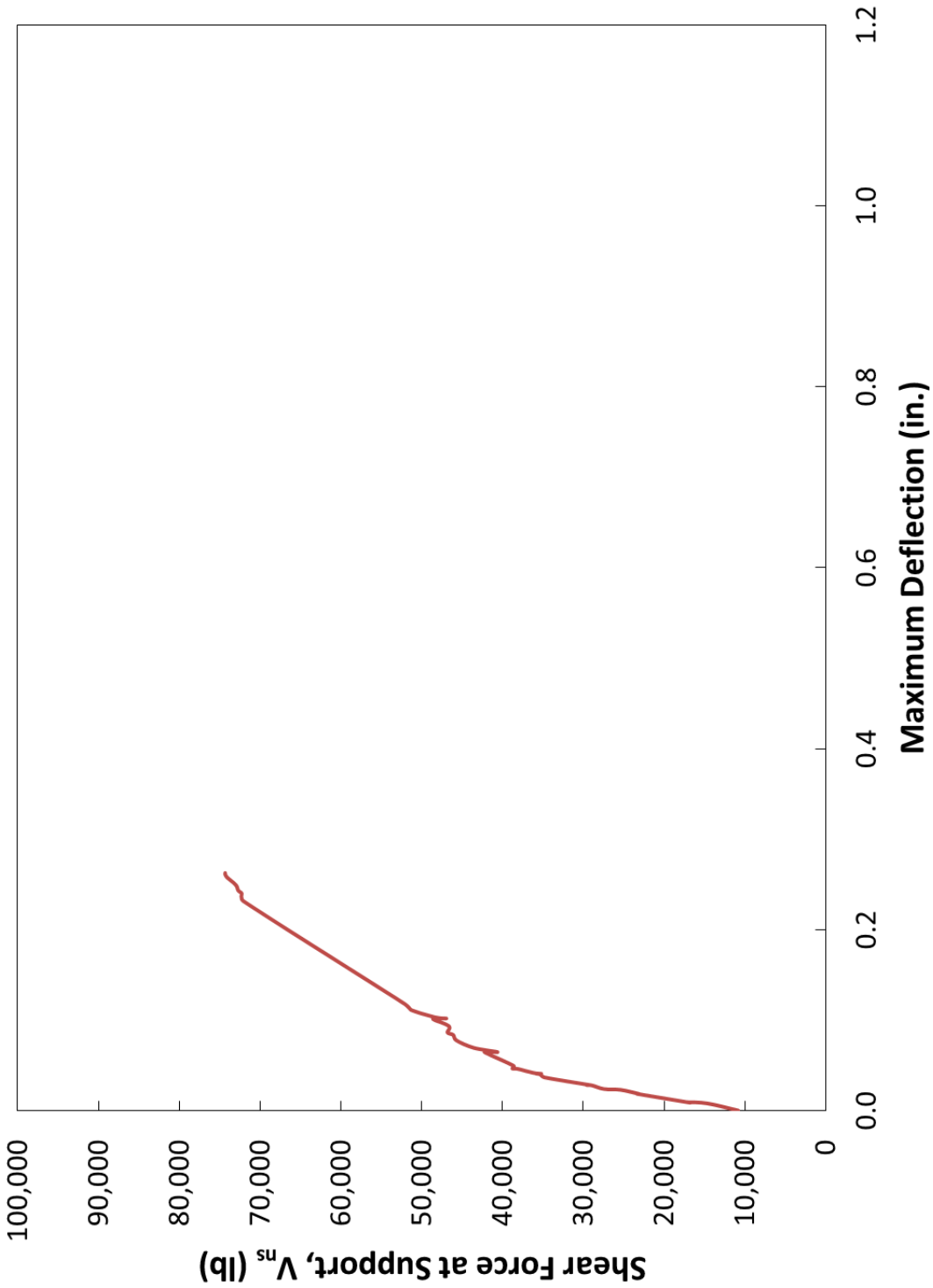

Figure D-5: LD7-S Load-Deflection Summary

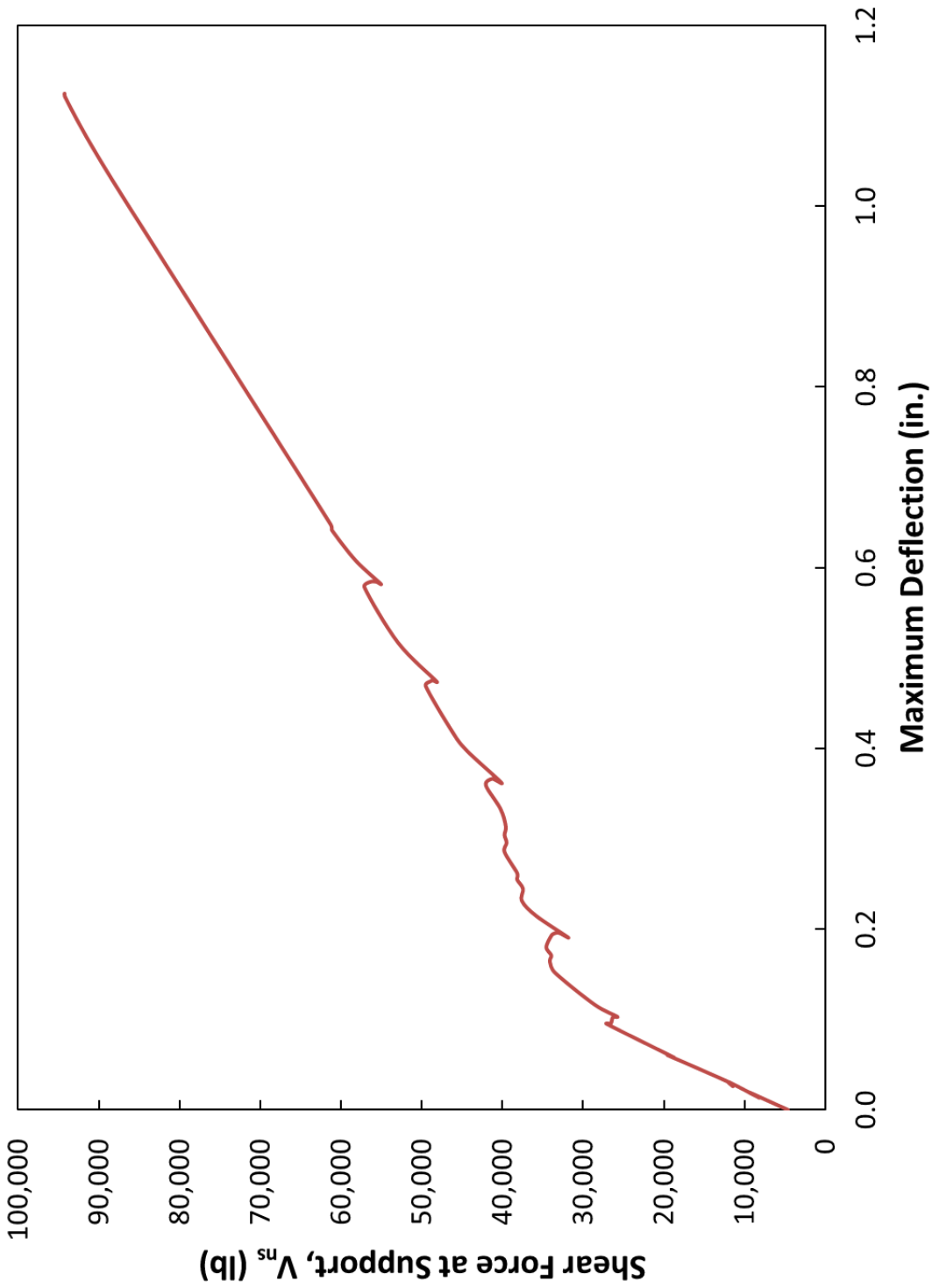

Figure D-6: LD8 Load-Deflection Summary

D.1 SUMMARY OF DATASET AND EQUATIONS FOR CONVERTING SHEAR

Depending on the test, each dataset was in the range of 4,500-13,000 data points. For the purposes of this document, representative data points were chosen to describe the full dataset in a concise manner. In this way, 4,500-13,000 data points were condensed to approximately 40-50 data points. The results plot almost identically to the original dataset, as shown in Figures D-1 through D-6. The plotted values are presented in Tables D-3 through D-8.

The data acquisition system used in each test provided values for load and displacement at both supports and at the theoretical location of maximum deflection: mid-span in the case of uniform load tests and at the load in the case of concentrated load tests. During weighing operations, the full specimen weights were measured, as well as the shear due to self-weight at the near support for concentrated load specimens, all of which can be seen in Table D-1. Using this combined information, the shear force at four different sections was calculated: the centerline of the near support (ns), (d) away from the edge of the support, (d_v) away from the edge of the support, and (x_r) away from the edge of the support. Table D-2 defines the value of the considered failure sections for each test. Equations D-1 through D-8 detail the shear force calculations.

Test LD5:

$$\boldsymbol{V_{ns} = R_{ns} + w_b * 38" + W_{ns}} \qquad \textit{Equation D-1}$$

$$\boldsymbol{V_x = V_{ns} + w_b * (x + 6") - w_a * (x + 3")} \qquad \textit{Equation D-2}$$

Tests LD6-N and LD6-S:

$$\boldsymbol{V_{ns} = R_{ns} + V_{sw} - w_b * 38"} \qquad \textit{Equation D-3}$$

$$\boldsymbol{V_x = V_{ns} - w_b * (x + 6")} \qquad \textit{Equation D-4}$$

Tests LD7-N and LD7-S:

$$\boldsymbol{V_{ns} = R_{ns} + V_{sw} - w_b * 34"}$$ ***Equation D-5***

$$\boldsymbol{V_x = V_{ns} - w_b * (x + 6")}$$ ***Equation D-6***

Test LD8:

$$\boldsymbol{V_{ns} = R_{ns} + w_b * 34" + W_{ns}}$$ ***Equation D-7***

$$\boldsymbol{V_x = V_{ns} + w_b * (x + 6") - w_a * (x + 6")}$$ ***Equation D-8***

where:

P	Total applied load = R_{ns}+R_{fs}
R_{ns}	Total applied load at the support closest to the failure crack
R_{fs}	Total applied load at the support furthest from the failure crack
w_b	Distributed self-weight of each specimen, shown in Table D-1
W_{ns}	Self-weight of the near support for uniform load tests, shown in Table D-1
W_{fs}	Self-weight of the far support for uniform load tests, shown in Table D-1
L	Total length of each specimen = 332 in. for LD5 and LD6 and 612 in. for LD7 and LD8
L_b	Length of air bladder = 250 in. for LD5 and 544 in. for LD8
w_a	Distributed load applied using bladder = (P+W_{ns}+W_{fs}+ w_b*L)/L_b
V_{sw}	Measured shear due to self-weight for concentrated load tests, shown in Table D-1
x	desired failure section, measured from the edge of the support
V_{ns}	Calculated shear at the centerline of the near support

V_x Calculated shear at the failure section (x)

δ_{ns} Average measured displacement at the near support

δ_{fs} Average measured displacement at the far support

δ_{max} Average measured displacement at the theoretical location of maximum deflection

Δ Calculated deflection at the theoretical location of maximum deflection

Table D-1: Self-Weight of Specimens and Supports

Specimen ID	w_b lbs/in.	W_{ns} lbs	W_{fs} lbs	V_{sw} lbs
LD5	43.513	1425.2	1442.0	-
LD6	46.179	-	-	3843.5
LD7	88.613	-	-	13848.8
LD8	87.845	1442.0	1425.2	-

Table D-2: Considered Failure Sections for Each Test

Test ID	d in.	d_v in.	x_r in.
LD5	21.3	19.2	16.5
LD6-N	21.3	19.2	28.0
LD6-S	21.3	19.2	31.3
LD7-N	45.3	40.8	90.5
LD7-S	45.3	40.8	84.0
LD8	45.3	40.8	60.0

Table D-3: LD5 Shortened Dataset

P lb	R_{ns} lb	R_{fs} lb	δ_{ns} in.	δ_{fs} in.	δ_{max} in.	Δ in.	V_{ns} lb
29.4	14.7	14.7	0.0000	0.0004	-0.0001	-0.0003	3093.4
4122.7	1732.3	2390.4	0.0059	0.0067	0.0079	0.0016	4811.1
10160.7	4688.4	5472.3	0.0144	0.0143	0.0290	0.0147	7767.1
14991.4	7261.3	7730.1	0.0142	0.0264	0.0477	0.0274	10340.0
16950.1	8234.4	8715.7	0.0164	0.0283	0.0573	0.0349	11313.1
18385.9	8920.0	9466.0	0.0178	0.0295	0.0686	0.0449	11998.7
19991.2	9694.0	10297.2	0.0194	0.0308	0.1055	0.0804	12772.7
19085.3	9251.7	9833.6	0.0190	0.0304	0.1106	0.0859	12330.4
18407.6	8883.0	9524.6	0.0184	0.0297	0.1103	0.0862	11961.7
12722.9	5963.6	6759.2	0.0125	0.0250	0.0900	0.0713	9042.4
20005.5	9715.9	10289.6	0.0195	0.0312	0.1212	0.0959	12794.7
22332.4	10880.7	11451.7	0.0219	0.0331	0.1328	0.1053	13959.4
26964.0	13166.0	13798.0	0.0257	0.0367	0.1707	0.1395	16244.7
30130.2	14699.3	15430.9	0.0294	0.0393	0.2025	0.1681	17778.0
29334.8	14323.3	15011.5	0.0292	0.0392	0.2060	0.1717	17402.0
28657.5	13962.2	14695.3	0.0285	0.0389	0.2056	0.1719	17040.9
25917.4	12531.7	13385.8	0.0260	0.0368	0.1932	0.1618	15610.4
26189.9	12671.8	13518.2	0.0261	0.0368	0.1961	0.1646	15750.5
32448.9	15834.3	16614.7	0.0320	0.0416	0.2259	0.1891	18913.0
36918.5	18038.5	18880.1	0.0355	0.0451	0.2544	0.2142	21117.2
38869.7	18982.0	19887.7	0.0370	0.0463	0.2724	0.2308	22060.7
40092.0	19571.7	20520.2	0.0378	0.0474	0.2867	0.2441	22650.5
39105.2	19107.3	19997.9	0.0375	0.0472	0.2876	0.2453	22186.0
36247.1	17647.3	18599.8	0.0353	0.0455	0.2786	0.2382	20726.0
43507.3	21266.7	22240.6	0.0404	0.0504	0.3145	0.2691	24345.4
50052.8	24488.0	25564.8	0.0459	0.0552	0.3580	0.3075	27566.7
49331.6	24134.4	25197.3	0.0457	0.0551	0.3605	0.3100	27213.1
47983.9	23456.1	24527.8	0.0447	0.0546	0.3585	0.3088	26534.8
45973.5	22424.0	23549.5	0.0436	0.0538	0.3500	0.3013	25502.7
49397.0	24141.3	25255.7	0.0458	0.0554	0.3699	0.3193	27220.0
52953.3	25910.5	27042.8	0.0480	0.0575	0.3874	0.3347	28989.2
60058.3	29367.6	30690.6	0.0531	0.0624	0.4329	0.3751	32446.3
59337.0	29028.7	30308.3	0.0529	0.0624	0.4361	0.3785	32107.4
56721.6	27701.2	29020.4	0.0514	0.0616	0.4271	0.3706	30779.9

Table D-3: LD5 Shortened Dataset continued

P lb	R_{ns} lb	R_{fs} lb	δ_{ns} in.	δ_{fs} in.	δ_{max} in.	Δ in.	V_{ns} lb
55801.3	27244.2	28557.1	0.0506	0.0610	0.4212	0.3654	30322.9
56655.3	27642.2	29013.1	0.0512	0.0614	0.4287	0.3724	30721.0
61875.7	30266.4	31609.3	0.0542	0.0644	0.4547	0.3954	33345.2
69187.4	33871.3	35316.1	0.0551	0.0691	0.5003	0.4382	36950.0
91658.0	44950.1	46707.9	0.0513	0.0833	0.6628	0.5955	48028.8
114704.8	56265.8	58439.1	0.0428	0.0978	0.8363	0.7660	59344.5
114910.9	56354.2	58556.7	0.0426	0.0980	0.8391	0.7688	59432.9
114947.8	56368.9	58578.8	0.0419	0.0979	0.8477	0.7778	59447.6
115087.5	56457.4	58630.2	0.0419	0.0979	0.8507	0.7807	59536.1

Table D-4: LD6-N Shortened Dataset

P lb	R_{ns} lb	R_{fs} lb	δ_{ns} in.	δ_{fs} in.	δ_{max} in.	Δ in.	V_{ns} lb
22.1	14.7	7.4	0.0002	-0.0001	0.0008	0.0007	2103.4
10362.4	6578.6	3783.8	0.0020	0.0010	0.0099	0.0083	8667.3
9802.8	6232.4	3570.4	0.0021	0.0009	0.0100	0.0083	8321.1
10944.3	6954.3	3989.9	0.0022	0.0009	0.0098	0.0081	9043.0
14088.9	8936.0	5152.9	0.0025	0.0013	0.0142	0.0122	11024.7
25047.7	15905.2	9142.5	0.0044	0.0024	0.0253	0.0217	17993.9
29576.8	18815.1	10761.7	0.0048	0.0026	0.0341	0.0301	20903.8
30166.1	19183.4	10982.7	0.0049	0.0026	0.0345	0.0305	21272.1
29753.8	18925.7	10828.1	0.0049	0.0027	0.0350	0.0310	21014.3
28987.9	18446.8	10541.1	0.0049	0.0027	0.0350	0.0309	20535.5
28472.1	18107.8	10364.3	0.0049	0.0027	0.0350	0.0309	20196.5
29930.2	19043.4	10886.9	0.0049	0.0027	0.0364	0.0324	21132.1
33509.6	21327.2	12182.4	0.0050	0.0029	0.0410	0.0368	23415.9
40116.8	25548.7	14568.1	0.0055	0.0036	0.0623	0.0575	27637.4
39468.6	25136.1	14332.5	0.0056	0.0037	0.0629	0.0580	27224.8
39395.0	25091.9	14303.1	0.0055	0.0037	0.0632	0.0583	27180.6
37900.1	24141.6	13758.5	0.0055	0.0037	0.0631	0.0583	26230.3
40529.6	25828.8	14700.7	0.0056	0.0038	0.0659	0.0610	27917.5
43180.7	27545.3	15635.4	0.0061	0.0039	0.0726	0.0673	29634.0
49103.8	31176.9	17927.0	0.0064	0.0045	0.0915	0.0857	33265.6
50068.6	31795.7	18272.9	0.0064	0.0045	0.0936	0.0878	33884.4
47815.2	30366.7	17448.5	0.0065	0.0046	0.0934	0.0876	32455.4
54001.2	34366.9	19634.4	0.0072	0.0048	0.1042	0.0979	36455.6
60091.5	38234.3	21857.1	0.0078	0.0052	0.1265	0.1197	40323.0
57573.3	36621.2	20952.1	0.0079	0.0051	0.1268	0.1200	38709.9
60776.8	38698.7	22078.1	0.0081	0.0054	0.1314	0.1243	40787.4
64348.4	40975.1	23373.3	0.0084	0.0057	0.1393	0.1320	43063.8
70073.2	44504.0	25569.2	0.0085	0.0064	0.1586	0.1509	46592.7
69005.4	43811.5	25193.9	0.0085	0.0064	0.1591	0.1514	45900.2
67663.7	42971.0	24692.8	0.0085	0.0064	0.1591	0.1514	45059.7
73333.9	46624.7	26709.2	0.0090	0.0066	0.1700	0.1619	48713.4
80168.5	50993.5	29174.9	0.0095	0.0069	0.1924	0.1839	53082.2
77495.5	49262.5	28233.0	0.0095	0.0070	0.1923	0.1837	51351.2
82701.0	52643.4	30057.6	0.0100	0.0071	0.2018	0.1929	54732.0

Table D-4: LD6-N Shortened Dataset continued

P lb	R_{ns} lb	R_{fs} lb	δ_{ns} in.	δ_{fs} in.	δ_{max} in.	Δ in.	V_{ns} lb
86162.3	54838.7	31323.6	0.0102	0.0072	0.2124	0.2034	56927.4
87460.1	55545.9	31914.2	0.0102	0.0073	0.2183	0.2092	57634.6
95105.0	60400.8	34704.2	0.0102	0.0076	0.2484	0.2392	62489.5
97004.8	61601.6	35403.3	0.0102	0.0078	0.2588	0.2495	63690.3
97608.8	61977.3	35631.5	0.0102	0.0077	0.2642	0.2549	64066.0
97616.1	61984.7	35631.5	0.0102	0.0078	0.2653	0.2560	64073.4

Table D-5: LD6-S Shortened Dataset

P lb	R_{ns} lb	R_{fs} lb	δ_{ns} in.	δ_{fs} in.	δ_{max} in.	Δ in.	V_{ns} lb
21.4	14.6	6.8	-0.0002	-0.0017	-0.0009	-0.0001	2103.3
2427.7	1546.5	881.2	0.0001	-0.0014	0.0003	0.0007	3635.2
6917.1	4389.4	2527.7	0.0011	-0.0011	0.0049	0.0047	6478.1
10354.4	6554.7	3799.7	0.0018	-0.0009	0.0082	0.0075	8643.4
9662.2	6142.1	3520.1	0.0020	-0.0009	0.0077	0.0068	8230.8
12017.8	7622.5	4395.3	0.0023	-0.0007	0.0108	0.0097	9711.2
15094.9	9581.6	5513.3	0.0029	-0.0005	0.0131	0.0114	11670.2
20064.1	12726.4	7337.7	0.0036	-0.0001	0.0173	0.0151	14815.0
19460.4	12343.4	7117.0	0.0037	0.0000	0.0174	0.0151	14432.1
20491.2	13006.2	7485.0	0.0038	0.0001	0.0177	0.0153	15094.9
30091.2	19119.0	10972.2	0.0048	0.0010	0.0321	0.0288	21207.7
28544.6	18139.2	10405.3	0.0049	0.0010	0.0328	0.0294	20227.9
32888.1	20923.1	11965.1	0.0051	0.0013	0.0378	0.0342	23011.8
36959.9	23545.0	13414.9	0.0060	0.0017	0.0486	0.0443	25633.7
37519.4	23928.0	13591.4	0.0060	0.0017	0.0526	0.0482	26016.7
40059.7	25540.9	14518.7	0.0064	0.0020	0.0621	0.0573	27629.6
38955.1	24848.5	14106.6	0.0064	0.0020	0.0625	0.0577	26937.2
37379.3	23832.1	13547.2	0.0064	0.0019	0.0622	0.0575	25920.8
41421.2	26446.6	14974.6	0.0067	0.0022	0.0690	0.0641	28535.3
44926.3	28670.9	16255.4	0.0071	0.0023	0.0783	0.0730	30759.6
50145.8	32036.2	18109.6	0.0076	0.0026	0.0961	0.0903	34124.9
48091.5	30710.5	17381.0	0.0077	0.0028	0.0959	0.0900	32799.2
52597.3	33612.2	18985.1	0.0080	0.0029	0.1042	0.0981	35700.9
60360.6	38361.9	21998.7	0.0088	0.0035	0.1296	0.1228	40450.6
58225.4	37007.1	21218.4	0.0088	0.0035	0.1298	0.1230	39095.7
59153.2	37618.3	21534.8	0.0089	0.0035	0.1303	0.1235	39707.0
66766.8	42516.1	24250.7	0.0095	0.0037	0.1495	0.1422	44604.8
66435.6	42332.0	24103.6	0.0095	0.0036	0.1539	0.1466	44420.7
70161.0	44732.7	25428.3	0.0099	0.0037	0.1678	0.1602	46821.4
69306.9	44173.0	25133.9	0.0100	0.0038	0.1687	0.1611	46261.7
67847.7	43222.3	24625.4	0.0100	0.0037	0.1686	0.1610	45311.0
70035.2	44651.4	25383.8	0.0099	0.0037	0.1706	0.1630	46740.1
74195.0	47317.4	26877.6	0.0103	0.0037	0.1806	0.1728	49406.1
80040.5	51058.6	28982.0	0.0108	0.0037	0.1993	0.1912	53147.2

Table D-5: LD6-S Shortened Dataset continued

P lb	R_{ns} lb	R_{fs} lb	δ_{ns} in.	δ_{fs} in.	δ_{max} in.	Δ in.	V_{ns} lb
77743.8	49556.4	28187.3	0.0108	0.0037	0.1998	0.1917	51645.1
82249.8	52509.8	29740.1	0.0110	0.0037	0.2084	0.2001	54598.4
86240.6	55035.9	31204.7	0.0112	0.0038	0.2204	0.2119	57124.6
87602.4	55897.6	31704.9	0.0113	0.0039	0.2288	0.2203	57986.3
87639.3	55912.3	31727.0	0.0114	0.0039	0.2316	0.2230	58001.0

Table D-6: LD7-N Shortened Dataset

P lb	R_{ns} lb	R_{fs} lb	δ_{ns} in.	δ_{fs} in.	δ_{max} in.	Δ in.	V_{ns} lb
58.9	66.5	-7.6	0.0006	0.0004	0.0010	0.0004	10902.5
5808.8	3621.1	2187.7	0.0011	0.0006	0.0051	0.0042	14457.1
10064.4	6270.6	3793.7	0.0013	0.0008	0.0099	0.0088	17106.6
9533.9	5954.1	3579.8	0.0013	0.0008	0.0096	0.0084	16790.0
15166.6	9472.4	5694.2	0.0018	0.0011	0.0154	0.0139	20308.3
20165.7	12593.1	7572.6	0.0022	0.0012	0.0222	0.0204	23429.0
19494.4	12172.9	7321.5	0.0024	0.0012	0.0221	0.0201	23008.9
22660.5	14152.9	8507.6	0.0027	0.0013	0.0234	0.0212	24988.9
30185.6	18863.6	11322.0	0.0037	0.0017	0.0324	0.0294	29699.6
29390.9	18363.2	11027.6	0.0038	0.0017	0.0325	0.0295	29199.2
31776.8	19857.6	11919.2	0.0040	0.0018	0.0344	0.0312	30693.6
35443.3	22154.0	13289.3	0.0041	0.0019	0.0384	0.0351	32990.0
40125.5	25068.5	15057.0	0.0044	0.0020	0.0440	0.0405	35904.4
38785.1	24251.3	14533.8	0.0044	0.0020	0.0441	0.0407	35087.3
41472.6	25914.8	15557.8	0.0045	0.0020	0.0480	0.0444	36750.8
44785.3	27990.2	16795.2	0.0047	0.0022	0.0493	0.0455	38826.1
48679.5	30418.4	18261.2	0.0049	0.0022	0.0590	0.0551	41254.3
47782.0	29889.1	17892.9	0.0049	0.0022	0.0598	0.0559	40725.1
47936.6	29977.4	17959.2	0.0050	0.0023	0.0634	0.0595	40813.3
50071.8	31287.6	18784.3	0.0051	0.0022	0.0674	0.0634	42123.5
49475.3	30934.2	18541.2	0.0051	0.0023	0.0670	0.0629	41770.1
46543.4	29093.2	17450.2	0.0051	0.0023	0.0681	0.0640	39929.1
53007.6	33126.5	19881.1	0.0055	0.0024	0.0771	0.0728	43962.4
58117.6	36313.4	21804.3	0.0062	0.0025	0.0927	0.0879	47149.3
58698.8	36681.0	22017.8	0.0063	0.0025	0.0962	0.0913	47517.0
60023.8	37490.3	22533.4	0.0065	0.0027	0.0997	0.0947	48326.3
56320.8	35186.7	21134.1	0.0064	0.0027	0.1010	0.0960	46022.7
58846.2	36754.4	22091.7	0.0066	0.0028	0.1034	0.0982	47590.4
61842.7	38631.2	23211.5	0.0068	0.0029	0.1100	0.1046	49467.1
63382.1	39588.3	23793.8	0.0068	0.0028	0.1112	0.1059	50424.2
70022.9	43710.0	26312.9	0.0072	0.0032	0.1359	0.1303	54545.9
69485.6	43393.6	26092.0	0.0072	0.0031	0.1363	0.1306	54229.6
68123.0	42532.3	25590.7	0.0072	0.0032	0.1353	0.1296	53368.2
66473.2	41494.2	24979.0	0.0072	0.0032	0.1356	0.1299	52330.2

Table D-6: LD7-N Shortened Dataset continued

P lb	R_{ns} lb	R_{fs} lb	δ_{ns} in.	δ_{fs} in.	δ_{max} in.	Δ in.	V_{ns} lb
72886.4	45490.9	27395.5	0.0074	0.0034	0.1463	0.1404	56326.9
76994.9	48044.9	28950.0	0.0080	0.0036	0.1571	0.1507	58880.8
79983.6	49899.1	30084.4	0.0085	0.0037	0.1703	0.1636	60735.1
77936.2	48632.8	29303.3	0.0086	0.0038	0.1712	0.1644	59468.8
76668.4	47844.7	28823.7	0.0085	0.0038	0.1712	0.1644	58680.7
79695.0	49721.8	29973.2	0.0087	0.0038	0.1757	0.1689	60557.8
83965.2	52378.7	31586.5	0.0090	0.0040	0.1844	0.1773	63214.7
85342.5	53240.4	32102.1	0.0090	0.0041	0.1877	0.1806	64076.4
90143.3	56288.3	33855.0	0.0095	0.0048	0.2057	0.1980	67124.2
86631.5	54094.9	32536.6	0.0095	0.0049	0.2057	0.1980	64930.9
91513.5	57120.2	34393.3	0.0095	0.0050	0.2139	0.2061	67956.2
98012.8	61174.6	36838.3	0.0096	0.0050	0.2318	0.2239	72010.5
118718.1	74064.0	44654.0	0.0108	0.0057	0.3093	0.3004	84900.0
119108.2	74299.5	44808.7	0.0109	0.0058	0.3122	0.3033	85135.5
121848.8	76001.2	45847.5	0.0111	0.0060	0.3236	0.3144	86837.2
122254.0	76259.2	45994.9	0.0112	0.0060	0.3277	0.3184	87095.2

Table D-7: LD7-S Shortened Dataset

P lb	R_{ns} lb	R_{fs} lb	δ_{ns} in.	δ_{fs} in.	δ_{max} in.	Δ in.	V_{ns} lb
0.0	0.0	0.0	-0.0001	0.0000	-0.0001	0.0000	10836.0
6121.8	3808.3	2313.5	0.0011	0.0004	0.0087	0.0078	14644.2
10127.3	6320.2	3807.2	0.0015	0.0006	0.0104	0.0092	17156.1
9543.9	5966.2	3577.7	0.0015	0.0007	0.0099	0.0086	16802.2
19979.5	12500.0	7479.5	0.0025	0.0013	0.0204	0.0184	23336.0
19588.2	12256.6	7331.6	0.0026	0.0013	0.0204	0.0183	23092.6
23307.4	14576.9	8730.4	0.0031	0.0015	0.0254	0.0229	25412.9
26584.7	16632.1	9952.6	0.0035	0.0017	0.0265	0.0238	27468.1
28941.4	18105.3	10836.1	0.0039	0.0017	0.0308	0.0277	28941.3
30060.6	18805.0	11255.5	0.0041	0.0018	0.0315	0.0282	29641.0
29515.3	18466.1	11049.2	0.0042	0.0019	0.0315	0.0282	29302.0
38286.3	23983.2	14303.1	0.0056	0.0025	0.0410	0.0366	34819.1
39111.2	24498.8	14612.4	0.0056	0.0025	0.0443	0.0399	35334.8
39980.1	25043.9	14936.2	0.0058	0.0027	0.0454	0.0408	35879.8
38904.1	24366.0	14538.1	0.0059	0.0025	0.0453	0.0406	35201.9
40354.9	25279.4	15075.6	0.0060	0.0026	0.0462	0.0414	36115.3
43588.4	27305.2	16283.2	0.0065	0.0029	0.0511	0.0460	38141.1
44596.6	27953.3	16643.3	0.0066	0.0029	0.0516	0.0464	38789.3
44353.6	27806.2	16547.5	0.0067	0.0031	0.0547	0.0494	38642.1
49972.6	31356.4	18616.2	0.0072	0.0031	0.0700	0.0643	42192.3
48860.0	30671.2	18188.9	0.0072	0.0032	0.0705	0.0648	41507.1
47549.3	29861.0	17688.3	0.0073	0.0033	0.0705	0.0647	40697.0
52137.5	32741.1	19396.4	0.0076	0.0034	0.0753	0.0693	43577.1
55532.4	34884.6	20647.8	0.0080	0.0037	0.0839	0.0776	45720.6
56165.3	35274.8	20890.5	0.0081	0.0037	0.0900	0.0836	46110.8
57247.0	35974.2	21272.8	0.0082	0.0038	0.0927	0.0861	46810.1
56937.6	35804.6	21132.9	0.0084	0.0039	0.0999	0.0932	46640.6
60007.8	37748.9	22258.9	0.0086	0.0040	0.1077	0.1009	48584.9
58792.6	36975.5	21817.1	0.0087	0.0041	0.1087	0.1017	47811.4
57431.5	36121.6	21309.9	0.0087	0.0041	0.1087	0.1017	46957.6
59559.1	37454.5	22104.5	0.0087	0.0041	0.1099	0.1029	48290.5
64360.5	40496.5	23863.9	0.0092	0.0044	0.1185	0.1111	51332.5
65582.9	41269.9	24313.0	0.0094	0.0045	0.1253	0.1177	52105.9
97083.6	61253.6	35830.0	0.0126	0.0054	0.2414	0.2315	72089.6

Table D-7: LD7-S Shortened Dataset continued

P lb	R_{ns} lb	R_{fs} lb	δ_{ns} in.	δ_{fs} in.	δ_{max} in.	Δ in.	V_{ns} lb
97377.8	61445.0	35932.8	0.0126	0.0054	0.2496	0.2397	72281.0
98018.4	61879.5	36138.9	0.0127	0.0055	0.2531	0.2431	72715.5
98482.1	62166.7	36315.4	0.0127	0.0054	0.2591	0.2492	73002.7
100174.5	63263.5	36911.0	0.0128	0.0059	0.2679	0.2577	74099.5
100527.9	63484.5	37043.4	0.0132	0.0058	0.2711	0.2607	74320.5
100564.7	63499.2	37065.5	0.0131	0.0058	0.2729	0.2626	74335.2

Table D-8: LD8 Shortened Dataset

P lb	R_{ns} lb	R_{fs} lb	δ_{ns} in.	δ_{fs} in.	δ_{max} in.	Δ in.	V_{ns} lb
486.2	206.1	280.1	0.2859	0.2749	0.2801	-0.0003	4634.8
10039.2	5047.9	4991.3	0.3209	0.3477	0.3536	0.0193	9476.7
7428.3	3794.4	3633.9	0.3297	0.3464	0.3513	0.0133	8223.2
15085.6	7552.5	7533.1	0.3396	0.3574	0.3791	0.0306	11981.3
13929.7	7015.7	6914.0	0.3392	0.3572	0.3740	0.0258	11444.4
15211.1	7589.5	7621.6	0.3400	0.3587	0.3800	0.0306	12018.2
30112.9	15105.4	15007.5	0.3561	0.3763	0.4264	0.0602	19534.2
28551.6	14340.4	14211.3	0.3553	0.3762	0.4235	0.0578	18769.1
45228.2	22687.6	22540.6	0.3695	0.3922	0.4759	0.0950	27116.3
44212.0	22165.3	22046.7	0.3695	0.3926	0.4762	0.0951	26594.1
43600.6	21878.3	21722.3	0.3692	0.3919	0.4832	0.1026	26307.0
42503.4	21356.0	21147.3	0.3684	0.3912	0.4827	0.1029	25784.8
48216.8	24180.2	24036.7	0.3726	0.3956	0.5004	0.1163	28608.9
58038.3	29078.0	28960.4	0.3807	0.4042	0.5440	0.1516	33506.7
59201.6	29673.6	29528.0	0.3816	0.4049	0.5560	0.1628	34102.3
59098.4	29666.3	29432.1	0.3818	0.4048	0.5599	0.1666	34095.0
58914.3	29533.8	29380.5	0.3818	0.4047	0.5642	0.1710	33962.6
60107.1	30144.2	29962.8	0.3826	0.4055	0.5738	0.1798	34573.0
58862.9	29511.7	29351.2	0.3824	0.4048	0.5862	0.1925	33940.5
58222.4	29210.2	29012.1	0.3822	0.4042	0.5880	0.1948	33639.0
56963.4	28592.5	28371.0	0.3815	0.4036	0.5882	0.1956	33021.2
54747.0	27496.5	27250.4	0.3803	0.4022	0.5821	0.1909	31925.3
62632.1	31394.3	31237.9	0.3856	0.4078	0.6111	0.2143	35823.0
66143.9	33151.8	32992.1	0.3880	0.4113	0.6304	0.2307	37580.5
65908.3	33034.1	32874.2	0.3880	0.4113	0.6442	0.2445	37462.8
67343.9	33762.1	33581.8	0.3887	0.4128	0.6554	0.2546	38190.9
67314.4	33747.4	33567.0	0.3891	0.4133	0.6628	0.2616	38176.1
70443.1	35321.0	35122.1	0.3913	0.4156	0.6886	0.2852	39749.7
69964.5	35063.5	34901.0	0.3909	0.4152	0.6982	0.2952	39492.2
70450.3	35320.9	35129.4	0.3916	0.4156	0.7076	0.3041	39749.7
70170.6	35166.5	35004.2	0.3914	0.4152	0.7171	0.3138	39595.2
71510.5	35850.3	35660.2	0.3921	0.4161	0.7375	0.3334	40279.1
75074.4	37622.9	37451.5	0.3949	0.4181	0.7651	0.3587	42051.7
73535.7	36843.4	36692.4	0.3942	0.4176	0.7720	0.3662	41272.1

Table D-8: LD8 Shortened Dataset continued

P lb	R_{ns} lb	R_{fs} lb	δ_{ns} in.	δ_{fs} in.	δ_{max} in.	Δ in.	V_{ns} lb
71216.1	35717.9	35498.2	0.3928	0.4167	0.7667	0.3620	40146.7
79830.1	40005.4	39824.7	0.3981	0.4227	0.8078	0.3974	44434.2
83555.8	41873.5	41682.3	0.4006	0.4254	0.8323	0.4194	46302.3
89975.8	45079.8	44896.0	0.4051	0.4294	0.8859	0.4687	49508.5
88870.8	44505.8	44365.0	0.4050	0.4293	0.8912	0.4740	48934.5
88164.3	44167.6	43996.7	0.4046	0.4292	0.8920	0.4751	48596.4
87222.1	43697.0	43525.1	0.4042	0.4288	0.8900	0.4735	48125.8
96820.8	48505.7	48315.1	0.4105	0.4359	0.9399	0.5167	52934.5
105082.0	52668.4	52413.6	0.4157	0.4419	1.0067	0.5779	57097.1
103757.0	51984.5	51772.6	0.4153	0.4425	1.0129	0.5840	56413.2
102107.7	51153.3	50954.4	0.4145	0.4419	1.0123	0.5841	55582.1
101070.0	50646.1	50424.0	0.4142	0.4413	1.0095	0.5817	55074.8
107313.6	53779.2	53534.4	0.4177	0.4448	1.0391	0.6078	58207.9
113159.3	56713.4	56445.9	0.4213	0.4492	1.0766	0.6414	61142.2
113439.1	56860.5	56578.6	0.4217	0.4493	1.0830	0.6476	61289.2
165767.6	83141.8	82625.8	0.4544	0.4840	1.4869	1.0177	87570.6
173638.5	87105.9	86532.6	0.4588	0.4887	1.5501	1.0764	91534.7
178924.8	89760.7	89164.1	0.4618	0.4926	1.5978	1.1206	94189.4
179013.0	89826.8	89186.1	0.4619	0.4927	1.6018	1.1246	94255.6

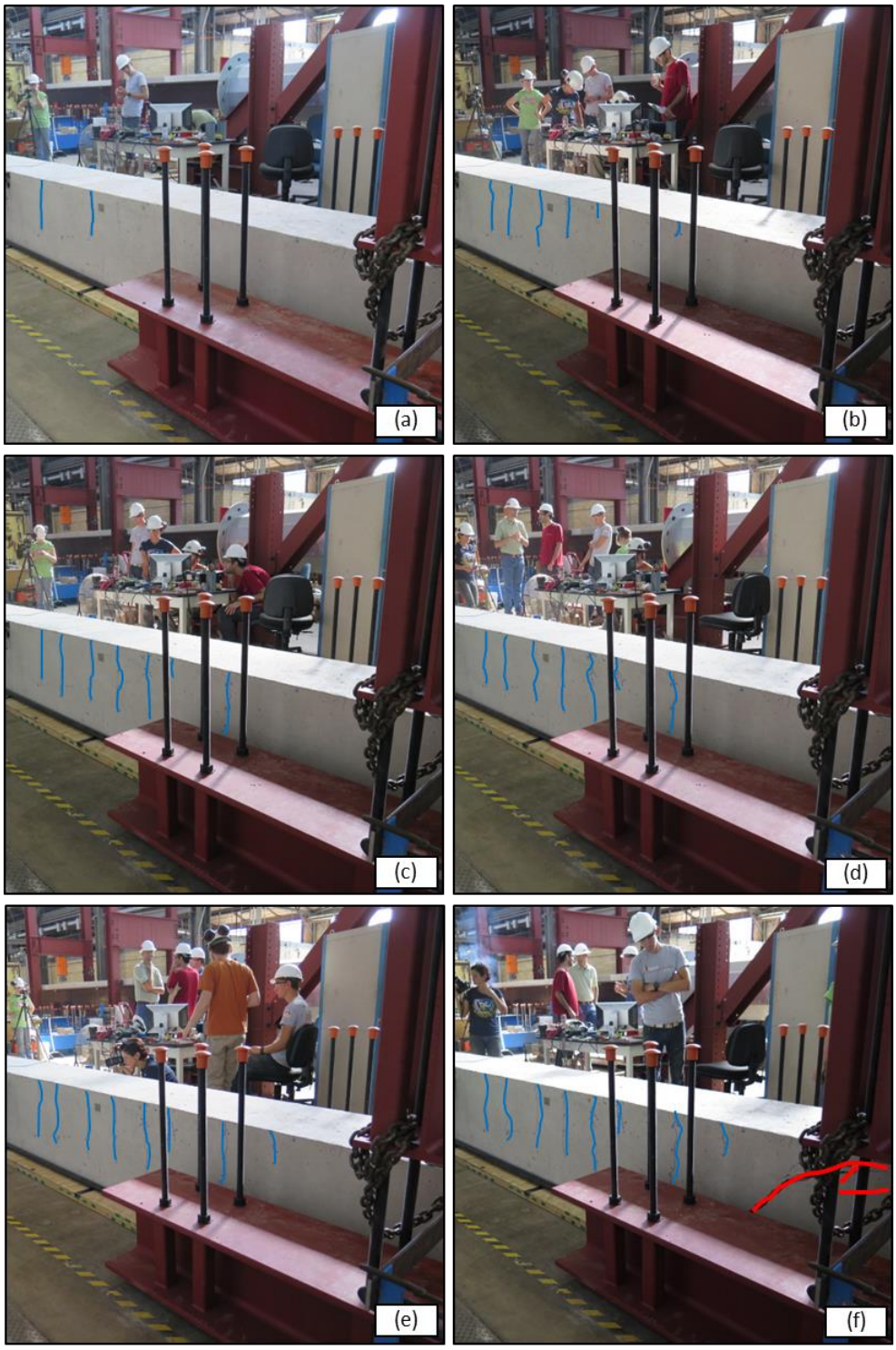

Figure D-7: LD5 Crack Pattern Monitoring at (a) 20 kip, (b) 30 kip, (c) 40 kip, (d) 50 kips, (e) 60 kip, and (f) Failure

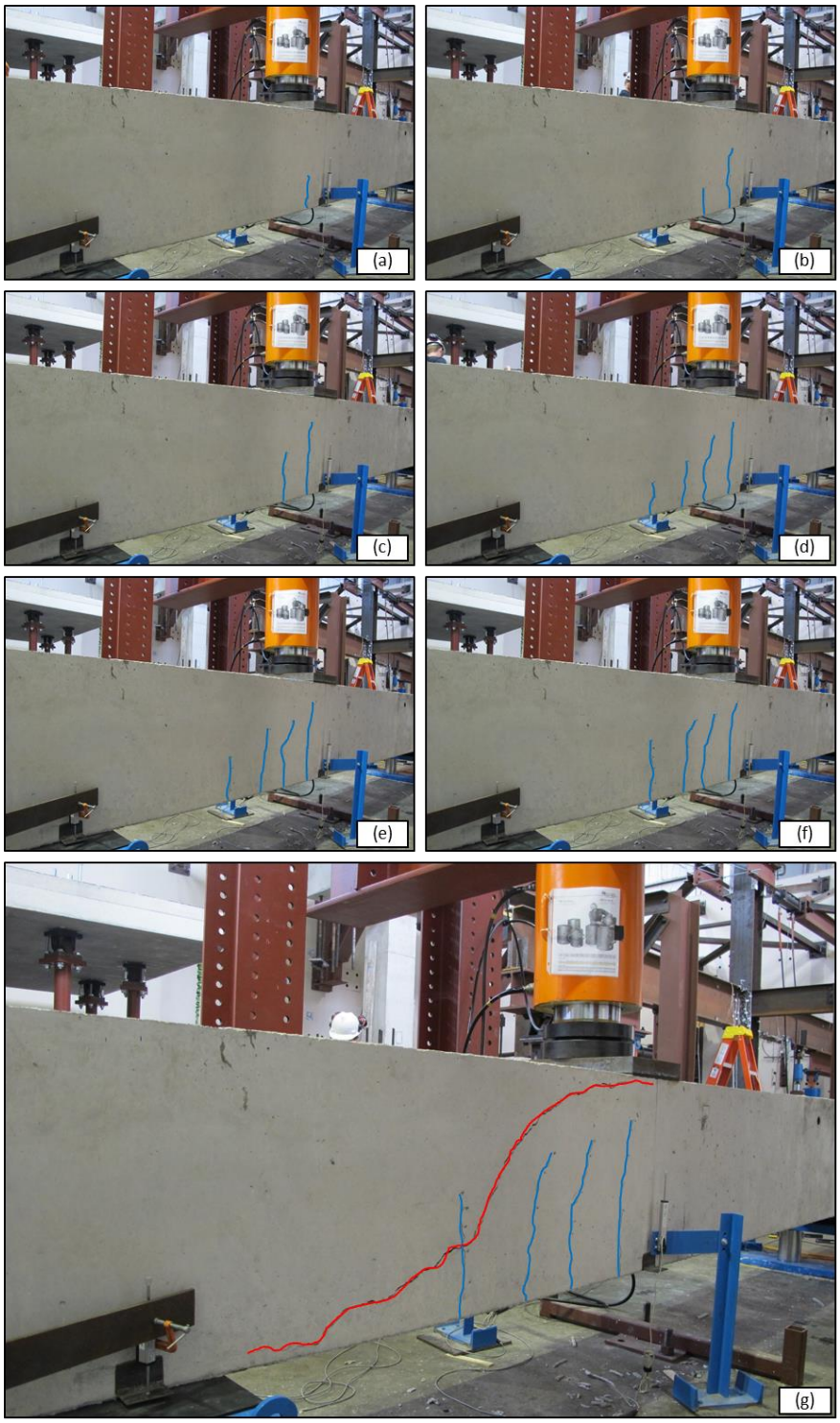

Figure D-8: LD6-N Crack Pattern Monitoring at (a) 30 kip, (b) 40 kip, (c) 50 kip, (d) 60 kips, (e) 70 kip, (f) 80 kip, and (g) Failure

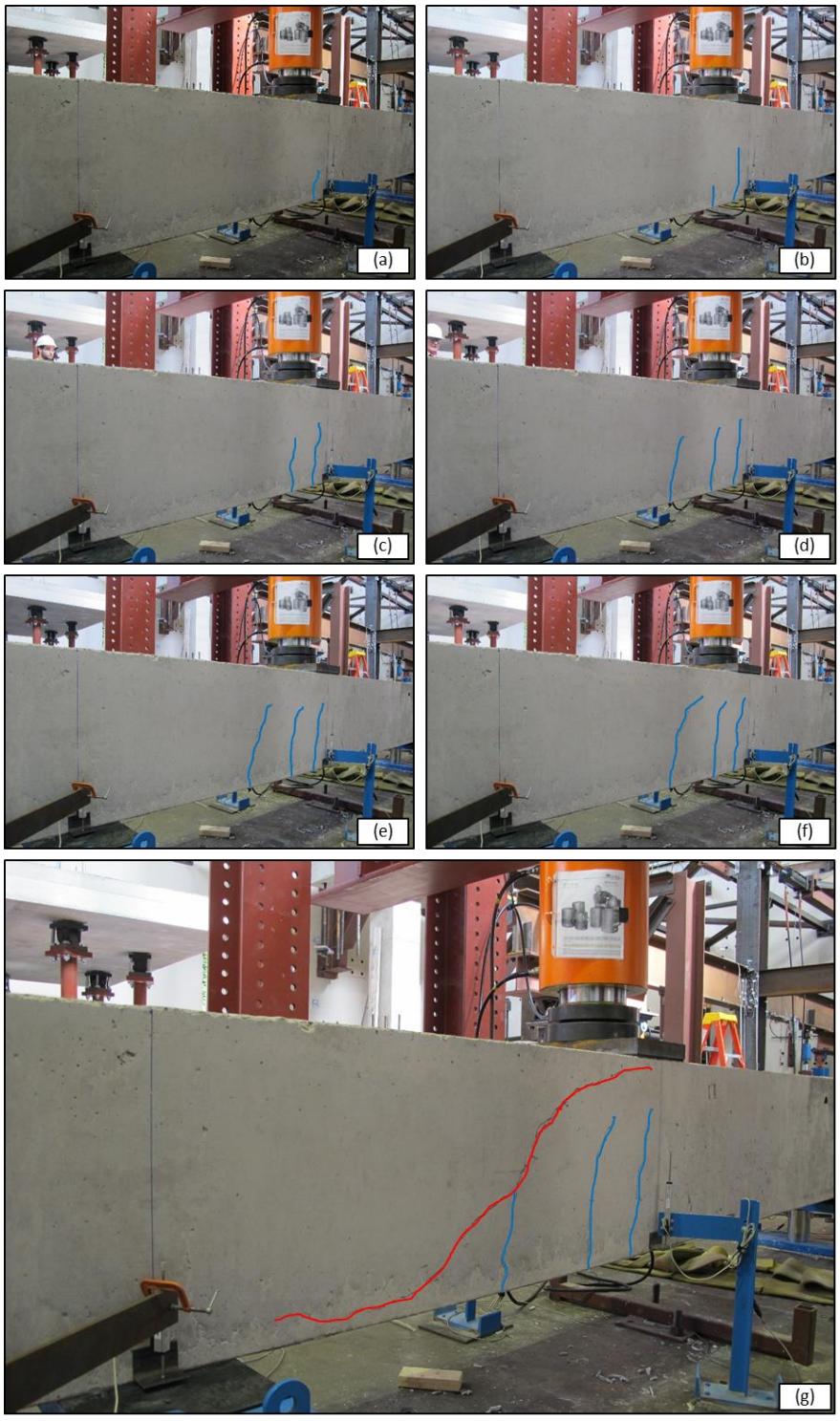

Figure D-9: LD6-S Crack Pattern Monitoring at (a) 30 kip, (b) 40 kip, (c) 50 kip, (d) 60 kips, (e) 70 kip, (f) 80 kip, and (g) Failure

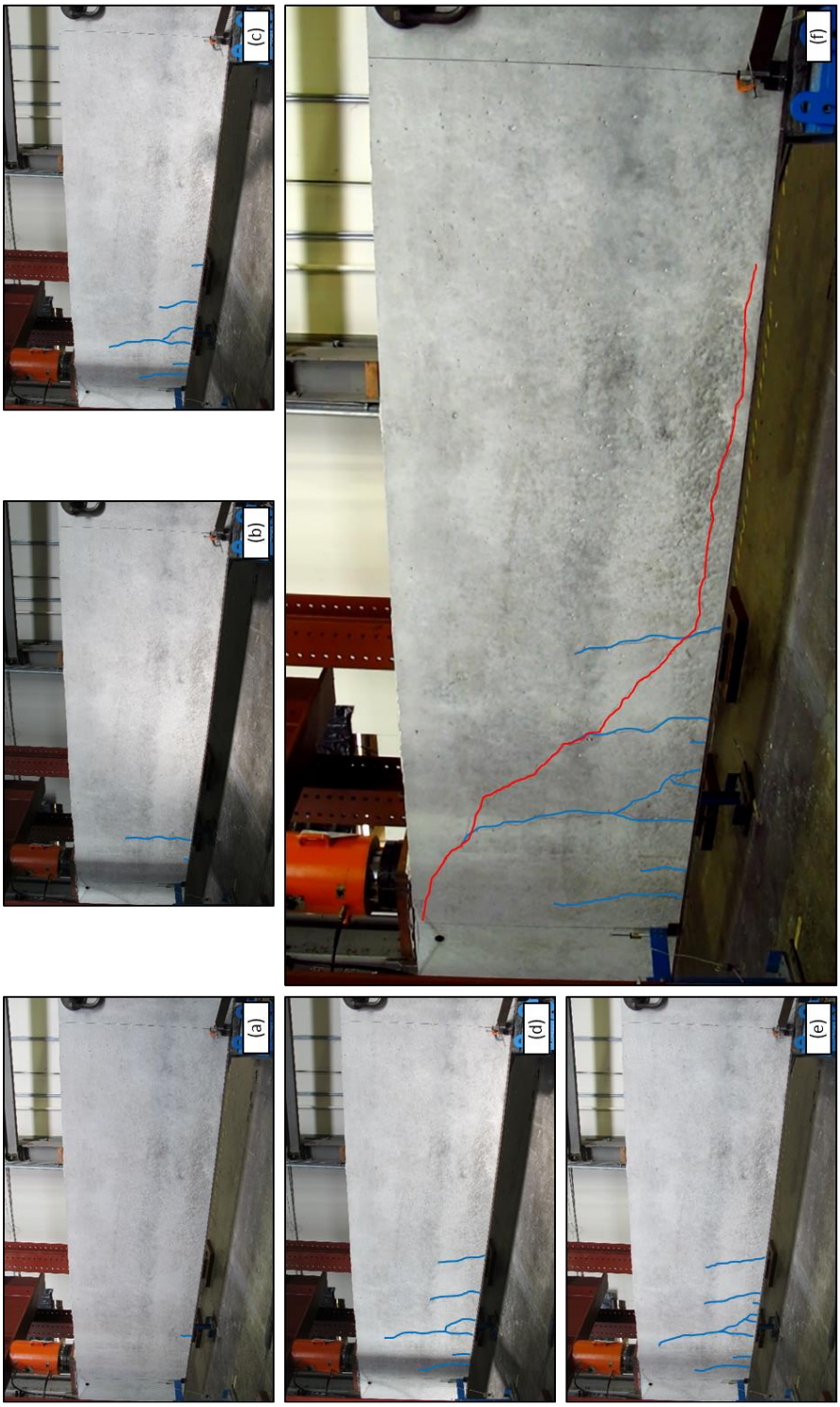

Figure D-10: LD7-N Crack Pattern Monitoring at (a) 50 kip, (b) 60 kip, (c) 70 kip, (d) 80 kips, (e) 90 kip, and (f) Failure

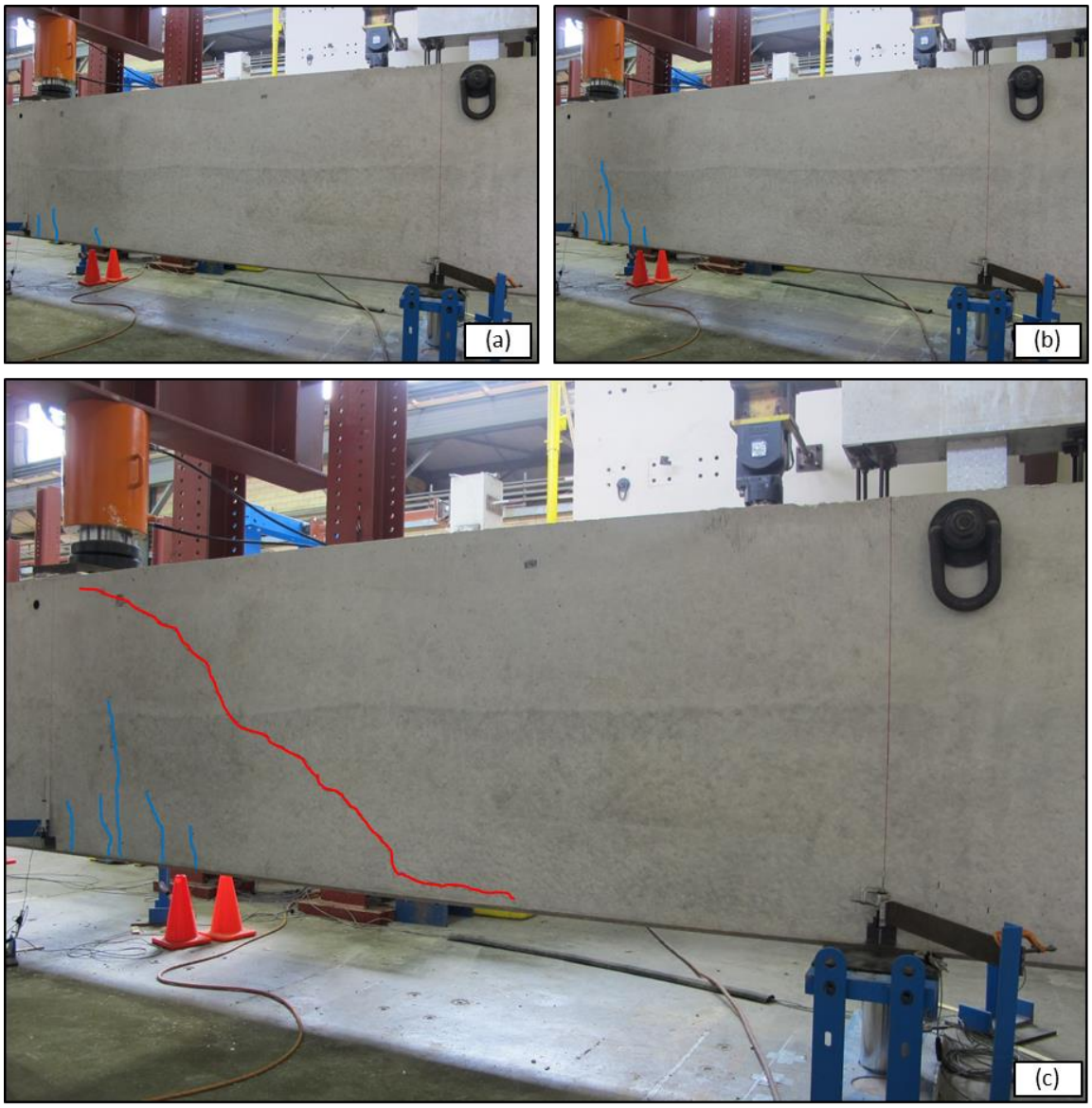

Figure D-11: LD7-S Crack Pattern Monitoring at (a) 50 kip, (b) 60 kip, and (c) Failure

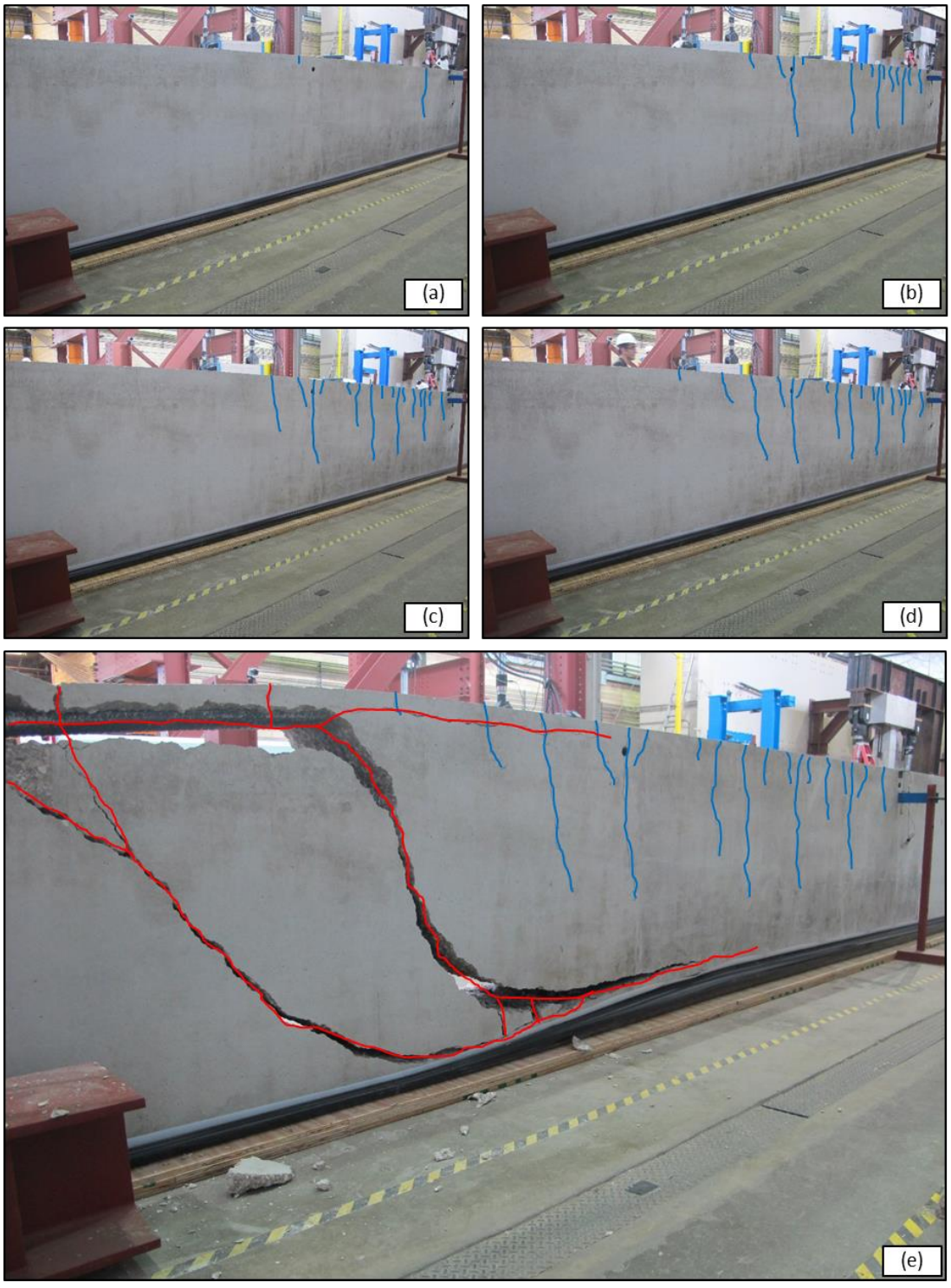

Figure D-12: LD8 Crack Pattern Monitoring at (a) 60 kip, (b) 75 kip, (c) 90 kip, (d) 105 kip, and (e) Failure

Figure D-13: LD5 Failure Photographs while: (a), (b), and (c) Partially Loaded, and (d) and (e) Unloaded

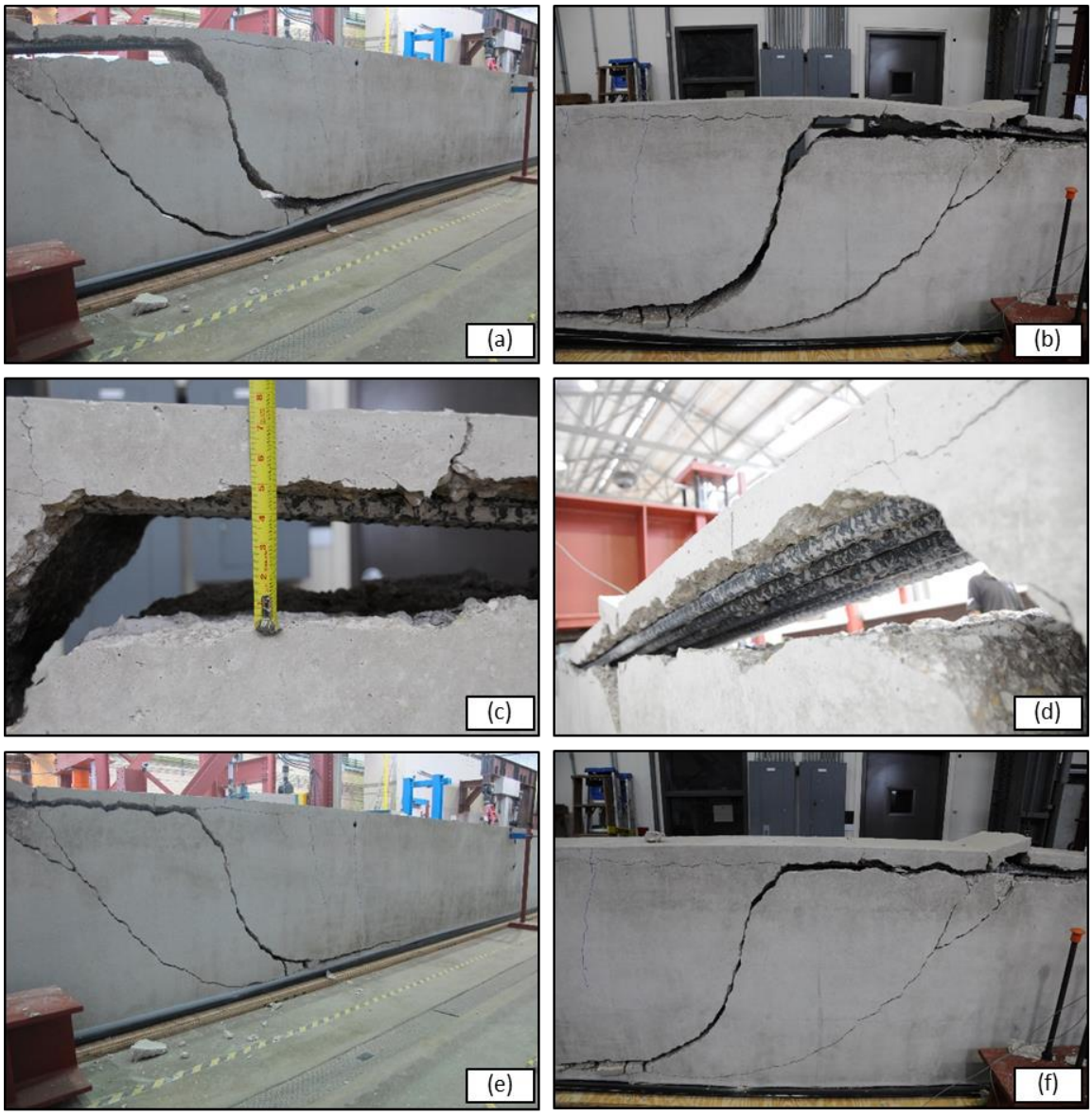

Figure D-14: LD5 Failure Photographs while: (a), (b), (c), and (d) Partially Loaded, and (e) and (f) Unloaded

ACTUAL STRUCTURAL RESPONSE LD5 8-5-2015

Time	Target Load	Actual Load	Comments and Observations
8:41	0	0	–
8:42	10	10.2	Adjusted balance of load
8:52	20	20.0	Flexural cracking at midspan
9:14	30	30.1	Additional flexural cracks, extensions
9:27	40	40.1	Same
9:39	50	50.1	Same
9:52	60	60.1	Limited additional flexural cracking
10:10	Failure	115.1	Well defined shear crack

Figure D-15: LD5 Observation Record

ACTUAL STRUCTURAL RESPONSE LD6-N 5-26-2015

Time	Target Load	Actual Load	Comments and Observations
7:58	0	0	—
7:59	10	10.3	None
8:04	20	19.9	None
8:10	30	30.2	Flexural cracking under load
8:15	40	40.1	Additional flexural cracks, extensions
8:22	50	50.1	Same
8:28	60	60.1	Same
8:33	70	70.1	Mostly extensions
8:38	80	80.1	Same
8:44	Failure	97.6	Well defined shear crack

Figure D-16: LD6-N Observation Record

ACTUAL STRUCTURAL RESPONSE LD6-S 5-26-2015

Time	Target Load	Actual Load	Comments and Observations
4:00	0	0	—
4:01	10	10.4	None
4:04	20	20.1	None
4:10	30	30.1	Flexural cracking under load
4:14	40	40.1	Additional flexural cracks, extensions
4:21	50	50.1	Same
4:26	60	60.4	Same
4:30	70	70.2	Mostly extensions
4:35	80	80.0	Same
4:39	Failure	87.6	Well defined shear crack

Figure D-17: LD6-S Observation Record

ACTUAL STRUCTURAL RESPONSE LD7-N 07-02-2015

Time	Target Load	Actual Load	Comments and Observations
8:24	0	0	—
8:25	10	10.1	None
8:32	20	20.2	None
8:38	30	30.2	None
8:43	40	40.1	None
8:49	50	50.1	Small flexural crack under load
8:58	60	60.0	Additional flexural cracks, extensions
9:07	70	70.0	Same
9:18	80	80.0	Mostly extensions
9:27	90	90.1	Same
9:37	Failure	122.3	Well defined shear crack

Figure D-18: LD7-N Observation Record

ACTUAL STRUCTURAL RESPONSE LD7-S 7-7-2015

Time	Target Load	Actual Load	Comments and Observations
9:03	0	0	—
9:04	10	10.1	None
9:09	20	20.0	None
9:14	30	30.1	None
9:18	40	40.0	None
9:27	50	50.0	Small flexural cracking under load
9:38	60	60.0	Additional flexural cracks, extensions
10:00	Failure	100.6	Well defined shear crack

Figure D-19: LD7-S Observation Record

ACTUAL STRUCTURAL RESPONSE LD8 9-25-15

Time	Target Load	Actual Load	Comments and Observations
2:20	0	0	-
2:20	10	10.0	Adjusted balance of load
2:33	15	15.1	None
2:39	30	30.1	None
2:46	45	45.2	None
2:54	60	60.0	Flexural cracking at midspan
3:12	75	75.1	Additional flexural cracks, extensions
3:32	90	90.0	Same
3:45	105	105.1	Same
4:10	Failure	179.0	Well defined shear crack

Figure D-20: LD8 Observation Record

Appendix E: ACI 318-14 and AASHTO LRFD 2014 Analysis

Appendix E presents sample calculations for ACI 318-14 Equation 22.5.5.1 and ACI 318-14 Table 22.5.5.1, subject to the limitations of Sections 7.4.3.2 and 9.4.3.2 of ACI 318-14, and AASHTO LRFD 2014 Sections 5.8.3.3 and 5.8.3.4. For more specific guidance, refer to ACI 318-14 and AASHTO LRFD 2014. Information is presented as follows:

- *ACI 318-14 Equation 22.5.5.1 Sample Calculations:* Figure E-1
- *ACI 318-14 Table 22.5.5.1 Sample Calculations:* Figure E-2 and Figure E-3
- *AASHTO LRFD 2014 Sample Calculations:* Figure E-4

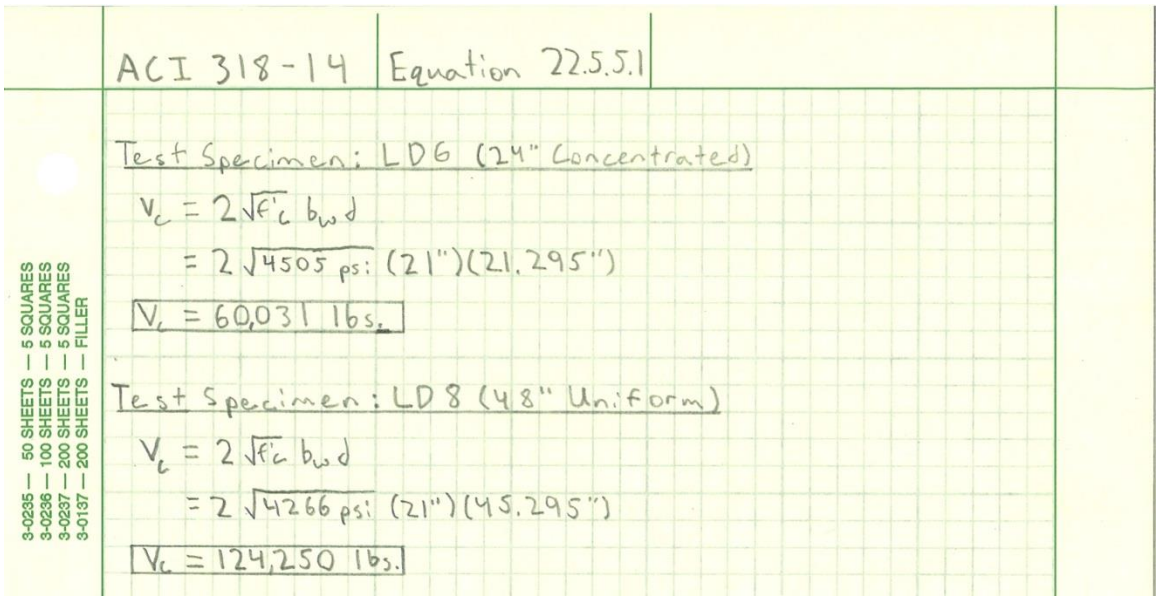

Figure E-1: ACI 318-14 Equation 22.5.5.1 Sample Calculations

Figure E-2: ACI 318-14 Table 22.5.5.1 Sample Calculations for Concentrated Load

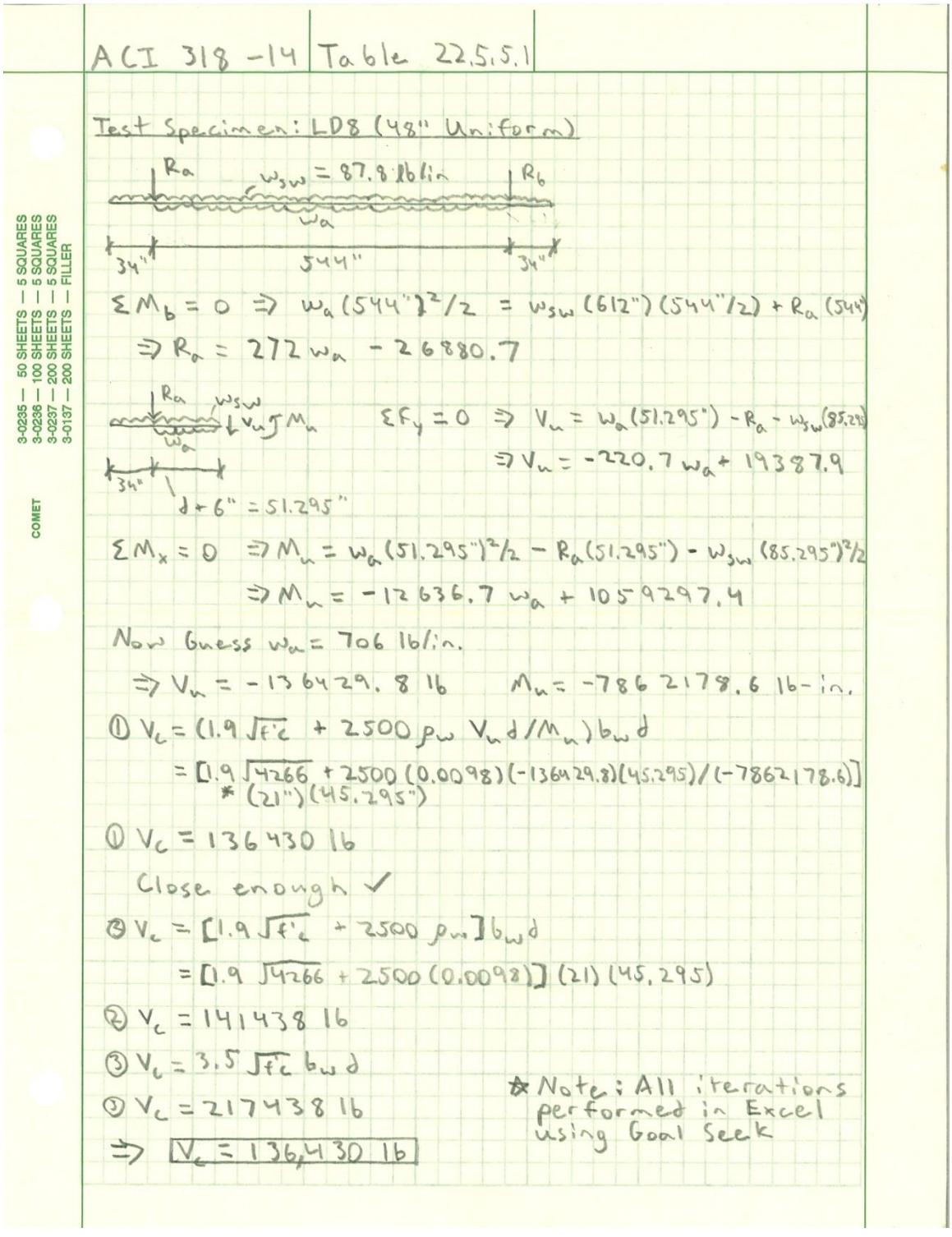

Figure E-3: ACI 318-14 Table 22.5.5.1 Sample Calculations for Uniform Load

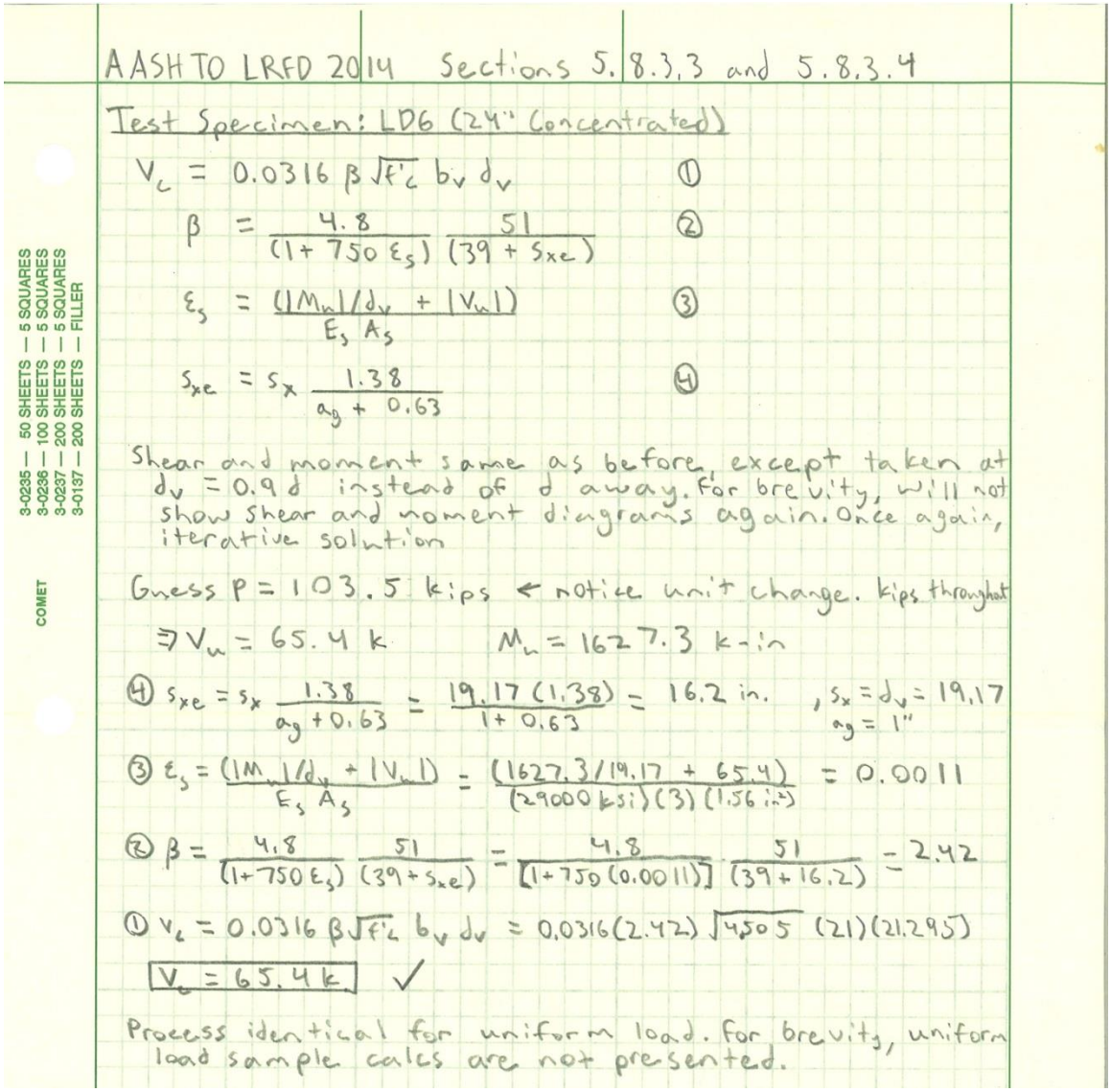

Figure E-4: AASHTO LRFD 2014 Sections 7.4.3.2 and 9.4.3.2 Sample Calculations for Concentrated Load

Appendix F: Literature Dataset Analysis

Three different literature sources were examined to make comparisons with the research presented in this thesis: 17 tests from Feldman and Siess (1955), 152 tests from Krefeld and Thurston (1966), and 6 tests from Dassow (2014). Each data point went through filtering operations as follows:

- shear span-to-depth ratio (a/d) greater than or equal to 2.4,
- no other failure modes such as flexure,
- concrete compressive strength (f'_c) greater than or equal to 2,500 psi (per ACI 318-14 Table 19.2.1.1),
- area of longitudinal tensile steel greater than or equal to the minimum area ($A_{s,min}$) (per ACI 318-14 Section 9.6.1.2 and Table 7.6.1.1),
- net tensile strain in the extreme layer of longitudinal steel (ε_t) greater than or equal to the yield strain (ε_y) when shear is neglected, and
- At least two concentrated load tests and two uniform load tests remaining for identical specimens after all other filtering operations (referred to in Appendix F as Criterion 6).

After filtering, 55 tests remained of 181 total tests, including the tests presented in this thesis. Of these remaining tests, 30 were concentrated load tests and 25 were uniform load tests. For more specific information on each testing program, refer to the original source material.

Appendix F presents the data from the original source material as well as the calculated shear force values at (d) away from the edge of the support (V_d). Dassow (2014) presented (V_d) so it was not calculated. In addition, the tables in Appendix F display the results of filtering operations for each literature source. Failed criteria are

highlighted in red for each test. Every test examined met the criterion for minimum area of longitudinal tensile steel ($A_{s,min}$), and hence, that value is not shown. All calculations were performed in an Excel spreadsheet, but sample calculations are also presented. Information in Appendix F is presented as follows:

- *Nomenclature*
- *Sample Calculations for Failure Criteria:* Figure F-1 and Figure F-2
- *Feldman and Siess (1955):*
  - Geometry and Support Conditions: Table F-1
  - Failure Information and Calculations: Table F-2
  - Final Dataset: Table F-3
  - Shear Force Calculations: Figure F-3 and Figure F-4
- *Krefeld and Thurston (1966):*
  - Geometry and Support Conditions: Table F-4 and Table F-5
  - Failure Information and Calculations: Table F-6 and Table F-7
  - Tests Failing to Meet Criterion 6: Table F-8
  - Final Dataset: Table F-9
  - Shear Force Calculations: Figure F-5
- *Dassow (2014):*
  - Geometry and Support Conditions: Table F-10
  - Failure Information and Calculations: Table F-11
  - Final Dataset: Table F-12

- *Klein (2015):*
    - Geometry and Support Conditions: Table F-13
    - Failure Information and Calculations: Table F-14
    - Final Dataset: Table F-15

F.1 NOMENCLATURE

f'_c	Concrete compressive strength
f_y	Steel yield strength
b	Width
h	Height
d	Effective depth
a	Shear span
a/d	Shear span-to-depth ratio
ρ	Longitudinal steel reinforcement ratio
LP width	Width of loading plate used to simulate uniform load – applies to Feldman and Siess (1955) and Krefeld and Thurston (1966)
SP width	Width of support plates
P_h	Total load at which diagonal cracking becomes horizontal, equated to first significant diagonal cracking – applies to Feldman and Siess (1955)
P_u	Ultimate total load – applies to Feldman and Siess (1955), Dassow (2014), and Klein (2015)
V_{crit}	Shear at the support at first diagonal cracking – applies to Krefeld and Thurston (1966)
V_{ult}	Shear at the support at ultimate load – applies to Krefeld and Thurston (1966)
P_{crit}	Total load at first diagonal cracking – applies to Dassow (2014) and Klein (2015)
w_b	Self-weight of specimen

V_d	Shear Force at (d) away from the edge of the support plate
v_d	Normalized shear stress at (d) away from the edge of the support plate
c	Depth of the neutral axis at flexural failure
ε_t	Net tensile strain in the extreme layer of longitudinal steel at flexural failure
Yield?	Is (ε_t) greater than or equal to (ε_y)? – yes or no (Y or N)
Other Failure?	Is there another failure type besides shear? – if yes, failure type listed; if no, "N"
Group	Originally termed "Series" in Krefeld and Thurston (1966). Many tests have the same name, and the series number distinguishes them. The name was changed to "Group" so as to avoid confusion with the Chapter 4 use of "Series".

Data Filtering | Sample Calculations

Test: Krefeld and Thurston 6AU (Series V Uniform):

Beam: $A_{s,min}$ = maximum of: $[3\sqrt{f'_c}/f_y]\,bd$

$[200/f_y]\,bd$

$f'_c = 2990$
$f_y = 39600$ $\Rightarrow A_{s,min} = 0.30\ in^2$

$A_{s,actual} = 2.54\ in^2$ ✓

Slab: $A_{s,min}$ = if $f_y < 60000$ $= 0.002\,bhd$

otherwise max of: $0.0018(60/f_y)\,bhd$

$0.0014\,bhd$

$\Rightarrow A_{s,min} = 0.144\ in^2$ ✓

Steel stress check

At flexural failure:

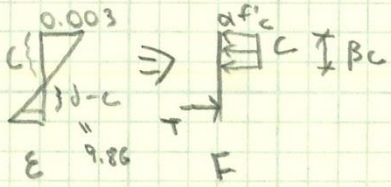

Assume steel yields

$T = C$

$A_s f_y = \alpha f'_c \beta c\, b$

$2.54(39.6) = (0.9)(2.99)(5/6)\,c\,(6)$

$\Rightarrow c = 7.47"$

★ Used real values of α + β because didn't want to exclude data points with lower-bound ACI approximation

Does steel yield?

$\varepsilon_s = 0.003\,\frac{(d-c)}{c} = 0.00096$

$\varepsilon_y = 39.6/29000 = 0.0013$ X NG

Must go back and assume steel doesn't yield

Figure F-1: Sample Calculations for Failure Criteria, Part 1

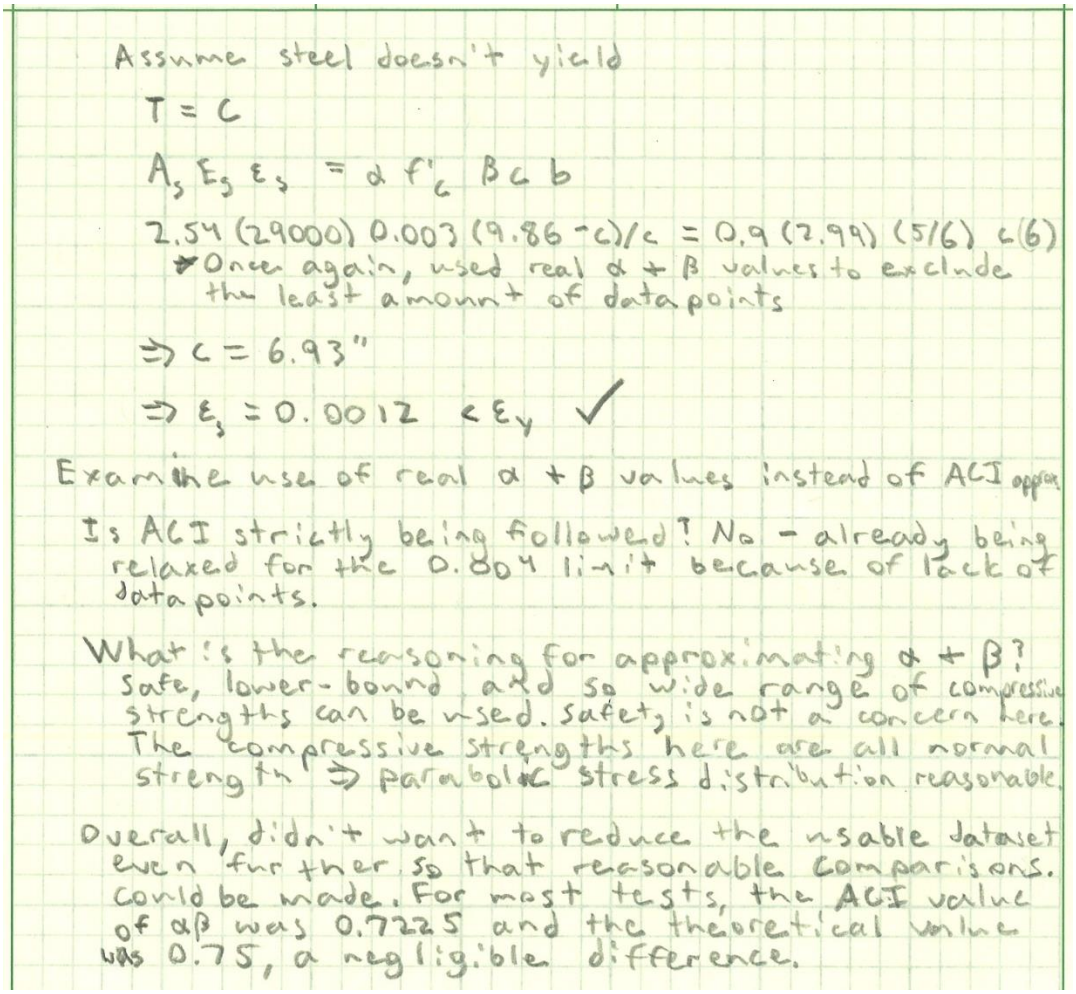

Figure F-2: Sample Calculations for Failure Criteria, Part 2

Table F-1: Geometry and Loading Conditions, Feldman and Siess (1955)

Loading	Name	f'_c psi	f_y ksi	b in.	h in.	d in.	a in.	a/d	ρ %	LP width in.	SP width in.
Concentrated	L-1	3050	44.0	6	12	9.94	20.0	2.01	3.35	-	6
	L-2	3120	45.0	6	12	9.94	30.0	3.02	3.35	-	6
	L-2a	5320	41.0	6	12	9.94	30.0	3.02	3.35	-	6
	L-3	4060	45.0	6	12	9.94	40.0	4.02	3.35	-	6
	L-4	3740	44.0	6	12	9.94	50.0	5.03	3.35	-	6
	L-5	4050	48.0	6	12	9.94	60.0	6.04	3.35	-	6
	L-6	4440	46.0	6	12	9.94	70.0	7.04	3.35	-	6
	L1R	3050	44.0	6	12	9.94	20.0	2.01	3.35	-	6
	L2R	3120	45.0	6	12	9.94	30.0	3.02	3.35	-	6
	L2aR	5230	41.0	6	12	9.94	30.0	3.02	3.35	-	6
	L3R	4060	45.0	6	12	9.94	40.0	4.02	3.35	-	6
Uniform	D-1	4470	42.8	6	12	9.94	27.5	2.77	3.35	6	6
	D-2	5590	44.5	6	12	9.94	27.5	2.77	3.35	6	6
	D-3	4820	45.5	6	12	9.94	33.0	3.32	3.35	6	6
	D-4	5020	44.6	6	12	9.94	22.0	2.21	2.21	6	6
	D-5	3740	52.3	6	12	10.88	16.5	1.52	1.35	6	6
	D-6	3450	45.0	6	12	9.94	27.5	2.77	3.35	6	6

Table F-2: Failure Information and Calculations, Feldman and Siess (1955)

Loading	Name	P_h kip	P_u kip	w_b lb/in.	V_d kip	v_d √psi	c in.	ε_t 10^{-3}	Yield?	Other Failure?
Concentrated	L-1	33.0	52.2	6.25	16.68	5.06	6.41	1.65	Y	N
	L-2	26.0	34.0	6.25	13.24	3.97	6.41	1.65	Y	N
	L-2a	28.7	36.0	6.25	14.59	3.35	3.43	5.71	Y	N
	L-3	24.0	24.0	6.25	12.30	3.24	4.93	3.05	Y	N
	L-4	23.0	23.0	6.25	11.86	3.25	5.23	2.70	Y	N
	L-5	22.9	22.9	6.25	11.88	3.13	5.27	2.66	Y	N
	L-6	21.1	21.1	6.25	11.04	2.78	4.60	3.48	Y	Flexure
	L1R	74.0	74.0	6.25	37.18	11.29	6.41	1.65	Y	N
	L2R	32.0	33.6	6.25	16.06	4.82	6.41	1.65	Y	N
	L2aR	41.6	41.6	6.25	20.86	4.84	3.48	5.56	Y	N
	L3R	27.9	27.9	6.25	14.09	3.71	4.93	3.05	Y	N
Uniform	D-1	38.2	41.7	-	17.23	4.32	4.26	4.01	Y	N
	D-2	39.8	49.6	-	17.95	4.03	3.54	5.43	Y	N
	D-3	38.8	42.3	-	18.79	4.54	4.20	4.11	Y	N
	D-4	52.6	52.6	-	21.97	5.20	2.61	8.44	Y	Flexure
	D-5	35.1	55.3	-	12.94	3.24	2.73	8.94	Y	N
	D-6	35.3	46.8	-	15.92	4.54	5.80	2.14	Y	N

Table F-3: Final Dataset, Feldman and Siess (1955)

Loading	Name	f'_c psi	d in.	a/d	ρ %	V_d kip	v_d √psi
Concentrated	L-2	3120	9.94	3.02	3.35	13.24	3.97
	L-2a	5320	9.94	3.02	3.35	14.59	3.35
	L-3	4060	9.94	4.02	3.35	12.30	3.24
	L-4	3740	9.94	5.03	3.35	11.86	3.25
	L-5	4050	9.94	6.04	3.35	11.88	3.13
	L2R	3120	9.94	3.02	3.35	16.06	4.82
	L2aR	5230	9.94	3.02	3.35	20.86	4.84
	L3R	4060	9.94	4.02	3.35	14.09	3.71
Uniform	D-1	4470	9.94	2.77	3.35	17.23	4.32
	D-2	5590	9.94	2.77	3.35	17.95	4.03
	D-3	4820	9.94	3.32	3.35	18.79	4.54
	D-6	3450	9.94	2.77	3.35	15.92	4.54

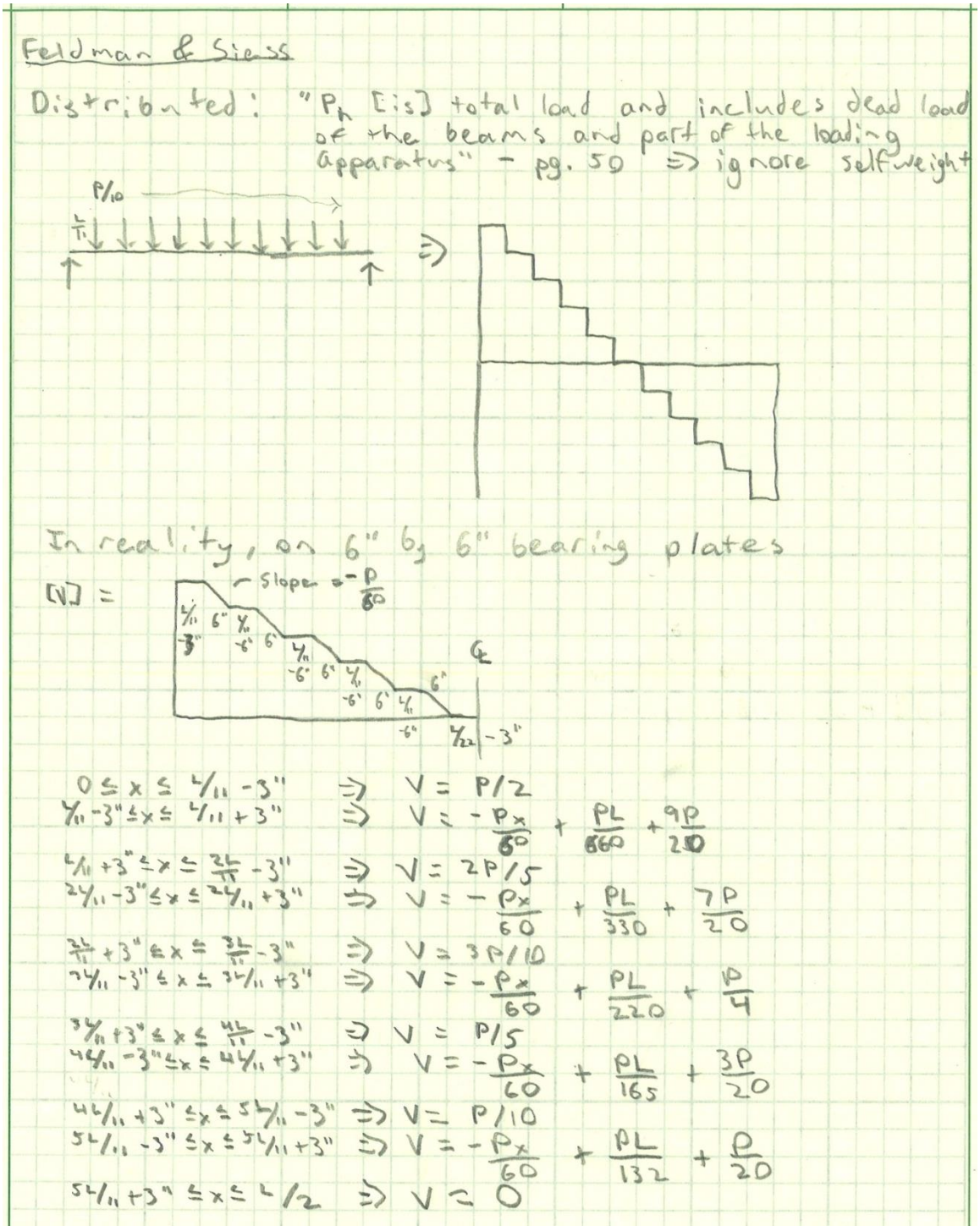

Figure F-3: Shear Force Calculations for Uniform Load, Feldman and Siess (1955)

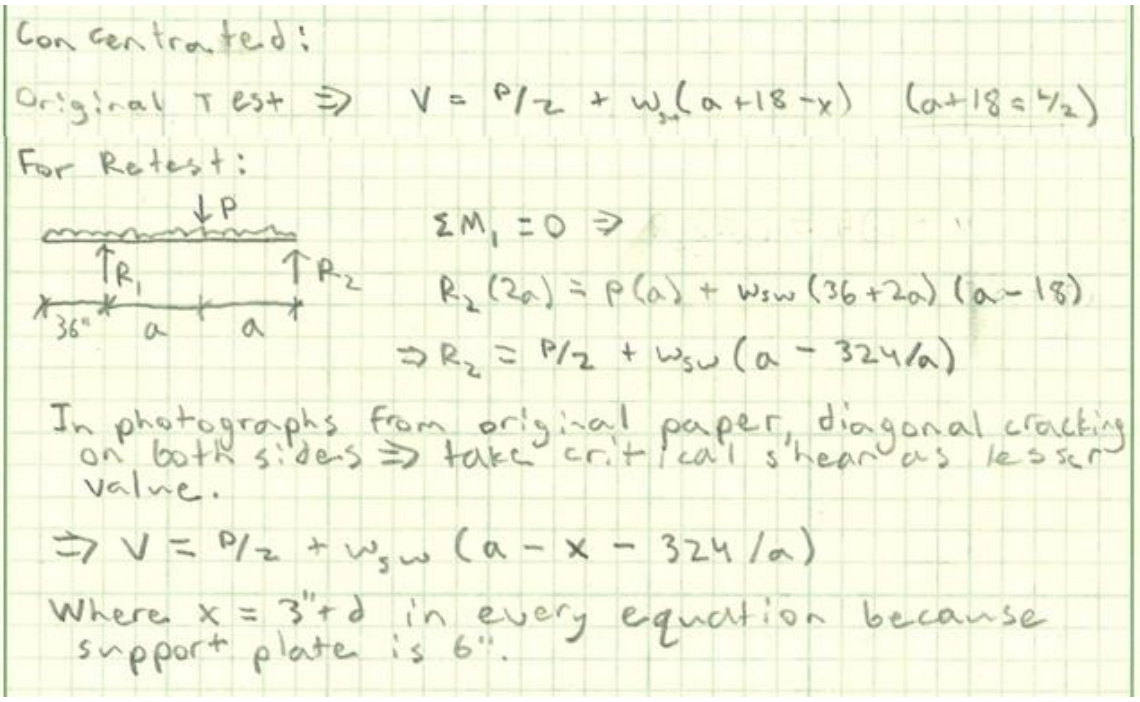

Figure F-4: Shear Force Calculations for Concentrated Load, Feldman and Siess (1955)

Table F-4: Geometry and Loading Conditions for Concentrated Load Tests, Krefeld and Thurston (1966)

Group	Name	f'_c psi	f_y ksi	b in.	h in.	d in.	a in.	a/d	ρ %	LP width in.	SP width in.
II	4A3	4440	53.0	8	18	15.36	36	2.34	2.07	-	7.5
	5A3	4330	53.0	8	18	15.36	36	2.34	3.10	-	7.5
	11A2	4380	53.0	6	15	12.36	36	2.91	3.43	-	7.5
	12A2	4360	53.0	6	12	9.36	36	3.85	4.52	-	7.5
III	18A2	2800	56.0	6	15	12.44	36	2.89	2.68	-	7.5
	18B2	2880	56.0	6	15	12.44	36	2.89	2.68	-	7.5
	18C2	3280	56.0	6	15	12.44	36	2.89	2.68	-	7.5
	18D2	3200	56.0	6	15	12.44	36	2.89	2.68	-	7.5
IV	13A2	2890	53.0	6	15	12.56	36	2.87	0.80	-	7.5
	14A2	3000	53.0	6	12	9.56	36	3.77	1.05	-	7.5
	15A2	2920	56.0	6	15	12.44	36	2.89	1.34	-	7.5
	15B2	3000	56.0	6	15	12.44	36	2.89	1.34	-	7.5
	16A2	3220	56.0	6	12	9.44	36	3.81	1.77	-	7.5
	17A2	3190	53.0	6	12	9.56	36	3.77	2.09	-	7.5
	18E2	2870	56.0	6	15	12.44	36	2.89	2.68	-	7.5
	19A2	2980	56.0	6	12	9.44	36	3.81	3.53	-	7.5
	20A2	3050	53.0	6	12	9.36	36	3.85	4.52	-	7.5
	21A2	2890	53.0	8	12	9.36	36	3.85	5.09	-	7.5
V	1AC	3180	53.0	6	12	10.06	48	4.77	0.99	-	7.5
	2AC	3340	57.1	6	12	10.00	48	4.80	1.32	-	7.5
	3AC	3020	53.0	6	12	10.06	48	4.77	1.99	-	7.5
	4AC	2390	57.1	6	12	10.00	48	4.80	2.63	-	7.5
	5AC	2660	56.0	6	12	9.94	48	4.83	3.35	-	7.5
	6AC	3310	53.0	6	12	9.86	48	4.87	4.29	-	7.5
	1CC	2750	53.0	6	12	10.06	60	5.96	0.99	-	7.5
	2CC	3020	57.1	6	12	10.00	60	6.00	1.32	-	7.5
	3CC	2970	53.0	6	12	10.06	60	5.96	1.99	-	7.5
	4CC	2980	57.1	6	12	10.00	60	6.00	2.63	-	7.5
	5CC	2950	56.0	6	12	9.94	60	6.04	3.35	-	7.5
	6CC	2980	53.0	6	12	9.86	60	6.09	4.29	-	7.5
	3EC	2730	53.0	6	12	10.06	72	7.16	1.99	-	7.5
	4EC	3080	57.1	6	12	10.00	72	7.20	2.63	-	7.5
	5EC	2830	56.0	6	12	9.94	72	7.24	3.35	-	7.5
	6EC	2770	53.0	6	12	9.86	72	7.30	4.29	-	7.5

Table F-4: Geometry and Loading Conditions for Concentrated Load Tests, Krefeld and Thurston (1966) continued

Group	Name	f'_c psi	f_y ksi	b in.	h in.	d in.	a in.	a/d	ρ %	LP width in.	SP width in.
V	3GC	3255	53.0	6	12	10.06	84	8.35	1.99	-	7.5
	4GC	3050	57.1	6	12	10.00	84	8.40	2.63	-	7.5
	5GC	3180	56.0	6	12	9.94	84	8.45	3.35	-	7.5
	6GC	3100	53.0	6	12	9.86	84	8.52	4.29	-	7.5
	3JC	3220	53.0	6	12	10.06	96	9.54	1.99	-	7.5
	4JC	3220	57.1	6	12	10.00	96	9.60	2.63	-	7.5
	5JC	3310	56.0	6	12	9.94	96	9.66	3.35	-	7.5
	6JC	3100	53.0	6	12	9.86	96	9.74	4.29	-	7.5
VII	6C	2920	56.0	6	12	9.94	36	3.62	3.35	-	7.5
VIII	3AAC	5010	53.0	6	12	10.06	36	3.58	1.99	-	7.5
	4AAC	4235	57.1	6	12	10.00	36	3.60	2.63	-	7.5
	5AAC	4760	56.0	6	12	9.94	36	3.62	3.35	-	7.5
	6AAC	4990	53.0	6	12	9.86	36	3.65	4.29	-	7.5
	3AC	4620	53.0	6	12	10.06	48	4.77	1.99	-	7.5
	4AC	4420	57.1	6	12	10.00	48	4.80	2.63	-	7.5
	5AC	4760	56.0	6	12	9.94	48	4.83	3.35	-	7.5
	6AC	4950	53.0	6	12	9.86	48	4.87	4.29	-	7.5
	4CC	5570	57.1	6	12	10.00	60	6.00	2.63	-	7.5
	5CC	5430	56.0	6	12	9.94	60	6.04	3.35	-	7.5
	6CC	5570	53.0	6	12	9.86	60	6.09	4.29	-	7.5
	4EC	5340	57.1	6	12	10.00	72	7.20	2.63	-	7.5
	5EC	5430	56.0	6	12	9.94	72	7.24	3.35	-	7.5
	6EC	4900	53.0	6	12	9.86	72	7.30	4.29	-	7.5
IX	3AAC	1820	53.0	6	12	10.06	36	3.58	1.99	-	7.5
	4AAC	1870	57.1	6	12	10.00	36	3.60	2.63	-	7.5
	5AAC	2230	56.0	6	12	9.94	36	3.62	3.35	-	7.5
	6AAC	1940	53.0	6	12	9.86	36	3.65	4.29	-	7.5
	3AC	1990	53.0	6	12	10.06	48	4.77	1.99	-	7.5
	4AC	1870	57.1	6	12	10.00	48	4.80	2.63	-	7.5
	5AC	2230	56.0	6	12	9.94	48	4.83	3.35	-	7.5
	6AC	1800	53.0	6	12	9.86	48	4.87	4.29	-	7.5
	3CC	1770	53.0	6	12	10.06	60	5.96	1.99	-	7.5
	4CC	2480	57.1	6	12	10.00	60	6.00	2.63	-	7.5
	5CC	2130	56.0	6	12	9.94	60	6.04	3.35	-	7.5

Table F-4: Geometry and Loading Conditions for Concentrated Load Tests, Krefeld and Thurston (1966) continued

Group	Name	f'_c psi	f_y ksi	b in.	h in.	d in.	a in.	a/d	ρ %	LP width in.	SP width in.
IX	6CC	1980	53.0	6	12	9.86	60	6.09	4.29	-	7.5
	4EC	2070	57.1	6	12	10.00	72	7.20	2.63	-	7.5
	5EC	2190	56.0	6	12	9.94	72	7.24	3.35	-	7.5
X	C	2430	57.1	8	21	19.00	60	3.16	1.56	-	7.5
XI	PCa	5260	53.0	6	12	9.86	72	7.30	4.29	-	7.5
	PCb	5260	53.0	6	12	9.86	72	7.30	4.29	-	7.5
s-I	OCa	5180	57.1	6	12	10.00	60	6.00	2.63	-	7.5
	OCb	5660	57.1	6	12	10.00	60	6.00	2.63	-	7.5
s-II	OCa	5550	56.0	10	20	17.94	72	4.01	2.23	-	7.5
	OCb	5550	56.0	10	20	17.94	72	4.01	2.23	-	7.5

Table F-5: Geometry and Loading Conditions for Uniform Load Tests, Krefeld and Thurston (1966)

Group	Name	f'_c psi	f_y ksi	b in.	h in.	d in.	a in.	a/d	ρ %	LP width in.	SP width in.
I	4A1	4240	49.3	8	18	15.36	18	1.17	2.07	8	6
	4B1	3990	52.9	8	18	15.36	18	1.17	2.07	8	6
	5A1	4270	45.6	8	18	15.36	18	1.17	3.10	8	6
	5B1	4290	52.3	8	18	15.36	18	1.17	3.10	8	6
II	4A2	4070	50.8	8	18	15.36	18	1.17	2.07	8	6
	5A2	4260	52.9	8	18	15.36	18	1.17	3.10	8	6
	11A1	3910	41.2	6	15	12.36	18	1.46	3.43	8	6
	12A1	4440	42.0	6	12	9.36	18	1.92	4.52	8	6
IV	13A1	2930	58.1	6	15	12.56	18	1.43	0.80	8	6
	14A1	3300	58.1	6	12	9.56	18	1.88	1.05	8	6
	15A1	2780	67.0	6	15	12.44	18	1.45	1.34	8	6
	16A1	3050	52.8	6	12	9.44	18	1.91	1.77	8	6
	17A1	2660	50.9	6	12	9.56	18	1.88	2.09	8	6
	17B1	3040	52.3	6	12	9.56	18	1.88	2.09	8	6
	18A1	2930	46.6	6	15	12.44	18	1.45	2.68	8	6
	19A1	3080	36.9	6	12	9.44	18	1.91	3.53	8	6
	20A1	3090	17.9	6	12	9.36	18	1.92	4.52	8	6
	21A1	3080	31.8	8	12	9.36	18	1.92	5.09	8	6
V	1AU	3180	54.9	6	12	10.06	24	2.39	0.99	11	6
	2AU	3070	57.1	6	12	10.00	24	2.40	1.32	11	6
	3AU	3290	49.7	6	12	10.06	24	2.39	1.99	11	6
	4AU	2590	39.6	6	12	10.00	24	2.40	2.63	11	6
	5AU	2990	38.9	6	12	9.94	24	2.41	3.35	11	6
	6AU	2990	39.6	6	12	9.86	24	2.43	4.29	11	6
	1CU	2750	54.9	6	12	10.06	30	2.98	0.99	14	6
	2CU	3020	53.7	6	12	10.00	30	3.00	1.32	14	6
	3CU	2970	46.2	6	12	10.06	30	2.98	1.99	14	6
	4CU	2980	40.0	6	12	10.00	30	3.00	2.63	14	6
	5CU	2960	32.5	6	12	9.94	30	3.02	3.35	14	6
	6CU	2980	25.3	6	12	9.86	30	3.04	4.29	14	6
	3EU	2550	50.6	6	12	10.06	36	3.58	1.99	14	6
	4EU	2935	47.4	6	12	10.00	36	3.60	2.63	14	6
	5EU	2800	37.1	6	12	9.94	36	3.62	3.35	14	6
	6EU	2910	25.3	6	12	9.86	36	3.65	4.29	14	6

Table F-5: Geometry and Loading Conditions for Uniform Load Tests, Krefeld and Thurston (1966) continued

Group	Name	f'_c psi	f_y ksi	b in.	h in.	d in.	a in.	a/d	ρ %	LP width in.	SP width in.
V	3GU	3280	54.9	6	12	10.06	42	4.17	1.99	14	6
	4GU	3205	57.1	6	12	10.00	42	4.20	2.63	14	6
	5GU	3085	37.7	6	12	9.94	42	4.23	3.35	14	6
	6GU	3080	43.4	6	12	9.86	42	4.26	4.29	14	6
	3JU	3220	54.9	6	12	10.06	48	4.77	1.99	14	6
	4JU	3220	30.0	6	12	10.00	48	4.80	2.63	14	6
	5JU	3120	53.7	6	12	9.94	48	4.83	3.35	14	6
	6JU	3045	34.6	6	12	9.86	48	4.87	4.29	14	6
VII	6U	2960	40.9	6	12	9.94	18	1.81	3.35	8	6
VIII	3AAU	5010	54.9	6	12	10.06	18	1.79	1.99	8	6
	4AAU	5280	52.0	6	12	10.00	18	1.80	2.63	8	6
	5AAU	4200	47.5	6	12	9.94	18	1.81	3.35	8	6
	6AAU	4990	42.9	6	12	9.86	18	1.83	4.29	8	6
	4AU	4590	43.2	6	12	10.00	24	2.40	2.63	11	6
	5AU	4590	44.3	6	12	9.94	24	2.41	3.35	11	6
	6AU	4950	40.3	6	12	9.86	24	2.43	4.29	11	6
	4CU	4680	45.5	6	12	10.00	30	3.00	2.63	14	6
	5CU	4680	36.8	6	12	9.94	30	3.02	3.35	14	6
	6CU	5340	36.1	6	12	9.87	30	3.04	4.29	14	6
IX	3AAU	1820	41.3	6	12	10.06	18	1.79	1.99	8	6
	4AAU	1780	27.9	6	12	10.00	18	1.80	2.63	8	6
	5AAU	2020	31.9	6	12	9.94	18	1.81	3.35	8	6
	6AAU	1940	28.6	6	12	9.86	18	1.83	4.29	8	6
	3AU	1990	44.5	6	12	10.06	24	2.39	1.99	11	6
	4AU	1840	51.2	6	12	10.00	24	2.40	2.63	11	6
	5AU	2170	34.8	6	12	9.94	24	2.41	3.35	11	6
	6AU	1800	24.4	6	12	9.86	24	2.43	4.29	11	6
	3CU	1770	35.2	6	12	10.06	30	2.98	1.99	14	6
	4CU	2480	36.4	6	12	10.00	30	3.00	2.63	14	6
	5CU	2130	29.0	6	12	9.94	30	3.02	3.35	14	6
	6CU	1980	29.2	6	12	9.86	30	3.04	4.29	14	6
	3EU	2200	54.9	6	12	10.06	36	3.58	1.99	14	6
	4EU	2070	33.5	6	12	10.00	36	3.60	2.63	14	6
	5EU	2190	36.5	6	12	9.94	36	3.62	3.35	14	6

Table F-5: Geometry and Loading Conditions for Uniform Load Tests, Krefeld and Thurston (1966) continued

Group	Name	f'_c psi	f_y ksi	b in.	h in.	d in.	a in.	a/d	ρ %	LP width in.	SP width in.
IX	6EU	1850	30.6	6	12	9.86	36	3.65	4.29	14	6
	3GU	1960	43.1	6	12	10.06	42	4.17	1.99	14	6
	4GU	1680	57.1	6	12	10.00	42	4.20	2.63	14	6
	5GU	1620	29.3	6	12	9.94	42	4.23	3.35	14	6
X	U	3060	41.5	8	21	19.00	30	1.58	1.56	14	6
s-II	OU	5390	36.1	10	20	17.94	36	2.01	2.23	14	6

Table F-6: Failure Information and Calculations for Concentrated Load Tests, Krefeld and Thurston (1966)

Group	Name	V_{crit} kip	V_{ult} kip	w_b lb/in.	V_d kip	v_d √psi	c in.	ε_t 10^{-3}	Yield?	Other Failure?
II	4A3	22.5	24.7	12.50	22.71	2.77	5.05	6.12	Y	N
	5A3	22.5	38.3	12.50	22.71	2.81	7.77	2.93	Y	N
	11A2	15.0	16.5	7.81	15.16	3.09	6.83	2.43	Y	N
	12A2	12.5	14.4	6.25	12.64	3.41	6.08	1.62	N	N
III	18A2	13.0	14.2	7.81	13.15	3.33	7.91	1.72	N	N
	18B2	13.0	16.2	7.81	13.15	3.28	7.85	1.75	N	N
	18C2	12.0	16.5	7.81	12.15	2.84	7.57	1.93	N	N
	18D2	12.0	13.5	7.81	12.15	2.88	7.63	1.89	N	N
IV	13A2	8.5	10.9	7.81	8.65	2.14	2.45	12.41	Y	N
	14A2	6.0	7.9	6.25	6.14	1.95	2.36	9.18	Y	N
	15A2	9.0	10.3	7.81	9.15	2.27	4.26	5.76	Y	N
	15B2	11.0	11.7	7.81	11.15	2.73	4.15	6.00	Y	N
	16A2	8.5	9.4	6.25	8.64	2.69	3.86	4.33	Y	N
	17A2	9.0	9.9	6.25	9.14	2.82	4.43	3.47	Y	N
	18E2	12.0	18.4	7.81	12.15	3.04	7.86	1.75	N	N
	19A2	9.5	10.4	6.25	9.64	3.12	6.34	1.47	N	N
	20A2	10.0	11.4	6.25	10.14	3.27	6.63	1.24	N	N
	21A2	14.0	17.2	8.33	14.19	3.53	6.88	1.08	N	N
V	1AC	7.4	7.4	6.25	7.61	2.24	2.22	10.58	Y	Flexure
	2AC	7.0	8.5	6.25	7.21	2.08	3.00	7.00	Y	N
	3AC	9.0	9.9	6.25	9.21	2.78	4.68	3.45	Y	N
	4AC	8.5	8.5	6.25	8.71	2.97	6.60	1.55	N	N
	5AC	8.5	9.4	6.25	8.71	2.83	6.78	1.40	N	N
	6AC	12.0	12.0	6.25	12.21	3.59	6.77	1.37	N	N
	1CC	6.0	6.0	6.25	6.29	1.99	2.57	8.74	Y	Flexure
	2CC	6.8	6.8	6.25	7.09	2.15	3.32	6.04	Y	Flexure
	3CC	8.0	8.0	6.25	8.29	2.52	4.76	3.34	Y	N
	4CC	9.0	9.0	6.25	9.29	2.84	6.22	1.82	N	N
	5CC	10.0	10.0	6.25	10.29	3.18	6.61	1.51	N	N
	6CC	10.0	10.0	6.25	10.29	3.19	6.94	1.26	N	N
	3EC	8.5	8.5	6.25	8.86	2.81	5.18	2.83	Y	Flexure
	4EC	9.4	9.4	6.25	9.76	2.93	6.17	1.87	N	N
	5EC	8.9	8.9	6.25	9.26	2.92	6.68	1.47	N	N
	6EC	9.5	9.5	6.25	9.86	3.17	7.05	1.19	N	N

Table F-6: Failure Information and Calculations for Concentrated Load Tests, Krefeld and Thurston (1966) continued

Group	Name	V_{crit} kip	V_{ult} kip	w_b lb/in.	V_d kip	v_d √psi	c in.	ε_t 10^{-3}	Yield?	Other Failure?
V	3GC	7.1	7.1	6.25	7.54	2.19	4.34	3.95	Y	Flexure
	4GC	8.0	8.3	6.25	8.44	2.55	6.18	1.85	N	N
	5GC	8.5	9.4	6.25	8.94	2.66	6.48	1.60	N	N
	6GC	9.1	9.1	6.25	9.54	2.90	6.88	1.30	N	N
	3JC	6.3	6.3	6.25	6.81	1.99	4.39	3.88	Y	Flexure
	4JC	7.1	7.1	6.25	7.61	2.24	6.09	1.93	N	Flexure
	5JC	9.0	9.0	6.25	9.51	2.77	6.42	1.65	N	Flexure
	6JC	7.9	7.9	6.25	8.41	2.55	6.88	1.30	N	Flexure
VII	6C	11.5	11.5	6.25	11.64	3.61	6.63	1.50	N	N
VIII	3AAC	12.0	12.5	6.25	12.14	2.84	2.82	7.70	Y	N
	4AAC	12.5	13.0	6.25	12.64	3.24	4.73	3.34	Y	N
	5AAC	12.0	12.8	6.25	12.14	2.95	5.23	2.70	Y	N
	6AAC	13.0	13.5	6.25	13.14	3.14	6.00	1.93	Y	N
	3AC	11.0	12.0	6.25	11.21	2.73	3.06	6.87	Y	N
	4AC	11.0	12.1	6.25	11.21	2.81	4.54	3.61	Y	N
	5AC	11.0	12.2	6.25	11.21	2.73	5.23	2.70	Y	N
	6AC	12.0	13.3	6.25	12.21	2.93	6.04	1.89	Y	N
	4CC	11.0	11.8	6.25	11.29	2.52	3.60	5.33	Y	N
	5CC	12.0	12.9	6.25	12.29	2.80	4.58	3.51	Y	N
	6CC	11.5	14.2	6.25	11.79	2.67	5.37	2.51	Y	N
	4EC	11.6	11.6	6.25	11.96	2.73	3.75	4.99	Y	Flexure
	5EC	9.0	12.0	6.25	9.36	2.13	4.58	3.51	Y	N
	6EC	9.0	11.0	6.25	9.36	2.26	6.11	1.85	Y	N
IX	3AAC	9.0	9.1	6.25	9.14	3.55	6.62	1.56	N	N
	4AAC	9.0	9.6	6.25	9.14	3.52	7.00	1.29	N	N
	5AAC	10.5	11.3	6.25	10.64	3.78	7.06	1.22	N	N
	6AAC	10.0	14.0	6.25	10.14	3.89	7.59	0.90	N	N
	3AC	8.0	8.3	6.25	8.21	3.05	6.47	1.66	N	N
	4AC	8.0	9.0	6.25	8.21	3.17	7.00	1.29	N	N
	5AC	9.5	9.8	6.25	9.71	3.45	7.06	1.22	N	N
	6AC	9.0	9.2	6.25	9.21	3.67	7.69	0.85	N	N
	3CC	6.0	7.0	6.25	6.29	2.48	6.67	1.53	N	N
	4CC	7.9	7.9	6.25	8.19	2.74	6.53	1.59	N	N
	5CC	7.5	7.7	6.25	7.79	2.83	7.14	1.18	N	N

Table F-6: Failure Information and Calculations for Concentrated Load Tests, Krefeld and Thurston (1966) continued

Group	Name	V_{crit} kip	V_{ult} kip	w_b lb/in.	V_d kip	v_d √psi	c in.	ε_t 10^{-3}	Yield?	Other Failure?
IX	6CC	8.5	8.9	6.25	8.79	3.34	7.56	0.91	N	N
	4EC	8.0	8.0	6.25	8.36	3.06	6.83	1.39	N	Flexure
	5EC	7.8	7.8	6.25	8.16	2.93	7.09	1.20	N	Flexure
X	C	19.0	19.0	14.58	19.54	2.61	9.28	3.14	Y	N
XI	PCa	12.0	12.0	6.25	12.36	2.88	5.69	2.20	Y	N
	PCb	12.0	12.0	6.25	12.36	2.88	5.69	2.20	Y	N
s-I	OCa	10.0	10.9	6.25	10.29	2.38	3.87	4.75	Y	N
	OCb	11.5	11.8	6.25	11.79	2.61	3.54	5.47	Y	N
s-II	OCa	31.0	33.0	17.36	31.87	2.38	5.38	7.00	Y	N
	OCb	29.0	30.0	17.36	29.87	2.24	5.38	7.00	Y	N

Table F-7: Failure Information and Calculations for Uniform Load Tests, Krefeld and Thurston (1966)

Group	Name	V_{crit} kip	V_{ult} kip	w_{sw} lb/in.	V_d kip	v_d √psi	c in.	ε_t 10^{-3}	Yield?	Other Failure?
I	4A1	37.5	90.6	12.50	18.97	2.37	4.92	6.36	Y	N
	4B1	42.5	98.1	12.50	21.47	2.77	5.61	5.21	Y	N
	5A1	47.5	123.1	12.50	23.97	2.99	6.78	3.80	Y	N
	5B1	42.5	140.1	12.50	21.47	2.67	7.74	2.95	Y	N
II	4A2	40.0	95.8	12.50	20.22	2.58	5.28	5.72	Y	N
	5A2	40.0	142.6	12.50	20.22	2.52	7.89	2.84	Y	N
	11A1	25.0	60.1	7.81	14.33	3.09	5.95	3.23	Y	N
	12A1	40.6	40.6	6.25	26.97	7.21	5.34	2.26	Y	Flexure
IV	13A1	26.6	26.6	7.81	15.07	3.69	2.64	11.25	Y	Flexure
	14A1	20.1	20.1	6.25	13.30	4.04	2.35	9.22	Y	Flexure
	15A1	16.0	34.8	7.81	9.19	2.34	5.36	3.97	Y	N
	16A1	13.0	23.7	6.25	8.70	2.78	3.85	4.36	Y	N
	17A1	13.0	27.5	6.25	8.65	2.93	5.10	2.62	Y	N
	17B1	14.0	28.8	6.25	9.31	2.94	4.59	3.25	Y	N
	18A1	21.0	54.3	7.81	12.01	2.97	7.07	2.28	Y	N
	19A1	19.0	36.0	6.25	12.65	4.02	5.32	2.32	Y	N
	20A1	18.0	37.6	6.25	12.04	3.86	3.27	5.59	Y	N
	21A1	27.0	50.6	8.33	18.03	4.34	6.56	1.28	Y	N
V	1AU	14.5	14.5	6.25	10.91	3.20	2.30	10.11	Y	Flexure
	2AU	17.1	17.1	6.25	12.85	3.87	3.27	6.19	Y	Flexure
	3AU	15.0	20.9	6.25	11.28	3.26	4.03	4.49	Y	N
	4AU	15.5	20.4	6.25	11.67	3.82	5.37	2.59	Y	N
	5AU	16.0	24.8	6.25	12.06	3.70	5.78	2.16	Y	N
	6AU	17.5	28.8	6.25	13.20	4.08	6.93	1.27	N	N
	1CU	10.9	10.9	6.25	8.75	2.76	2.66	8.34	Y	Flexure
	2CU	11.0	12.2	6.25	8.84	2.68	3.12	6.61	Y	N
	3CU	11.0	16.1	6.25	8.83	2.68	4.15	4.28	Y	N
	4CU	12.5	17.9	6.25	10.00	3.05	4.71	3.37	Y	N
	5CU	15.0	18.6	6.25	11.96	3.69	4.88	3.11	Y	N
	6CU	16.5	17.5	6.25	13.15	4.07	4.79	3.17	Y	N
	3EU	13.9	13.9	6.25	11.52	3.78	5.29	2.70	Y	Flexure
	4EU	12.5	16.4	6.25	10.41	3.20	5.67	2.29	Y	N
	5EU	12.0	17.4	6.25	10.02	3.18	5.89	2.06	Y	N
	6EU	14.0	15.4	6.25	11.65	3.65	4.91	3.03	Y	N

Table F-7: Failure Information and Calculations for Uniform Load Tests, Krefeld and Thurston (1966) continued

Group	Name	V_{crit} kip	V_{ult} kip	w_{sw} lb/in.	V_d kip	v_d √psi	c in.	ε_t 10^{-3}	Yield?	Other Failure?
V	3GU	13.3	13.3	6.25	11.47	3.32	4.46	3.76	Y	Flexure
	4GU	15.9	15.9	6.25	13.65	4.02	6.10	1.92	N	Flexure
	5GU	12.5	14.8	6.25	10.84	3.27	5.43	2.49	Y	N
	6GU	16.9	16.9	6.25	14.52	4.42	6.89	1.30	N	Flexure
	3JU	10.9	10.9	6.25	9.85	2.88	4.55	3.64	Y	Flexure
	4JU	11.0	12.8	6.25	9.95	2.92	3.27	6.17	Y	N
	5JU	14.9	14.9	6.25	13.31	3.99	6.52	1.58	N	Flexure
	6JU	12.9	12.9	6.25	11.61	3.56	6.41	1.61	Y	Flexure
VII	6U	19.0	38.3	6.25	12.35	3.81	6.14	1.86	Y	N
VIII	3AAU	34.4	34.4	6.25	22.12	5.18	2.92	7.33	Y	Flexure
	4AAU	20.0	41.2	6.25	12.96	2.97	3.46	5.68	Y	N
	5AAU	45.1	45.1	6.25	29.12	7.53	5.03	2.93	Y	Flexure
	6AAU	20.0	48.3	6.25	13.04	3.12	4.85	3.10	Y	N
	4AU	17.0	26.4	6.25	12.78	3.14	3.30	6.08	Y	N
	5AU	21.0	29.8	6.25	15.76	3.90	4.29	3.95	Y	N
	6AU	20.0	34.8	6.25	15.06	3.62	4.60	3.44	Y	N
	4CU	16.5	21.9	6.25	13.11	3.19	3.41	5.79	Y	N
	5CU	19.0	21.4	6.25	15.07	3.69	3.49	5.53	Y	N
	6CU	20.5	24.2	6.25	16.27	3.76	3.82	4.76	Y	N
IX	3AAU	13.0	28.8	6.25	8.45	3.28	6.05	1.99	Y	N
	4AAU	12.0	25.1	6.25	7.83	3.09	5.50	2.45	Y	N
	5AAU	30.2	30.2	6.25	19.55	7.29	7.02	1.25	Y	Flexure
	6AAU	17.5	30.1	6.25	11.43	4.39	7.59	0.90	N	N
	3AU	11.0	21.8	6.25	8.33	3.09	5.96	2.06	Y	N
	4AU	10.0	18.3	6.25	7.61	2.95	7.03	1.27	N	N
	5AU	24.0	24.0	6.25	17.98	6.47	7.11	1.20	N	Flexure
	6AU	14.0	17.8	6.25	10.61	4.23	7.65	0.87	Y	N
	3CU	10.0	13.3	6.25	8.05	3.17	5.30	2.69	Y	N
	4CU	11.0	15.9	6.25	8.84	2.96	5.15	2.82	Y	N
	5CU	12.0	18.1	6.25	9.63	3.50	6.05	1.93	Y	N
	6CU	12.0	16.1	6.25	9.65	3.66	7.56	0.91	N	N
	3EU	10.0	13.0	6.25	8.39	2.96	6.30	1.79	N	N
	4EU	9.5	11.3	6.25	8.00	2.93	5.68	2.28	Y	N
	5EU	11.0	14.4	6.25	9.22	3.30	7.09	1.20	N	N

Table F-7: Failure Information and Calculations for Uniform Load Tests, Krefeld and Thurston (1966) continued

Group	Name	V_{crit} kip	V_{ult} kip	w_{sw} lb/in.	V_d kip	v_d √psi	c in.	ε_t 10^{-3}	Yield?	Other Failure?
IX	6EU	11.0	13.9	6.25	9.24	3.63	7.65	0.86	N	N
	3GU	8.8	10.7	6.25	7.74	2.90	5.86	2.15	Y	N
	4GU	9.9	9.9	6.25	8.66	3.52	7.17	1.18	N	Flexure
	5GU	9.0	10.9	6.25	7.93	3.30	7.55	0.95	N	N
X	U	35.0	56.6	14.58	22.74	2.70	5.36	7.64	Y	N
s-II	OU	48.0	63.7	17.36	36.08	2.74	3.57	12.07	Y	N

Table F-8: Tests Failing to Meet Criterion 6, Krefeld and Thurston (1966)

Loading	Group	Name	f'_c psi	d in.	a/d	ρ %	V_d kip	v_d √psi
ρ = 0.80%								
Concentrated	IV	13A2	2890	12.56	2.87	0.80	8.65	2.14
ρ = 1.05%								
Concentrated	IV	14A2	3000	9.56	3.77	1.05	6.14	1.95
ρ = 1.32%								
Concentrated	V	2AC	3340	10.00	4.80	1.32	7.21	2.08
Uniform	V	2CU	3020	10.00	3.00	1.32	8.84	2.68
ρ = 1.34%								
Concentrated	IV	15A2	2920	12.44	2.89	1.34	9.15	2.27
		15B2	3000	12.44	2.89	1.34	11.15	2.73
ρ = 1.77%								
Concentrated	IV	16A2	3220	9.44	3.81	1.77	8.64	2.69
ρ = 1.99%								
Concentrated	V	3AC	3020	10.06	4.77	1.99	9.21	2.78
		3CC	2970	10.06	5.96	1.99	8.29	2.52
	VIII	3AAC	5010	10.06	3.58	1.99	12.14	2.84
		3AC	4620	10.06	4.77	1.99	11.21	2.73
Uniform	V	3CU	2970	10.06	2.98	1.99	8.83	2.68
ρ = 2.09%								
Concentrated	IV	17A2	3190	9.56	3.77	2.09	9.14	2.82
ρ = 2.23%								
Concentrated	s-II	OCa	5550	17.94	4.01	2.23	31.87	2.38
		OCb	5550	17.94	4.01	2.23	29.87	2.24
ρ = 3.43%								
Concentrated	II	11A2	4380	12.36	2.91	3.43	15.16	3.09

Table F-9: Final Dataset, Krefeld and Thurston (1966)

Loading	Group	Name	f'_c psi	d in.	a/d	ρ %	V_d kip	v_d √psi
ρ = 2.63%								
Concentrated	VIII	4AAC	4235	10.00	3.60	2.63	12.64	3.24
		4AC	4420	10.00	4.80	2.63	11.21	2.81
		4CC	5570	10.00	6.00	2.63	11.29	2.52
	s-I	OCa	5180	10.00	6.00	2.63	10.29	2.38
		OCb	5660	10.00	6.00	2.63	11.79	2.61
Uniform	V	4AU	2590	10.00	2.40	2.63	11.67	3.82
		4CU	2980	10.00	3.00	2.63	10.00	3.05
		4EU	2935	10.00	3.60	2.63	10.41	3.20
		4JU	3220	10.00	4.80	2.63	9.95	2.92
	VIII	4AU	4590	10.00	2.40	2.63	12.78	3.14
		4CU	4680	10.00	3.00	2.63	13.11	3.19
ρ = 3.35%								
Concentrated	VIII	5AAC	4760	9.94	3.62	3.35	12.14	2.95
		5AC	4760	9.94	4.83	3.35	11.21	2.73
		5CC	5430	9.94	6.04	3.35	12.29	2.80
		5EC	5430	9.94	7.24	3.35	9.36	2.13
Uniform	V	5AU	2990	9.94	2.41	3.35	12.06	3.70
		5CU	2960	9.94	3.02	3.35	11.96	3.69
		5EU	2800	9.94	3.62	3.35	10.02	3.18
		5GU	3085	9.94	4.23	3.35	10.84	3.27
	VIII	5AU	4590	9.94	2.41	3.35	15.76	3.90
		5CU	4680	9.94	3.02	3.35	15.07	3.69
ρ = 4.29%								
Concentrated	VIII	6AAC	4990	9.86	3.65	4.29	13.14	3.14
		6AC	4950	9.86	4.87	4.29	12.21	2.93
		6CC	5570	9.86	6.09	4.29	11.79	2.67
		6EC	4900	9.86	7.30	4.29	9.36	2.26
	XI	PCa	5260	9.86	7.30	4.29	12.36	2.88
		PCb	5260	9.86	7.30	4.29	12.36	2.88
Uniform	V	6CU	2980	9.86	3.04	4.29	13.15	4.07
		6EU	2910	9.86	3.65	4.29	11.65	3.65
	VIII	6AU	4950	9.86	2.43	4.29	15.06	3.62
		6CU	5340	9.87	3.04	4.29	16.27	3.76

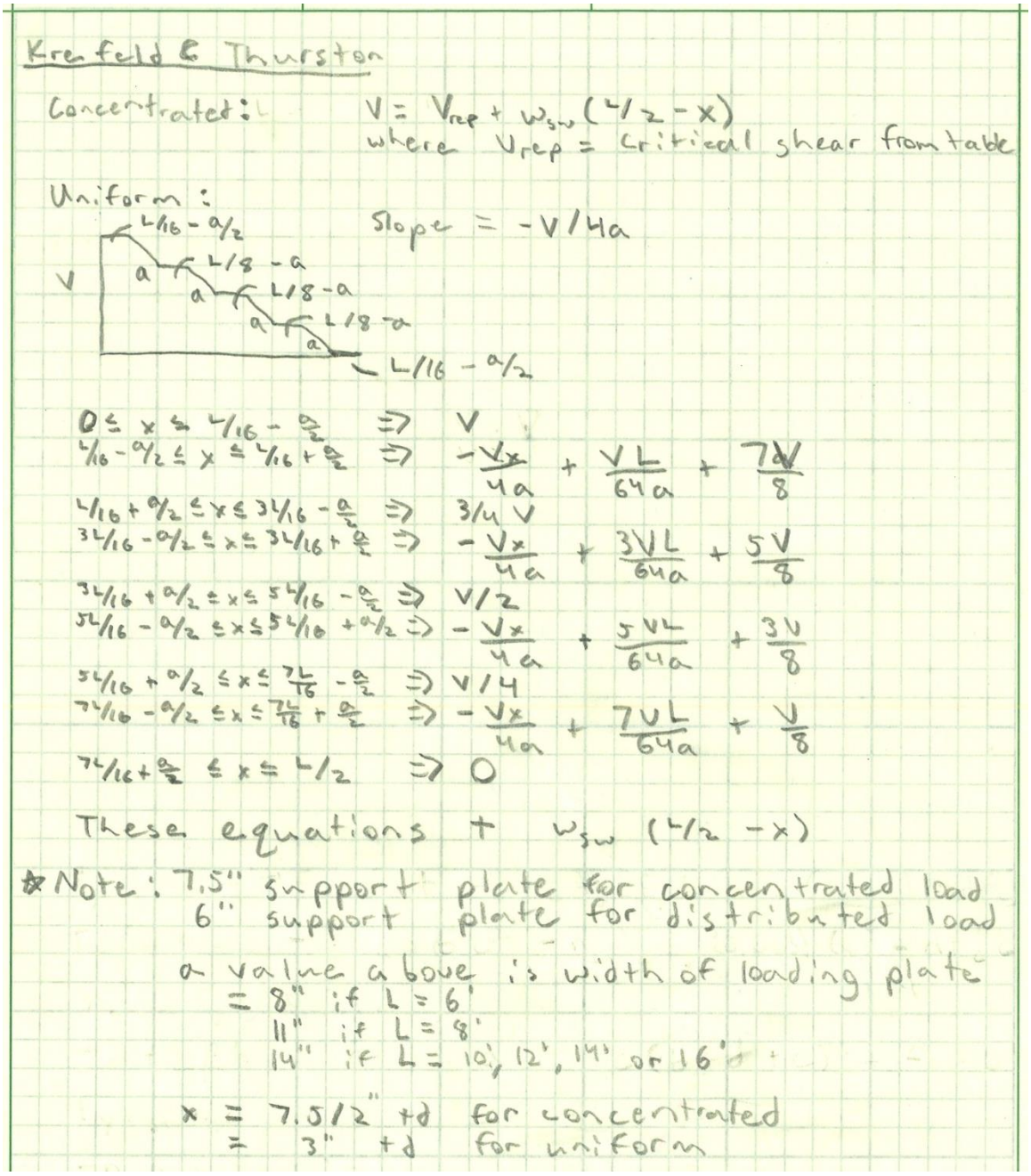

Figure F-5: Sample Calculations, Krefeld and Thurston (1966)

Table F-10: Geometry and Loading Conditions, Dassow (2014)

Loading	Name	f'_c psi	f_y ksi	b in.	h in.	d in.	a in.	a/d	ρ %	SP width in.
Concentrated	LD1-N	3658	69.3	36	24	21.30	53.2	2.50	1.02	12
	LD1-S	3658	69.3	36	24	21.30	53.2	2.50	1.02	12
	SR2-S	4360	69.3	36	24	21.30	53.2	2.50	1.02	12
Uniform	LD2	4071	69.3	36	24	21.30	54.0	2.54	1.02	12
	LD3	3522	69.3	36	24	21.30	54.0	2.54	1.02	12
	LD4	3713	67.4	36	24	21.30	54.0	2.54	1.02	12

Table F-11: Failure Information and Calculations, Dassow (2014)

Loading	Name	P_{crit} kip	P_u kip	w_b lb/in.	V_d kip	v_d √psi	c in.	ε_t 10^{-3}	Yield?	Other Failure?
Concentrated	LD1-N	119.5	119.5	71.69	87.82	1.89	5.47	8.67	Y	N
	LD1-S	131.4	131.4	71.69	95.99	2.07	5.47	8.67	Y	N
	SR2-S	117.2	155.6	74.05	85.86	1.70	4.59	10.91	Y	N
Uniform	LD2	234.0	258.3	74.23	91.04	1.86	4.92	9.99	Y	N
	LD3	233.6	327.0	73.40	91.43	2.01	5.68	8.24	Y	N
	LD4	274.3	274.3	73.77	106.85	2.29	5.24	9.18	Y	N

Table F-12: Final Dataset, Dassow (2014)

Loading	Name	f'_c psi	d in.	a/d	ρ %	V_d kip	v_d √psi
Concentrated	LD1-N	3658	21.30	2.50	1.02	87.82	1.89
	LD1-S	3658	21.30	2.50	1.02	95.99	2.07
	SR2-S	4360	21.30	2.50	1.02	85.86	1.70
Uniform	LD2	4071	21.30	2.54	1.02	91.04	1.86
	LD3	3522	21.30	2.54	1.02	91.43	2.01
	LD4	3713	21.30	2.54	1.02	106.85	2.29

Table F-13: Geometry and Loading Conditions, Klein (2015)

Loading	Name	f'_c psi	f_y ksi	b in.	h in.	d in.	a in.	a/d	ρ %	SP width in.
Concentrated	LD6-N	4505	74.5	21	24	21.30	64	3.01	1.05	12
	LD6-S	4505	74.5	21	24	21.30	64	3.01	1.05	12
	LD7-N	3465	64.8	21	48	45.30	136	3.00	0.98	12
	LD7-S	3618	64.8	21	48	45.30	136	3.00	0.98	12
Uniform	LD5	4805	71.8	21	24	21.30	64	3.01	1.05	12
	LD8	4266	64.8	21	48	45.30	136	3.00	0.98	12

Table F-14: Failure Information and Calculations, Klein (2015)

Loading	Name	P_{crit} kip	P_u kip	w_b lb/in.	V_d kip	v_d √psi	c in.	ε_t 10^{-3}	Yield?	Other Failure?
Concentrated	LD6-N	115.1	115.1	46.18	62.81	2.09	4.91	10.00	Y	N
	LD6-S	97.6	97.6	46.18	56.74	1.89	4.91	10.00	Y	N
	LD7-N	87.6	87.6	88.61	82.55	1.47	11.11	9.23	Y	N
	LD7-S	122.3	122.3	88.61	69.79	1.22	10.64	9.77	Y	N
Uniform	LD5	100.6	100.6	43.51	47.86	1.54	4.44	11.39	Y	N
	LD8	179.0	179.0	87.85	76.54	1.23	9.03	12.05	Y	N

Table F-15: Final Dataset, Klein (2015)

Loading	Name	f'_c psi	d in.	a/d	ρ %	V_d kip	v_d √psi
d = 21.30 in.							
Concentrated	LD6-N	4505	21.30	3.01	1.05	62.81	2.09
	LD6-S	4505	21.30	3.01	1.05	56.74	1.89
Uniform	LD5	4805	21.30	3.01	1.05	47.86	1.54
d = 45.30 in.							
Concentrated	LD7-N	3465	45.30	3.00	0.98	82.55	1.47
	LD7-S	3618	45.30	3.00	0.98	69.79	1.22
Uniform	LD8	4266	45.30	3.00	0.98	76.54	1.23

References

AASHTO LRFD Bridge Design Specifications, Customary U.S. Units. Washington, DC: American Association of State Highway and Transportation Officials, 2014.

ACI Committee 318. Building Code Requirements for Structural Concrete (ACI 318-11) and Commentary. Farmington Hills, MI: American Concrete Institute, 2014.

ACI-ASCE Committee 326, “Shear and Diagonal Tension,” ACI Journal Proceedings, V. 59, No. 1, January 1962, pp. 1-30.

ACI-ASCE Committee 326, “Shear and Diagonal Tension,” ACI Journal Proceedings, V. 59, No. 2, February 1962, pp. 277-334.

ACI-ASCE Committee 445, “445R-99: Recent Approaches to Shear Design of Structural Concrete (Reapproved 2009),” ACI Technical Documents, November 1999, pp. 1-55.

ASTM Standard A615/A615M, 2009, "Standard Specification for Deformed and Plain Carbon-Steel Bars for Concrete Reinforcement," ASTM International, West Conshohocken, PA, 2009, DOI: 10.1520/A0615_A0615M, www.astm.org.

ASTM Standard C31/C31M, 2010, "Standard Practice for Making and Curing Concrete Test Specimens in the Field," ASTM International, West Conshohocken, PA, 2010, DOI: 10.1520/C0031_C0031M, www.astm.org.

Bentz, Evan C., and Michael P. Collins, "Development of the 2004 Canadian Standards Association (CSA) A23.3 Shear Provisions for Reinforced Concrete," Canadian Journal of Civil Engineering, V. 33, No. 5, 2006, pp. 521-534.

Bentz, Evan C., Frank J. Vecchio, and Michael P. Collins, "Simplified Modified Compression Field Theory for Calculating Shear Strength of Reinforced Concrete Elements," ACI Structural Journal, V. 103, No. 4, July 2006, pp. 614-24.

Dassow, Nicholas A., "Effect of Uniform Load on the Shear Strength of Slender Beams without Shear Reinforcement," Thesis, University of Texas at Austin, 2014.

Elstner, Richard C., and Hognestad, Eivind, "Laboratory Investigation of Rigid Frame Failure," ACI Journal Proceedings, V. 53, No.1, January 1957, pp. 637-668.

Feldman, A., and C. P. Siess, "Effect of Moment-Shear Ratio on Diagonal Tension Cracking and Strength in Shear of Reinforced Concrete Beams," University of Illinois Civil Engineering Studies, Structural Research Series No. 107, June 1955.

Kani, G. N. J., "Basic Facts Concerning Shear Failure," ACI Journal Proceedings, V. 63, No. 6, June 1966, pp. 675-692.

Kani, G. N. J., "How Safe are Our Large Reinforced Concrete Beams?" ACI Journal Proceedings, V. 64, No. 3, March 1967, pp. 128-141.

Krefeld, William J., and Charles W. Thurston, "Studies of the Shear and Diagonal Tension Strength of Simply Supported Reinforced Concrete Beams," ACI Journal Proceedings, V. 63, No. 4, April 1966, pp. 451-476.

Leonhardt, F., and R. Walther, "Schubversuche an einfeldrigen Stahlbetonbalken mit und ohne Schubbewehrung," DAfStb, H. 151, Berlin, 1962, pp. 277-290.

Leonhardt, F., and R. Walther, "The Stuttgart Shear Tests," C&CA Translation, No. 111, Cement and Concrete Association, London, 1964.

MacGregor, James G., and James K. Wight. Reinforced Concrete: Mechanics and Design. 6th ed. Upper Saddle River, NJ: Prentice Hall, 2012.

Regan, P. E., "Shear in Reinforced Concrete – an Experimental Study," CIRIA-Report, April 1971.

Reineck, Karl-Heinz, Evan C. Bentz, Birol Fitik, Daniel A. Kuchma, and Oguzhan Bayrak, "ACI-DAfStb Database of Shear Tests on Slender Reinforced Concrete

Beams without Stirrups," ACI Structural Journal, V. 110, No. 5, September-October 2013, pp. 867-876.

Sherwood, Edward G., Adam S. Lubell, Evan C. Bentz, and Michael P. Collins, "One-Way Shear Strength of Thick Slabs and Wide Beams," ACI Structural Journal, V. 103, No. 6, November-December 2006, pp. 794-802.

Shioya, T., "Shear Properties of Large Reinforced Concrete Member," Special Report of Institute of Technology, Shimizu Corporation, No. 25, February 1989.

Uzel, Almila, Bogdan Podgorniak, Evan C. Bentz, and Michael P. Collins, "Design of Large Footings for One-Way Shear," ACI Structural Journal, V. 108, No. 2, March-April 2011, pp. 131-138.

Vecchio, Frank J., and Michael P. Collins, "The Modified Compression-Field Theory for Reinforced Concrete Elements Subjected to Shear," ACI Journal Proceedings, V. 83, No. 2, March 1986, pp. 219-31.